Dissertation
submitted to the
Combined Faculties for the Natural Sciences and for Mathematics
of the Ruperto-Carola University of Heidelberg, Germany
for the degree of
Doctor of Natural Sciences

Characterization of Innate Cellular Modulators of Retroviral Infection

presented by

M.Sc. Elina Eriksson
born in Taxinge, Sweden
Oral examination:

Referees: Prof. Dr. Hans-Georg Kräusslich
Prof. Dr. Oliver Keppler

ABSTRACT

HIV-1 is a retrovirus that causes AIDS, a condition that is characterized by progressive failure of the immune system and emerging opportunistic infections. Research aiming at understanding mechanisms for retroviral spread and pathogenesis has recently started to focus on the innnate immune system and factors that have been demonstrated to either enhance or block infection in tissue-culture experiments. The work presented in this thesis aimed to characterize the expression and function of three cellular proteins; CD317, SAMHD1, and Siglec-1, that function as modulators of retroviral infection.

In the **first project**, we investigated the *in vivo* expression pattern of the intrinsic immunity factor CD317 (BST-2, tetherin) in humans. CD317 restricts the release of enveloped viruses including HIV from infected cells. An additional proposed function for CD317 is as a selective target for immunotherapy of multiple myeloma, due to its apparently highly restricted expression on the surface of terminally differentiated B cells. To facilitate further studies of the biological functions, regulation, and therapeutic potential of CD317, we performed microarray-based expression profiling in 468 tissue samples from 25 healthy organs from more than 210 patients. CD317 protein could be detected in all organs investigated and in a number of specialized cell types, several of which are targeted *in vivo* by pathogenic viruses restricted by CD317 in tissue culture. We found limited co-expression of CD317 with the IFN biomarker MxA *in vivo* and low or no stimulation in organ explants exposed to recombinant IFNα, indicating that interferons may only partially regulate CD317. The study identified multiple thus far unknown interaction sites of viruses with CD317 and refutes the concept of its limited constitutive expression and strict IFN inducibility. Furthermore, CD317's widespread expression questions its suitability as a target for immunotherapy.

The **second project** involved characterizations of the restriction factor SAMHD1 in resting CD4+ T cells. SAMHD1 was reported to potently limit productive HIV-1 infection in a myeloid cell-specific manner by restricting HIV at the level of reverse transcription, and this block could be overcome by the Vpx protein of SIV and HIV-2. Our study demonstrated that SAMHD1 is also expressed abundantly in resting CD4+ T cells, where it locates to both the nucleus and cytoplasm. A staining protocol for SAMHD1 detection by flow cytometry was established, which enabled kinetic monitoring of its expression at a single cell level. Endogenous SAMHD1 levels were depleted in cells which either expressed Vpx following plasmid transfection or infection with Vpx-carrying HIV virions. In the latter case the restriction was alleviated, suggesting that reverse transcription is actively suppressed in resting CD4+ T cells, and that SAMHD1 is at least partly responsible for this restriction.

The **third project** focused on the surface receptor Siglec-1 (sialoadhesin, CD169) that mediates *trans*-enhancement of HIV-1 infection through recognition of sialic acid moieties in virus membrane gangliosides. Our study demonstrated that mouse Siglec-1, expressed on macrophages, captures murine leukemia virus (MLV) particles and mediates their transfer to proliferating B- and T-lymphocytes. To investigate the interaction between Siglec-1 and virus and its importance for mediating *trans*-infection, we analyzed the potential of sialic acid precursor analogs to modulate the MLV/Siglec-1 interaction. MLV released from N-substituted D-mannosamine analog-pretreated cells displayed strikingly different capacities for Siglec-1-mediated capture and *trans*-infection. The N-acyl side chain of sialic acid was thus revealed as a critical functional determinant for the mouse Siglec-1-MLV interaction.

In conclusion, the findings presented in this thesis provide new insights into the physiological expression pattern, regulation and function of the innate immunity factors CD317, SAMHD1 and Siglec-1. Characterizing the infection-modifying properties of these proteins might lead to a better understanding of their impact on retroviral spread and pathogenesis.

ZUSAMMENFASSUNG

HIV-1 ist ein Retrovirus, das AIDS auslöst, eine Krankheit, die durch progredientes Versagen des Immunsystems und damit einhergehenden opportunistischen Infektionen gekennzeichnet ist. Seit kurzem stehen Proteine der angeborenen Immunität, die einerseits die Infektion mit HIV-1 in Zellkulturexperimenten erleichtern oder andererseits hemmen, im Mittelpunkt derjenigen Forschung, die das Verständnis für die retrovirale Pathogenese und Ausbreitung im Körper zum Ziel hat. Die vorliegende Arbeit widmete sich der Charakteriserung von Expression und Funktion dreier zellulärer Proteine: CD317, SAMHD1 und Siglec-1, welche alle drei den Ablauf der retroviralen Infektion modulieren.

Im **ersten Projekt** wurde das Muster der *in-vivo*-Expression des intrinsischen Immunitätsfaktors CD317 (BST-2, Tetherin) im Menschen untersucht. CD317 hemmt die Freisetzung behüllter Viren wie HIV von infizierten Zellen in Kultur. Zusätzlich wurde CD317 aufgrund seiner hochselektiven Expression auf terminal differenzierten B-Zellen als spezifischer Angriffspunkt für die Immuntherapie des Multiplen Myeloms diskutiert. Wir erstellten mithilfe eines *Microarray*-Gewebe-Systems ein Expressionsprofil in 468 Gewebeproben aus 25 gesunden Organen von mehr als 210 Patienten. Das CD317-Protein konnte in allen untersuchten Organen in mehreren spezialisierten Zelltypen detektiert werden; einige dieser sind Zielzellen von pathogenen Viren *in vivo*, welche von CD317 gehemmt werden. Wir fanden nur geringe Koexpression von CD317 mit dem Interferon-Biomarker MxA *in vivo* und nur geringe oder gar keine Stimulation in Organexplantaten, die wir mit rekombinantem IFNα behandelt hatten. Diese Befunde legen nahe, dass CD317 allenfalls teilweise von Interferonen reguliert wird. Die vorliegende Arbeit identifizierte mehrere bisher unbekannte Interaktionsorte von Virus mit CD317 und gibt Grund zum Anlass, das Konzept einer sehr limitierten konstitutiven Expression sowie der strikten IFN-Abhängigkeit in Zweifel zu ziehen. Darüber hinaus stellt die ubiquitäre Expression in Frage, dass CD317 ein geeigneter Angriffspunkt für immuntherapeutische Ansätze sein könnte.

Das **zweite Projekt** untersuchte das antivirale Potential des Restriktionsfaktors SAMHD1in ruhenden CD4+-T-Zellen mittels Durchflusszytometrie. SAMHD1 wurde beschrieben, die Infektion von HIV-1 auf der Ebene der reversen Transkription in Zellen myeloischer Herkunft effizient zu begrenzen; dieser Block kann durch die Expression des Vpx-Proteins von SIV oder HIV-2 überwunden werden. Die vorliegende Arbeit führte aus, dass – konträr zum angenommenen Expressionsmuster – SAMHD1 ebenfalls in hohem Maße in ruhenden T-Zellen exprimiert wird, in denen es sowohl im Zellkern als auch im Zytoplasma vorkommt. Ein Protokoll zur Anfärbung und Detektion von SAMHD1 mithilfe von Durchflusszytometrie wurde etabliert. Dieses gestattete die Untersuchung der antiviralen Aktivität auf Einzelzellebene. Endogenes SAMHD1 konnte durch Transfektion von Vpx oder Infektion mit HIV-1 oder HIV-2, die Vpx inkorporiert hatten, abgebaut werden. Letzteres führte zu einer Reversion der Restriktion in ruhenden T-Zellen und zeigte, dass SAMHD1 zumindest teilweise für diese Restriktion verantwortlich ist.

Das **dritte Projekt** konzentrierte sich auf den Zelloberflächenrezeptor Siglec-1 (Sialoadhesin, CD169), welcher die *trans*-Infektion von HIV-1 durch die Erkennung von Sialinsäurebestandteilen in Gangliosiden der viralen Membran vermittelt. Die vorliegende Arbeit konnte zeigen, dass Maus-Siglec-1, das auf Makrophagen exprimiert wird, Partikel des murinen Leukämievirus (MLV) einfangen und die Übertragung auf proliferierende B- und T-Lymphozyten ermöglichen kann. Um die Wechselwirkungen zwischen Siglec-1 und Virus sowie deren Bedeutung für die Vermittlung der *trans*-Infektion zu untersuchen, analysierten wir den Effekt hierauf von Analoga der Vorläufersubstanzen der Sialinsäure. MLV, das aus Zellen freigesetzt wurde, die mit N-substituierter D-Mannosaminanaloga behandelt worden waren, zeigten deutlich veränderte Fähigkeiten für die Siglec-1-vermittelte *trans*-Infektion. Die N-Alkylseitenkette von Sialinsäure wurde als krtische funktionelle Determinante für die murine Siglec-1-MLV-Interaktionen identifiziert.

Zusammenfassend tragen die in dieser Arbeit vorgestellten Erkenntnisse über das physiologische Expressionsmuster, die Regulation sowie die Funktion von CD317, SAMHD1 und Siglec-1 zu einem breiteren wie tieferen Verständnis bei. Diese Faktoren der angeborenen Immunität sind Modulatoren der Infektion. Die Charakterisierung der infektionsmodulierenden Eigenschaften können einen wichtigen Beitrag zum Verständnis von Ausbreitung und Pathogenese retroviraler Infektionen leisten.

LIST OF PUBLICATIONS

This thesis is based on the following publications, which will be refered to in the text by their Roman numerals:

I. **Elina Erikson**, Tarek Adam, Sarah Schmidt, Judith Lehmann-Koch, Benjamin Over, Christine Goffinet, Christoph Harter, Isabelle Bekeredjian-Ding, Serkan Sertel, Felix Lasitschka, and Oliver T. Keppler. 2011. In vivo expression profile of the antiviral restriction factor and tumor-targeting antigen CD317/BST-2/HM1.24/tetherin in humans. *Proceedings of the National Academy of Sciences of the United States of America 108:13688-13693*.

II. Hanna-Mari Baldauf, Xiaoyu Pan, **Elina Erikson**, Sarah Schmidt, Waaqo Daddacha, Manja Burggraf, Kristina Schenkova, Ina Ambiel, Guido Wabnitz, Thomas Gramberg, Sylvia Panitz, Egbert Flory, Nathaniel R. Landau, Serkan Sertel, Frank Rutsch, Felix Lasitschka, Baek Kim, Renate König, Oliver T. Fackler, and Oliver T. Keppler. 2012. SAMHD1 restricts HIV-1 infection in resting CD4(+) T cells. *Nature medicine **18:**1682-1687.*

III. Sarah Schmidt, Kristina Schenkova, Tarek Adam, **Elina Erikson**, Judith Lehmann-Koch, Serkan Sertel, Bruno Verhasselt, Oliver T. Fackler, Felix Lasitschka, and Oliver T. Keppler. 2015. SAMHD1's protein expression profile in humans. *Journal of leukocyte biology. In press.*

IV. **Elina Erikson**, Parastoo Azadi, Martin Frank, Ina Ambiel, Katharina Klingeberg, Maria Pino, Paul-Robin Wratil, Nuria Izquierdo-Useros, Javier Martinez-Picado, Ronald L. Schnaar, Chris Meier, Paul R. Crocker, Werner Reutter, and Oliver T. Keppler. Mouse Siglec-1 mediates trans-Infection of murine leukemia virus in a sialic acid N-acyl side chain-dependent manner. *Manuscript in preparation.*

Other publications:

Nuria Izquierdo-Useros, Maier Lorizate, Maria C. Puertas, Maria T. Rodriguez-Plata, Nadine Zangger, **Elina Erikson**, Maria Pino, Itziar Erkizia, Bärbel Glass, Bonaventura Clotet, Oliver T. Keppler, Amalio Telenti, Hans-Georg Krausslich, and Javier Martinez-Picado. 2012. Siglec-1 is a novel dendritic cell receptor that mediates HIV-1 trans-infection through recognition of viral membrane gangliosides. *PLoS biology **10:**e1001448.*

Maria Pino, Itziar Erkizia, Susana Benet, **Elina Erikson**, Maria Teresea Fernández-Figueras, Dolores Guerro, Judith Dalmau, Dan Ouchi, Antonio Rausell, Angela Ciuffi, Oliver T. Keppler, Amalio Telenti, Hans-Georg Kräusslich, Javier Martinez-Picado and Nuria Izquierdo-Useros. HIV-1 immune activation induces Siglec-1 expression on myeloid cells fom blood and lymphoid tissues and enhances trans-infection. *Submitted for publication*.

ABBREVIATIONS

AIDS	Acquired Immune Deficiency Syndrome
AIM2	Absent in melanoma 2
AMP	Adenosine monophosphate
APC	Allophycocyanin
APOBEC	Apolipoprotein B mRNA editing enzyme catalytic polypeptide
BSA	Bovine serum albumin
BST-2	Bone marrow stromal cell antigen 2
CA	Capsid protein
CD	Cluster of differentiation
cGAMP	Cyclic guanosine monophosphate adenosine
cGAS	cGAMP synthase
CMAH	Cytidine monophosphate-N-acetylneuraminic acid hydroxylase
CpG	C-phosphate-G
CRF	Circulating recombinant form
DAI	DNA-dependent activator of IRFs
DC	Dendritic cell
DC-SIGN	Dendritic cell-specific intercellular adhesion molecule 3-grabbing nonintegrin
DNA	Deoxyribonucleic acid
DNAPKcs	DNA-dependent protein kinase catalytic subunit
dNTP	Deoxynucleoside triphosphate
Env	Envelope glycoprotein
FACS	Fluorescence activated cell sorting
FCS	Fetal calf serum
FITC	Fluorescein isothiocyanate
GMP	Guanosine monophosphate
GPI	Glycosylphosphatidylinositol
GTP	Guanosine triphosphate
HIV	Human Immunodeficiency Virus
HLH	Human lymphoid histoculture
HSV	Herpesvirus
IF	Immunofluorescence
IHC	Immunohistochemistry
IFI16	IFNγ-inducible protein 16
IFN	Interferon
IN	Integrase
IRF	Interferon regulatory factor
ISG	Interferon-stimulated genes
KSHV	Kaposi's sarcoma-associated Herpesvirus
MA	Matrix protein
ManN	N-substituted D-mannosamine
MDA5	Melanoma differentiation-associated gene 5
Mre	Meiotic recombination 11
MX2	Myxovirus resistance protein 2
MxA	Myxovirus resistance protein A
NC	Nucleocapsid protein
Nef	Negative factor
Neu5Ac	N-acetylneuraminic acid
Neu5Gc	N-glycolylneuraminic acid
NFκB	Nuclear factor κB
PBMC	Peripheral blood mononuclear cells
PBS	Phosphate buffered saline
pDC	Plasmacytoid dendritic cell
PE	Phycoerythrin

PECAM	Platlet endothelium cell adhesion molecule
PFA	Paraformaldehyd
PIC	Pre-integration complex
RIG	Retinoic acid inducible gene
RNA	Ribonucleic acid
RT	Reverse transcriptase
RTC	Reverse transcription complex
SAMHD1	Sterile alpha motif domain and HD domain-containing protein 1
Siglec	Sialic acid-binding immunoglobulin-like lectin
SIV	Simian Immunodeficiency Virus
STING	Stimulator of IFN genes
Tat	Transactivator of transcription
TBK	Tank-binding kinase
TBS	Tris buffered saline
TLR	Toll-like receptor
TMA	Tissue microarray
TRIF	TIR-domain-containing adapter-inducing interferon-β
Trim	Tripartite interaction motif
Vif	Viral infectivity factor
Vpu	Viral protein U
Vpx	Viral protein X

1 INTRODUCTION

1.1 INTERPLAY BETWEEN INTRINSIC AND INNATE IMMUNITY IN VIRAL DEFENCE

1.1.1 Intrinsic immunity and interferon-induced antiviral restriction

In response to viral infections, host cells have evolved a set of genes that restrict viral replication. These genes that encode proteins with suppressive or preventive effects, form part of the intrinsic immune system. Contrary to the conventional innate and adaptive immune responses, intrinsic immunity does not necessarily need factors that trigger its action – it is already there and active. Intrinsic immune factors can be constitutively expressed and can function signal-independent and block viral replication directly, thus providing a "front-line immune defense" against infections (14). However, some of these conserved intrinsic immunity proteins can also be further induced by type I interferons (IFNs). Similar to the induction of the innate immune response, these intrinsic antiviral factors require the host to first shape an antiviral state in order to get upregulated, underlying a possible interplay between the two types of immune responses.

1.1.2 Viral activation of the IFN system

Viruses are intracellular pathogens and contain protein as well as nucleic acid structures that are recognised as foreign by intracellular pattern-recognition receptors. Recent interest focused on recognition of intracellular pathogen-derived nucleic acids. In general, viral RNA as well as DNA can be sensed and induce the activation of proinflammatory pathways through IFN secretion.

1.1.2.1 IFN activation through RNA sensors

Type I IFN genes encode a family of cytokines that comprise 13 IFN-α subtypes and IFN-β (66). These genes can be activated by viral DNA and RNA species through recognition by cytosolic pattern recognition receptors (PRRs) or endosomal Toll-like receptors (TLRs) that work as microbial sensors in the cell. Double standed RNA (dsRNA), for example – which is the genetic material of many viruses – can be detected by receptors both in the cytosol and in endosomes. When the cytoplasmic sensors retinoic acid inducible gene (RIG-I) and melanoma differentiation-associated gene 5 (MDA5) are activated by dsRNA, this leads to phosphorylation, activation and nuclear translocation of Interferon regulatory factor (IRF)3 and Nuclear factor κB (NFκB). These proteins are the main interferon regulatory transcription factors, which induce transcription of IFNβ genes (84, 211). When TLR3 recognizes dsRNA in endosomes, it signals independently of RIG-I and activates IRF3 via the adaptor molecule TIR-domain-containing adapter-inducing IFNβ (TRIF), that signals directly to the kinase Tank-binding kinase (TBK)1, which phosphorylates IRF3 for nuclear translocation (84). TLR7, which recognizes viral single standed RNA (ssRNA), is also located in endosomes and is predominantly expressed by plasmacytoid dendritic cells (pDC) and B cells (9, 91). TLR7 (and TLR9, which senses double stranded CpG-rich DNA) signal via Myeloid differentiation primary response

gene 88 (MyD88) to activate the transcription factor IRF7 (supposedly by phosphorylation (89)), which is constitutively expressed in pDC and regulates IFNα/β transcription. Type I IFNs that are secreted then bind to interferon cell surface receptors (IFNARs) and activate expression of IFN stimulated genes (ISGs) via the JAK-STAT pathway (Fig. 1.1) (84).

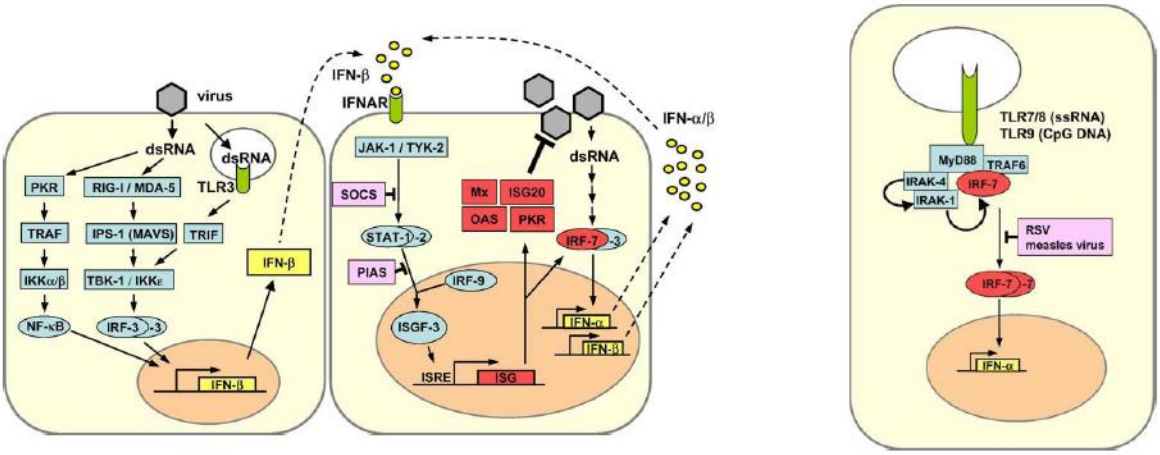

Fig. 1.1 Production of an antiviral state. The IFN response circuit is shown as the classical pathway (left) and within pDC or B cells expressing TLR7 and 9 (right). Activation of viral sensing receptors leads to expression of type I IFN genes. Type I IFNs are secreted and bind to cell surface IFNARs and induce transcription of ISGs (84).

1.1.2.2 IFN activation through DNA sensors

Signaling events mediated by the presence of intracellular DNA receptors has recently gained increasing interest. Besides sensing DNA viruses, recent studies suggest that DNA receptors can also be triggered by reverse transcribed retroviral cDNA (61, 102, 146). Cytosolic IFN-inducing DNA receptors typically signal through the Stimulator of IFN genes (STING)- dependent pathway. The adaptor protein STING resides in the endoplasmatic reticulum and on mitochondria-associated membranes (95, 217) and can, upon activation, recruit TBK1 and IRF3 via its C terminus, wich is believed to exend into the cytoplasm (Fig. 1.2). TBK1 can thereby phosphorylate IRF3, leading to nuclear translocation and induction of IFNβ genes.

Upstream of STING, many different receptors have been suggested to induce this signalling pathway. DNA-dependent activator of IRFs (DAI), also known as ZBP1, was the first candidate DNA sensor to be discovered. DAI was found to bind dsDNA and has been reported to interact with TBK1 and IRF3. However, DAI has been shown not to play an essential role for DNA sensing in leukocytes and in many human cell types (94, 136, 196). Like the RNA sensors RIG-I and MDA5, the DNA sensor DDX41 belongs to the DExD/H-Box helicases (DDX) protein family. While RIG-I and MDA5 have defined signaling (CARD)- and nucleic acid binding (DDX)- domains, DDX41 is thought to bind DNA using its DEADc domain, and also use the same domain to interact with STING (216).

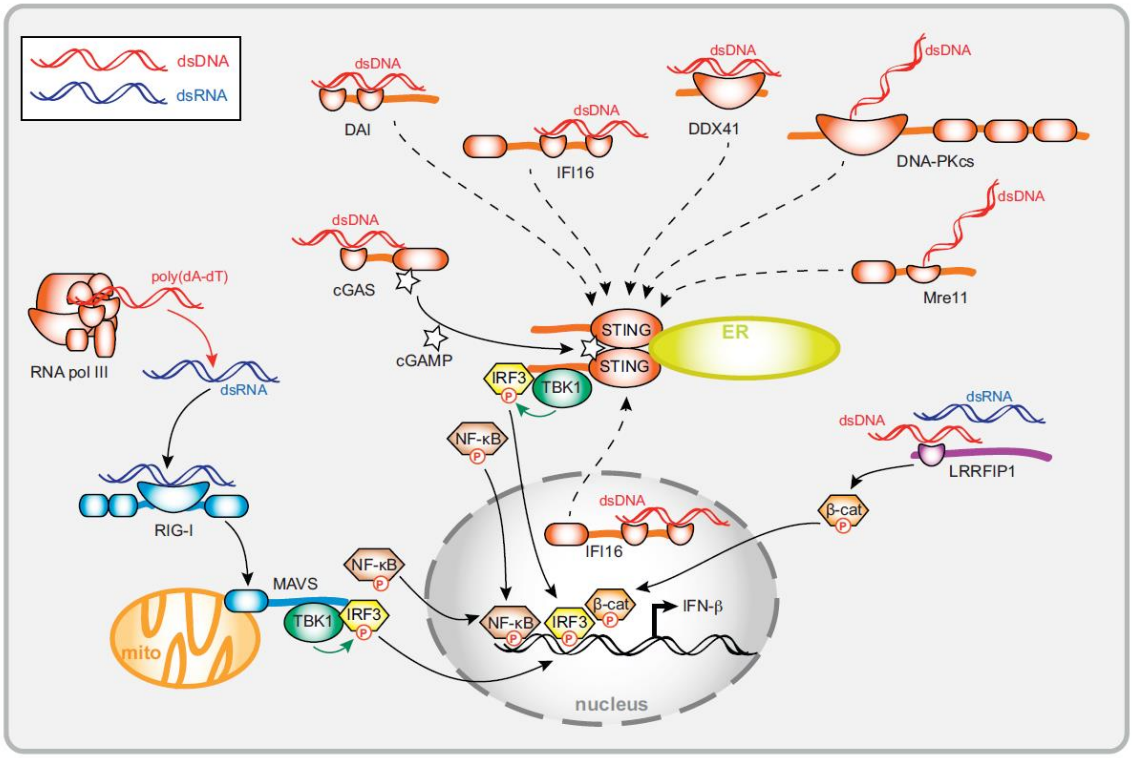

Fig. 1.2 Intracellular DNA receptors involved in the induction of interferon-β. Various DNA sensors have been proposed to activate a STING-dependent signalling pathway leading to activation of the transcription factors IRF3 and NFκB, which trigger transcription of IFNβ mRNA (195).

Not only pathogen-derived DNA or RNA, but also nucleic acids released from host cells during tissue damage, have the potential to activate the immune system, and studies on the link between DNA damage and innate immune responses indicated that DNA damage events can trigger type I IFN induction (112, 118). Later studies then identified the DNA damage factors Meiotic recombination 11 (Mre11) and the DNA-dependent protein kinase catalytic subunit (DNAPKcs) as initiators of the STING-pathway that trigger off repair pathways for dsDNA breaks (125, 195). When it comes to sensing of retroviral DNA intermediates, several receptors leading to STING activation have recently been identified. The IFNγ-inducible protein 16 (IFI16) and absent in melanoma 2 (AIM2) are members of the pyrin and HIN domain-containing (PYHIN) family of proteins, and are able to bind DNA via their HIN domains (106). While AIM2 localizes to the cytoplasm and is essential for interleukin-1β (IL-1β) production in response to dsDNA and induces the inflammasome, IFI16 shuttles between the nucleus and the cytoplasm and induces inflammasome activation, as well as STING-dependent IFNβ responses upon dsDNA binding (196). According to this mode of activation, a role for IFI16 in the recognition of HIV-1-derived dsDNA has been demonstrated (102, 146). It was also recently demonstrated that viral intracellular DNA induces the synthesis of a second messenger molecule, cyclic GMP-AMP (cGAMP), which can activate STING, leading to IFN induction (186, 206). The sensor of retroviral – including HIV-1, murine leukemia virus (MLV) and simian immunodeficiency virus (SIV) – DNA intermediates was then identified as the enzyme that

synthesizes cGAMP; cyclic GMP-AMP synthase (cGAS), which hence induces IFNβ in a STING-dependent manner (61).

1.2 INTRINSIC IMMUNE FACTORS AGAINST HIV-1

1.2.1 Introduction to HIV-1

1.2.1.1 Discovery and characterization

HIV-1 was first isolated from human lymph nodes in 1983 and based on its expression of reverse transcriptase, its shape and its size, it was classified as a member of the *Retroviridae* family (7). With further cloning and analysis of the genome, HIV-1 was categorized as a member of the genus Lentivirus. Like other lentiviruses, HIV-1 has a long period until disease onset and its primary cell targets are lymphocytes and macrophages of hematopoietic origin. When phylogenetic analyses of HIV-1 viruses from different parts of the world were performed, it became clear that this was a genetically extremely variable virus. Most of the variation can be attributed to the surface envelope (Env) glycoprotein (see section 1.2.2.2). HIV-1 isolates are divided into four groups: M (main), O (outlier), N (non-M, non-O) and P (pending the identification of further human cases). The largest group M is further divided into the following subgroups referred to as clades: A, B, C, D, F, G, H, J and K, as well as 15 recombinant forms (CRF). Soon after the isolation of HIV-1, lentiviruses were discovered and isolated from cats (feline immunodeficiency virus, FIV) (159) and a variety of nonhuman primates (simian immunodeficiency virus, SIV) (42). It is now well established that HIV-1 and HIV-2, a distinct, less pathogenic type of HIV (72), originate from at least two different strains of SIV (62): HIV-1 (M) is derived from SIVcpz (infecting chimpanzees, which are apes) and HIV-2 is derived from SIVsmm (infecting sooty mangabeys, which are monkeys). These viruses are thought to have been transmitted from primates to humans in the beginning of the 20th century (50, 205).

1.2.1.2 The AIDS/HIV pandemic and treatment

Today, there are more than 34 million people infected with HIV-1 worldwide and every year an estimate of 1.8 million people die from AIDS (UNAIDS). The HIV infection begins with an acute phase, characterized by high viral loads produced by activated lymphocytes in lymph nodes, which give rise to lymph node swelling, a cytokine storm and flu-like symptoms. The acute phase is followed by an asymptomatic phase typically starting 3-4 months after infection and this phase is characterized by low rate of viral replication and progressive depletion of CD4+ T cells from peripheral blood and lymph nodes. The asymptomatic phase may last for years (typically 8-10 years in HIV-1 infection (88)), but once the T cell count drops below 200 cells per mL, the untreated disease course enters its end stage. In this symptomatic phase, virus replication increases, something which – along with chronic immune stimulation – is associated with destruction of lymphoid cells and of the normal

architecture of the lymphoid tissue. The infected individual now develops symptoms of AIDS, including dysfunction of the immune system and emergence of opportunistic infections.

The development of anti-retrovirals for slowing the onset of AIDS progressed during the 1990s, and now many HIV-1 infected people can live their whole life without developing AIDS (144). These drugs are targeting several different steps of the viral life cycle and can thereby keep the viral replication low. However, due to factors including lack of education and medical infrastructure, this medical treatment is primarily available to HIV-1-infected individuals in developed countries. To reduce the rate of HIV-1 transmission globally, development of a prophylactic vaccine to prevent infection is of utmost importance. HIV-1 vaccine research is in part focused on the use of vectors and/or DNA plasmids aimed at eliciting an effective T cell response or subunit-based vaccines aimed at eliciting protective antibodies, or the combination of both (123). Other potential therapeutic strategies currently investigated include the use of broadly neutralizing antibodies (bNAbs) that target different vulnerable sites on the Env glycoprotein (203), gene editing of the CCR5 gene (189), the search for and application of antimicrobial molecules (149) and development of microbicides that can be applied topically (134).

1.2.2 Antiviral factors acting at different steps in the HIV-1 life cycle

1.2.2.1 Viral genes

Like other lentiviruses, and compared to simple retroviruses, the genome of the integrated form of HIV-1 cDNA (provirus) is relatively large (~9.8 kilobases in length), flanked on both ends by a repeated sequence known as the long terminal repeats (LTRs). The HIV-1 genome contains more than the genes gag, pol and env coding for structural proteins and common to all retroviruses. In order to replicate, HIV also needs additional regulatory genes, *tat* (transactivator of transcription) and *rev* (regulator of expression of virion proteins). The four remaining genes; *vif* (viral infectivity factor), *vpu* (viral protein U), *vpr* (viral protein R) and *nef* (negative factor), encode accessory proteins that are not essential for replication in tissue culture, but seem to have a larger impact on virus production and pathogenesis *in vivo*. Many SIVs and HIV-2 encode one additional accessory gene, *vpx* (viral protein X), which is related to Vpr and thought to have arisen as a result of non-homologous recombination between different SIVs (180).

1.2.2.2 The viral particle and its life cycle

Each HIV-1 particle contains a set of structural as well as non-structural proteins, and the HIV-1 viral assembly and replication cycle requires the collaborate effort of its genes that encode both structural and non-structural proteins (55). The gag gene encodes Gag (p55), a polyprotein precursor that is cleaved by the viral protease (PR) into the mature Gag proteins matrix (MA/p17), capsid (CA/p24), nucleocapsid (NC/p7), p6, spacer peptide p1 and p2. Gag (p55) proteins assemble together with Gag-

Pol polyprotein precursor Gag-Pol (p160) which is the result of a rare frame shift during Gag (p55) translation. Gag-Pol contains the viral enzymes; protease (PR), integrase (IN) and reverse transcriptase (RT), which are cleaved during maturation. The envelope (Env) glycoproteins are also synthesized from the Env precursor (gp160) that is processed by a cellular protease resulting in the generation of the surface (SU) Env glycoprotein gp120 and the transmembrane (TM) glycoprotein gp41. The structural proteins; MA, CA, NC and p6 (Gag) assemble together with the viral enzymes; PR, IN and RT (GagPol); and the envelope glycoproteins are incorporated into budding viral particles at the plasma membrane. In addition to these structural and enzymatic proteins, also the accessory protein Vpr is incorporated into new virions through interaction with p6 in Gag and in the case of HIV-2, also Vpx is incorporated.

The HIV particle is covered by a lipid bilayer, derived from the host cell membrane during the budding process. When HIV-1 enters the cell, the Env subunit gp120 interacts with CD4 on the cell surface, resulting in a conformational change that allows binding of the chemokine receptors CCR5 or CXCR4. Following this interaction, either the virus membrane fuses with the cellular membrane so that its core can be released into the cytoplasm, or the clathrin-mediated endocytosis process is triggered. When the HIV-1 core is uncoated (a process which is still poorly understood (13, 208)), this leads to formation of the reverse transcription complex (RTC), containing the viral RNA and the proteins needed for reverse transcription (20, 51). The viral RNA is then converted into (linear) double-stranded DNA, and the pre-integration complex (PIC) travels through the nuclear pore complex into the nucleoplasm, where the viral genome integrates into the host genome by the enzymatic activity of IN. Once the transcription of the proviral DNA template is initiated in the HIV long terminal repeat (LTR), the binding of the cellular RNA polymerase II in presence of the regulatory protein Tat leads to efficient transcriptional activity. The viral RNAs that are generated during transcription resemble cellular mRNAs but can be fully spliced, unspliced or partially spliced. The process in which partially spliced or unspliced mRNAs are transported from the nucleus into the cytoplasm requires the presence of the viral regulatory protein Rev (164) and the cellular factor CRM1 (56). Rev binds to the Rev-response element, leading to unrecognized export of partially spliced mRNAs which would otherwise be recognized by host cell mechanisms including e.g. nonsense-mediated decay. After viral protein synthesis at the ribosomes, the proteins are transported to the cell membrane where the virus assembles. The Gag protein binds tRNA to its MA domain – this prevents that Gag binds to intracellular membranes, thereby facilitating recruitment to the plasma membrane – and it also recruits both cellular and viral transcripts to the plasma membrane via its NC domain. At the plasma membrane the viral genomic RNAs are selectively incorporated into virions due to specific A-rich nucleotide sequences (129). When all viral components have assembled, a budding process is initiated by interaction of Gag polyprotein parts with the cellular ESCRT machinery and the viral particles pinch off from the cell membrane, resulting in the onset of the final steps necessary to generate infectious particles. The Gag polyprotein is then processed into its subunits MA, CA, NC and

p6. In this process, called maturation, structural changes occur that allow the virion to enter, uncoat and replicate in the next host cell: the RNA genome is condensed and stabilized and the conical capsid assembles around the RNA-NC-complex (187). During this life cycle, host cell restriction factors can act at virtually all steps. However, many restriction factors inhibit incoming viral capsids or reverse transcription complexes, suggesting that the very early steps are vulnerable targets for intrinsic immune factors.

1.2.2.3 HIV-1 restriction factors

Common traits shared by HIV-1 restriction factors are that they typically act in a species specific way, are under positive selection, and often IFN-inducible (140). One antiretroviral restriction factor whose expression is increased as a consequence of IFN treatment is the ubiquitin ligase Trim5α, which belongs to the Trim (tripartite interaction motif) family of proteins. Trim5α blocks HIV-1 replication in rhesus macaques, likely by targeting its capsid protein for degradation by the proteasome (191). Since some lentiviral capsids bind to the host cell protein cyclophilin A (CypA), the sensitivity of TRIM5α towards HIV-1 is compromised. Additionally, while human Trim5α largely lacks the ability to bind HIV-1 capsid, productive infection of nonhuman primate cells with HIV-1 is efficiently restricted (46). In general, TRIM5α proteins are poor inhibitors of retroviruses that are found naturally in the same host species, but are often active against retroviruses that are found in other species, a common feature of species-specificity of restriction factors.

Different restriction factors target different steps of viral replication. For instance, several members of the *APOBEC3* (apolipoprotein B mRNA editing enzyme catalytic polypeptide 3) family of genes are also interferon-inducible and impose their restriction by targeting retroviral replication at the level of reverse transcription. When viral RNA is copied into cDNA, APOBEC3G/F deaminate the single stranded DNA, converting cytosine to uracil (U) resulting in the pairing of U's with A's. Since uracil-containing DNA is less stable, it usually gets degraded. However, if it stays intact and the provirus gets integrated into the host genome, the mutations will in many circumstances prevent it from producing viable progeny. Furthermore APOBEC3G has a preference for GG dinucleotides (141) and that means TGG (tryptophan) codons can be converted into stop-codons (TAA). In addition to the deaminating activity, A3G also has a deamination-independent antiviral activity by blocking reverse transcription, likely through interacting and physically preventing elongation of RT (15). In order to replicate successfully, viruses have evolved strategies to overcome these cellular barriers of the host. For example, the HIV-1 accessory protein Vif accomplishes this by binding both APOBEC3G and proteins cullin 5 and elongins B and C, belonging to an E3 ubiquitin ligase complex, thus resulting in the polyubiquitination of APOBEC3G and proteasomal degradation (213).

Another factor recently found to have anti-HIV-1 activity is the type I interferon-inducible human protein MX2 (74, 111, 137). MX2 seems to act at the level of nuclear import and/or at the level of integration (49, 74), because in MX2-expressing cells the cDNA synthesis occurs normally, while

integration of HIV-1 provirus is impaired. Similar to TRIM5α, MX2's anti-HIV activity seems to be sensitive to capsid-CypA binding. However, since the viral inhibition is manifested as the failure to accumulate viral cDNA in the nucleus, the anti-viral action of MX2 is distinct from TRIM5α- or APOBEC3G-mediated inhibition of early reverse transcription or SAMHD1-mediated restriction (see next section) (74).

1.2.2.4 SAMHD1

The sterile alpha motif (SAM) domain and HD domain-containing protein 1 (SAMHD1) has been reported to potently restrict productive HIV-1 infection at an early stage of the viral replication cycle in non-dividing cells of myeloid origin, like monocytes, macrophages and DC (92, 131) and this block is overcome by the Vpx protein of SIV and HIV-2 through a proteasome-dependent mechanism involving DCAF1 and DDB1 (1, 92, 184). Vpx has also been described to promote the nuclear entry of the PIC and the accumulation of full-length viral DNA (54, 58). The HIV-1 replication block in myeloid cells and the delivery of the Vpx protein to overcome this restriction, has been known for some time (73, 75, 179). The interaction of Vpx with DCAF1, a component of the CRL4A/DDB1/DCAF1 ubiquitin ligase complex, and the involvement of the proteasome system are required for the Vpx-dependent enhancement of infection (75, 179, 184). Vpx is believed to primarily counteract SAMHD1 by CRL4A/DDB1/DCAF1 ubiquitin ligase-dependent degradation of the restriction factor, rendering non-cycling myeloid cells permissive for infection (11, 184).

The block imposed by SAMHD1 is at the level of reverse transcription, during which the HIV-1 RNA is copied into cDNA. The HD-domain of SAMHD1 has nucleotide-phosphohydrolase activity (3), and SAMHD1 is a dGTP-stimulated triphosphohydrolase that can dehydrolyze deoxynucleoside triphosphates (dNTPs) into deoxynucleoside and triphosphate thus postulated to lower the dNTP pool levels enough to sufficiently reduce viral DNA synthesis in non-cycling cells (166). The HD-domain alone has also been shown to be sufficient to restrict infection of different viruses (204). Thus the findings on SAMHD1 restriction activities suggested that the overall decrease in the level of dNTPs may be primarily responsible for the block imposed on lentiviral reverse transcription. A second enzymatic activity was recently described for the HD-domain of SAMHD1; it also posesses nuclease activity by which it can target single-stranded DNA and RNA (10), and an even more recent study suggests that SAMHD1 inhibits HIV-infection through degradation of viral RNA rather than through its dNTPase activity (175). Furthermore, the SAMHD1 restriction activity has been demonstrated to be determined by its phosphorylation status, which correlates with whether the cells are cycling (phosphorylated SAMHD1) or non-cycling (dephosphorylated SAMHD1) (34). The phosphorylation site on SAMHD1 has been mapped to residue T592 and phosphorylation at this site renders SAMHD1 incapable of blocking retroviral infection (34). However, the modification of this phosphorylation site does not affect the ability of SAMHD1 to decrease cellular dNTP levels (204). The ribonuclease activity, on the other hand, was described to be negatively regulated by phosphorylation at residue

T592 (175). Hence the mechanistic details on antiviral restriction imposed by SAMHD1 are still not fully elucidated and remain an active field of research.

1.2.2.5 Tetherin/CD317

Though originally discovered as a plasma cell antigen highly expressed by multiple myeloma cells (71), and later suggested as a target for cellular immunotherapy (103), CD317 (also known as BST-2, Tetherin or HM1.24) was not identified as an antiviral restriction factor until 2008. Tetherin inhibits the release of retroviruses and its action is antagonized by the HIV-1 accessory protein Vpu (153, 198). When infected with HIV-1, some cell lines, e.g. HeLa cells, require Vpu for efficient viral particle release, while others do not require the action of this viral accessory protein for final release from the cell surface. Vpu has mainly two functions; 1) it interacts with newly synthesized CD4 (the primary receptor for all primate lentiviruses) at the endoplasmatic reticulum (ER) and targets the receptor for proteasomal degradation, 2) Vpu enhances the release of viral particles by counteracting CD317. The latter is mechanistically not fully understood but may involve targeting CD317 for proteasomal and/or lysosomal degradation or the sequestration of CD317 resulting in reduction of its cell surface exposure (67). CD317 is a glycosylated type II transmembrane protein of 30-36 kDa. It has an unusual topology, shared only by a minor isoform of the prion protein (147). CD317 has a short N-terminal domain that is cytoplasmic, a transmembrane region that anchors the protein in the membrane and a coiled-coil extracellular domain prior to the C-terminus of the protein. The C-terminus has a glycosylphosphatidylinositol (GPI) anchor that enables the protein to localize to lipid rafts at the plasma membrane, a site where HIV budding preferentially occurs (128). CD317 localizes not only to the plasma membrane, but also to membranes on intracellular organelles, including endosomes and the trans-Golgi network (83). Mechanistically, the tethering action of the CD317 protein is thought to involve one or both of its anchors to become incorporated into the viral particle while the extracellular coiled-coil domain typically forms homodimers. Thereby can CD317 efficiently tether enveloped viral particles to the cell surface (160). In addition to the tethering action, reports have also demonstrated a role for CD317 in signal transduction (59, 190). These studies show that CD317-mediated restriction of the release of enveloped viruses triggers proinflammatory gene expression through induction of NfκB activation. Both the extracellular domain that is essential for virus restriction, and amino acids in the N-terminal cytoplasmic tail, were required for NFκB-mediated transcription of proinflammatory genes (59).

In addition to HIV-1, several other enveloped viruses are also restricted by CD317 and have evolved counteracting factors to overcome the impaired release of budding virions from the cell surface. In contrast to HIV-1, most other primate lentiviruses do not contain a *vpu* gene, neither HIV-2 nor SIV encode a Vpu protein, instead they use Env (HIV-2, SIV) and Nef (SIV) to antagonize CD317 (133, 153, 215). Ebola virus uses its glycoprotein (109) and Kaposi's sarcoma herpesvirus (KSHV) has been suggested to use its protein processing K5 ubiquitin ligase activity (142) to circumvent the block that

CD317 constitutes. Since most other primate lentiviruses do not contain a *vpu* gene while HIV-1 does, this may have important implications for the role of Vpu in the pathogenesis of AIDS (121, 128). Recent studies describe how Nef proteins of HIV-1 group O – which is believed to be derived from a different ancestor than group M and has not evolved a Vpu-based tetherin antagonism (176) – can antagonize human CD317, and this is something that might explain the epidemic spread of HIV-1 group O (124).

1.3 CARBOHYDRATE RECEPTORS AND RETROVIRAL *TRANS*-INFECTION

1.3.1 DC-SIGN and the concept of *trans*-infection

The important role of dendritic cells (DC) in HIV infection came from the discovery that these cells facilitate HIV infection when cocultured with T cells (23, 165). This process, whereby uninfected immature DC (23, 76) capture virus and mediate viral transfer to neighboring cells without becoming infected themselves is termed *trans*-infection. The HIV glycoprotein gp120 binds to dendritic cell–specific intercellular adhesion molecule 3-grabbing nonintegrin (DC-SIGN) (41, 64), a cell surface C-type lectin expressed on immature dendritic cells, mostly present in skin and mucosa. Isolated primary DC-SIGN+ cells from rectal mucosa were shown to mediate transmission of HIV-1 to T cells through DC-SIGN (82), this confirming a role of the receptor as a mediator of transmission of HIV in physiologically relevant cells. DC-SIGN is expressed as a tetramer and recognizes mannose, fucose, N-Acetylglucosamine (GlcNAc) and mannan, through a Ca2+-dependent mechanism (52). In contrast to CD4 and chemokine receptors, DC-SIGN does not mediate entry of HIV bound to it (64, 130). However, at low viral multiplicty of infection (MOI), DC-SIGN-expressing cells pulsed with HIV transmit virus to appropriate target cells and retain infectious particles for several days in culture. After binding, the DC-SIGN cytoplasmic tail mediates internalization of HIV, keeping it intact for efficient infection in *trans* in a low pH nonlysosomal compartment (130). Later studies on DC transfer, however, demonstrate that the long-term transfer of HIV require infection of the DC and show that de novo synthesized viral particles are primarily transferred to T cells at the later time points (21, 26). These more recent studies distinguish between a first-phase transmission, which occurs early and peaks within the first couple of hours after virus exposure, and a second phase, in which virus can be transmitted up to 5 days after exposure (26, 194). The latter one is supposed to involve the de novo pathway of viral transmission, while the early phase *trans*-infection is characterized by transfer of primarily surface-bound HIV particles to CD4+ T cells (21, 26).

Since DC-SIGN is expressed at high levels on immature dendritic cells, it is suggested to be important for DC-mediated transport of virus from mucosal sites to secondary lymphoid tissues where it could efficiently transfer virus to T cells (64). DC-SIGN is able to capture and enhance transmission of a variety of HIV and SIV strains, but cannot bind to HIV particles pseudotyped with the retroviral

ecotropic Moloney murine leukemia virus (MLV) envelope glycoprotein (130), this suggesting some species specificity. Although the function of DC-SIGN to capture and transfer HIV-1 particles to CD4+ T cells is well established (4, 64, 82, 130), some studies question the actual contribution of DC-SIGN in HIV *trans*-infection, since virus transfer can occur through DC-SIGN-independent mechanisms as well (6, 80, 207). These studies used monocyte-derived DC, suggesting that other receptors expressed on this *in vitro*-differentiated cell type are contributing to the *trans*-infection of HIV-1. Indeed, studies suggested several other receptors (e.g galactosyl ceramide, the mannose receptor, the HIV-1 receptor CD4 and Syndecan-3) to be involved (43, 139, 154, 193). Recent studies have also demonstrated an important role for the sialic acid-binding immunoglobulin-like lectin 1 (Siglec-1) in HIV-1 *trans*-infection mediated by monocyte-derived DC (see section 1.3.3). In order to define the role of different receptors in HIV *trans*-infection and their potential effect on HIV transmission *in vivo*, isolation of primary DC subsets from tissues relevant for HIV-transmission (e.g. subepithelium of the genital and rectal mucosa) would be required, the difficulty of which makes such studies demanding to conduct.

1.3.2 Siglec-1/Sialoadhesin/CD169

1.3.2.1 Discovery and characterisation

The adhesion molecule and carbohydrate recognition receptor Siglec-1, also termed Sialoadhesin or CD169, was first described in 1985 as a non-phagocytic sheep erythrocyte receptor, expressed on resident bone marrow macrophages that cluster with developing haematopoietic cells (36). Therefore, Siglec-1 was suggested to directly regulate haematopoiesis (40), and later studies by Chow et al. showed Siglec-1+ bone marrow macrophages to be important for erythroblast development (29, 30). However, Siglec-1 -/- mice are viable and show no developmental abnormalities. They have a small increase in CD8+ T cells and a small decrease in B220+ B cells in spleens and lymph nodes with slightly less follicular B cells and an increase in numbers of marginal zone B cells in spleen, a phenomenon indicative of reduced immunoglobulin M (IgM) levels (155).

There are 14 Siglecs in humans and they all recognize sialic acids. Being the largest member of the immunoglobulin (Ig) superfamily, Siglec-1 is a type I transmembrane glycoprotein and has 17 Ig-like domains, with 16 extracellular C2-like domains extending from the cell surface and one extracellular N-terminal V-set domain at the top. The V-set domain was shown to be necessary and sufficient for sialic acid binding (152). Unlike most other Siglecs, Siglec-1 has a short, poorly conserved cytoplasmic tail that lacks tyrosine-based signalling motifs, suggesting a primary role as binding partner in cell-cell interactions rather than cell signaling (38).

Sialic acids are typically located at the exposed ends of oligosaccharide chains, and Siglec-1 binding is influenced by the type of sialic acid and its linkage to the subterminal sugar. In glycoproteins and glycolipids, sialylated oligosaccharide ligands are attached to protein and lipid carriers. These

glycoconjugates have the potential to function as 'counter-receptors' for Siglecs and other glycan-binding proteins (35, 38). Siglec-1 preferentially recognizes sialic acids that are α2 → 3 linked, which means that the gangliosides GD1a and GM3 which express terminal α2 → 3 linked sialic acid are recognized by Siglec-1, whereas GM1 and GM2 which express a less exposed sialic acid residue, and GD3 and GQ1b which contain terminal α2 → 8 linked sialic acid, do not bind at all or only weakly (37). Studies that investigated the interaction between Siglec-1 and one of the most common sialic acids in mammals, *N*-acetylneuraminic acid (Neu5Ac), demonstrated by site-directed mutagenesis (200), X-ray crystallography (143), and NMR (39) that the arginine-97 residue (which is conserved in Siglec-1 in all species) forms a key salt bridge with the carboxylate group of Neu5Ac and two conserved tryptophans at positions 2 and 106 to make hydrophobic interactions with the N-acetyl group and the C-9 glycerol group respectively (Fig. 1.3).

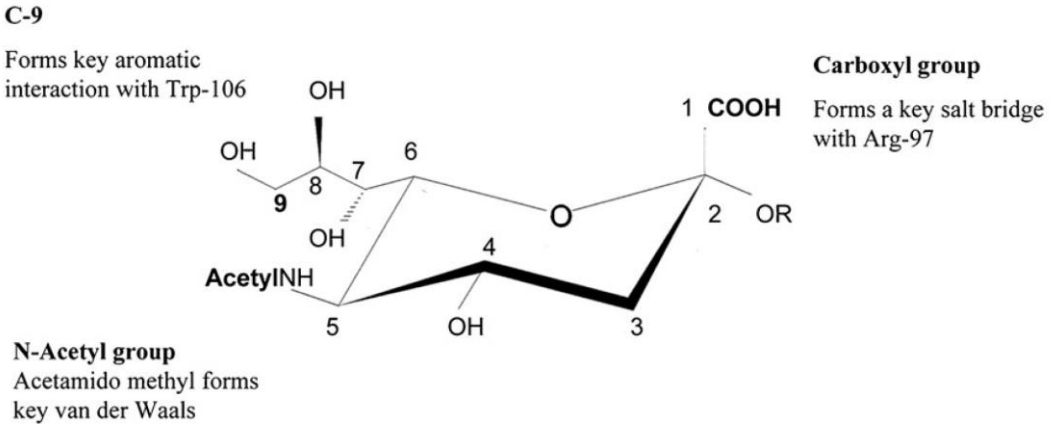

Fig. 1.3 The features of *N*-acetylneuraminic acid important for interaction with Siglec-1. Indicated are the functional groups that form contacts with the binding site of Siglec-1. The Siglec-1 residues indicated are conserved in all Siglec-1 orthologs (122).

The functional groups of sialic acids involved in binding to Siglec-1 were investigated using synthetic N-acetylneuraminic acid analogues either on resialylated human erythrocytes or as free α-glycosides in hapten inhibition studies (115, 116). These studies confirmed that Siglec-1 specifically binds Neu5Ac, but does not recognize two other important sialic acids; Neu5Gc or Neu5Ac9Ac. In contrast to mice, humans lack Neu5Gc due to a mutation in the CMAH (cytidine monophosphate-N-acetylneuraminic acid hydroxylase) gene, which encodes the enzyme required for the conversion of Neu5Ac to Neu5Gc (183).

1.3.2.2 Expression profile and IFN induction

In humans, Siglec-1 is expressed on tissue macrophages in the spleen, lymph nodes, bone marrow, liver, colon and lungs (86). In rodents, Siglec-1 is abundantly expressed on macrophages in the subcapsular sinus (SCS) and medullary cords of the lymph node (Fig. 1.4), as well as on marginal

zone metallophilic macrophages in the spleen. Their strategic localization along lymphatic vessels and at portals of entry for blood, suggests a function for these cells in regulating the immune response to pathogens that they encounter in the lymph and in blood.

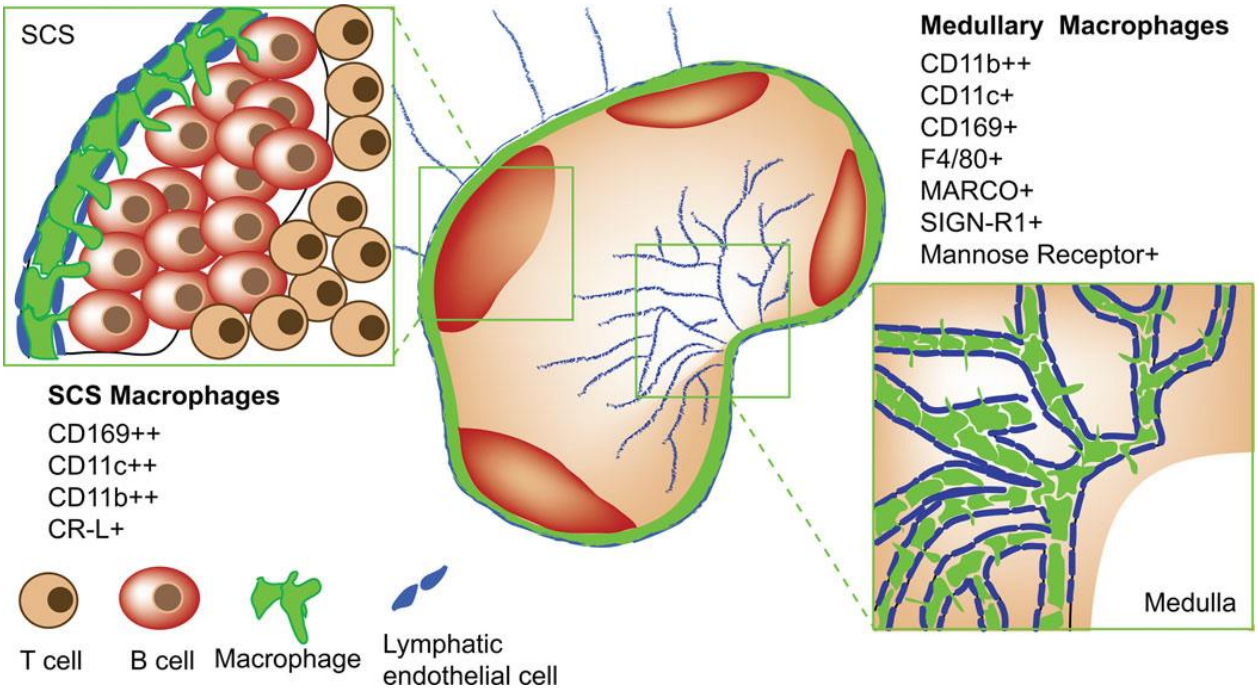

Fig. 1.4 Lymph node macrophages localize to strategic positions. Diagram showing anatomical distribution of lymph node sinus-resident macrophages along with the surface markers they express (127).

IFN alpha has been shown to upregulate Siglec-1 expression on macrophages in all species examined. In addition, molecules that trigger type I IFN responses like LPS and poly I:C stimulation of TLR4 and 3, respectively, have this effect by activating the TRIF-dependent pathway of type I IFN induction (212). Although there is no *in vivo* evidence for DC expression of Siglec-1, it can be induced on monocyte-derived DC *in vitro* after treatment with inactivated human rhinovirus (119) or after LPS or type I IFN stimulation (100, 168). Siglec-1 has also been reported to be expressed on monocytes in patients suffering from viral infections or autoimmune diseases with upregulated type I IFN levels as a marker, like HIV-1 infection (167, 199), systemic lupus erythematosus and systemic sclerosis (212).

1.3.3 The role of Siglec-1 in viral infection

Siglec-1 is a surface receptor involved in *trans*-enhancement of HIV-1 infection and its expression on monocytes directly correlates with plasma viral load in HIV-1 patients (170). Siglec-1 was shown to bind the virus through recognizing the sialic acid residues on the viral envelope glycoprotein gp120. The Siglec-1+ monocytes enhanced HIV-1 infectivity by absorbing the cell-free virus from the culture and *trans*-infecting permissive reporter cells. In another study, the sialic acid on gp120 binding to

Siglec-1 was shown to have a crucial role in infection of macrophages (218). However, it was recently demonstrated that Siglec-1 expressed on *in vitro* differentiated DC can recognize sialic acid-containing gangliosides in the HIV-1 particles, independent of gp120 leading to capture, internalization and subsequent transfer to target cells (98, 100, 168, 169). The ganglioside recognized by Siglec-1 in these studies was GM3, a glycolipid that had previously been observed in the membranes of HIV-1 and several other viruses including Semliki forest virus (SFV), vesicular stomatitis virus (VSV) and MLV (27, 98, 110). Mouse studies show that within minutes upon peripheral inoculation, viral particles are captured by lymph node resident (CD169++) sinus macrophages, preventing their systemic dissemination (93, 108). While (CD169+) medullary macrophages are poorly selective in their filtering ability and can bind bacteria, nanoparticles and apoptotic cells, the subcapsular sinus macrophages seem to be specialized in binding viruses and immune complexes (77). As compared to medullary macrophages, the subcapsular sinus macrophages are less endocytic and able to retain viral particles on their surface for at least several hours after capture (108, 161, 171, 192), through a yet not understood mechanism. Most of the *in vivo* studies on viral capture in mice have been perfomed using VSV, a rhabdovirus causing fatal paralytic disease in mammals. When VSV is captured by subcapsular sinus macrophages, the virus can readily replicate in these cells, something that was shown to be critical for host survival: the enforced viral replication at this site results in that the macrophages – before being killed by the cytopathic VSV – secrete large amounts of IFNα/β that establishes a local antiviral state, this preventing further viral replication, thereby protecting the host from central ascending nervous system paralysis and death (93, 148). There are also mechanisms attributed to subcapsular sinus macrophages that are not dependent on virus replication in these cells, that might affect viral pathogenesis. For instance the local accumulation of virus and increased antigen availability may promote adaptive immunity (87, 90) and it has also been described in a study that subcapsular sinus macrophages can translocate surface-bound viral particles across the subcapsular sinus floor (which is normally impermeable to particles larger than 4 nm, such as viruses (57)) and present them to migrating B cells in underlying follicles (108). In this study, it was demonstrated that after infection, virions were detectable at B cell-macrophage interfaces for at least 4 hours, and the authors suggest that particles probably reached the lymph node parenchyma by moving along the macrophage surface. Interestingly, while the above mentioned studies investigated the function of the Siglec-1+ subcapsular sinus macrophages to capture and retain virus particles, none of the studies attributed this function to the Siglec-1 receptor itself.

2 OBJECTIVES

2.1 OVERALL AIM OF THIS THESIS

The work presented in this thesis aimed to characterize the expression and function of cellular proteins working as modulators of retroviral infection. Investigating these cellular factors using primary cells and *ex vivo* tissue models could lead to a better understanding of the *in vivo* determinants of retrovirus transmission and viral spread.

2.2 PROJECT-SPECIFIC AIMS

2.2.1 *In vivo* expression profiling of CD317

CD317 was originally referred to as bone marrow stromal antigen 2 (BST-2) because it was found to be expressed by bone marrow stromal cell lines (96). Moreover, the protein has previously been described to be constitutively expressed by some human cancer cells, e.g. from breast cancers (22) and multiple myelomas, as well as by terminally differentiated B-cells (71). In mice, CD317 is a marker for pDC (16), but the protein has also been shown to be expressed by mouse plasma cells (188). However, most expression studies of the restriction factor have focused on IFN induction in cell lines or isolated primary T cells normally expressing no or low levels of CD317, trying to assess whether viral target cells have the ability to upregulate the protein after IFN treatment. Focusing on the antiviral activities of CD317, it is important to investigate expression of the restriction factor *in vivo,* since a broader knowledge about which cell types express the protein either constitutively or after induction would help to understand more about its antiviral potential under physiological conditions. Furthermore, considering that CD317 is suggested as a specific target for immunotherapy in B-cell malignancies (103), detailed knowledge of its full expression pattern is essential in order to avoid potential side effects. This project aims to address questions regarding *in vivo*-expression levels and tissue distribution of CD317 under physiological conditions.

2.2.2 Investigating the antiviral activity of SAMHD1 in resting T cells by flow cytometry

SAMHD1 was recently reported as a potent restriction factor that limits productive HIV-1 infection in monocytes and dendritic cells. Interestingly, CD4+ T cells in a resting state are largely refractory to HIV-1 infection and only become permissive upon activation (185, 214). The first aim therefore of my studies on SAMHD1 was to determine whether, in contrast to its proposed cell type-specific expression pattern, SAMHD1 is also expressed in resting CD4+ T cells. Furthermore, the focus was on deciphering the antiviral role of SAMHD1 in the T cell lineage using different experimental strategies including monitoring SAMHD1 levels during the course of an infection, and establishing a flow cytometry compatible protocol to investigate SAMHD1 *in vivo*-expression levels in specific cell types.

2.2.3 The role of murine Siglec-1+ macrophages in retroviral *trans*-infection

To investigate whether the ability of Siglec-1 to transfer virus to lymphocytes that get productively infected is common for retroviruses other than HIV-1, the aim of the third project was to explore the potential role of mouse Siglec-1 in modulating the infection of murine leukemia virus (MLV). An *ex vivo* co-culture system was established where wild-type or Siglec-1-/- bone marrow-derived macrophages (BMDM) are pulsed with virus and co-cultivated with mouse lymphocytes. In order to investigate which binding properties are necessary for viral transfer, dependency of the sialic acid N-acyl chain was tested by pretreatment of cells with sialic acid precursor analogs to biosythetically incorporate N-acyl-modified sialic acids in the virus producer cells, and consequently in the MLV membrane. This project aimed to contribute to a deeper understanding of the role of Siglec-1 in retroviral *trans*-infection and the determinants of virus-cell interaction, something that could be important for viral spread and pathogenesis *in vivo*.

3 MATERIAL AND METHODS

3.1 MATERIAL

3.1.1 Antibodies

Table 1. Primary antibodies used in this work.

Unconjugated Antibodies

Antibody	Species	Clone	Dilution (application)	Source
mAbα-CD3	rabbit IgG	SP7	1:200 (IF)	Neo Markers
mAbα-CD3	mouse IgG2a	PS1	1:500 (IF)	BioGenex
mAbα-CD4	mouse IgG1	IF6	1:25 (IF)	Invitrogen (Zymed)
mAbα-CD14	mouse IgG1	2Q1233	1:25 (Flow)	Abcam
mAb α-CD19	mouse IgG1	LE-CD19	1:100 (IF)	Acris
mAb α-CD21	mouse IgG1	1F8	1:50 (IF)	Dako
mAb α-CD23	mouse IgG1	1B12	1:10 (IF)	Neo Markers
mAb α-CD31	mouse IgG1	JC70A	1:25 (IF)	Dako
mAb α-CD66b	mouse IgG1	80H3	1:100 (IF)	Dianova
mAb α-CD68	mouse IgG3	PG-M1	1:100 (IF)	Dako
mAb α-CD138	mouse IgG1	MI15	1:25 (IF)	Dako
mAb α-DC-SIGN	mouse IgG1	AZN-D1	1:100 (IF)	Teunis Geijtenbeek
mAbα-CD303/BDCA2	mouse IgG1	124B3.13	1:50 (IF)	Dendritics
mAbα-D2-40	mouse IgG1	D2-40	1:50 (IF)	Dako
mAbα-CD106	mouse IgG1	51-10C9	1:50 (Flow)	BD Pharmingen
pAbα-sIgD	rabbit IgG		1:1500 (IF)	Dako
mAbα-HM1.24/CD317	mouse IgG2a	HM1.24	1:200 (IHC, IF); 1:400 (Flow)	Chugai Pharmaceuticals
mAbα-CD317/BST2	mouse IgG1	26F8	1:50 (IHC)	eBioscience
pAb α-BST-2/CD317	rabbit IgG		1:5000 (WB)	Klaus Strebel
pAb α-SAMHD1	rabbit IgG		1:100 (IHC, FACS)	Proteintech Europe
pAbα-TRIM5α	rabbit IgG		1:400 (IHC)	LifeSpan Biosciences
pAbα-TRIM5γ	rabbit IgG		1:400 (IHC)	LifeSpan Biosciences
pAbα-MXA	rabbit IgG	#166	1:500 (IHC, WB)	Otto Haller, Georg Kochs
mAbα-MXA	mouse IgG2a	M143	1:1000 (WB)	Otto Haller, Georg Kochs
pAbα-MLV p30	rat IgG	R187	1:50 (Flow)	Sarah S, AG Keppler (Hybridoma from Carol Stocking, via Jens Bohne)
pAbα-ERK 2	rabbit IgG		1:1000 (WB)	Santa Cruz Biotechnology
mAbα-mSiglec1	rat IgG2a		1:100 (blocking, IF)	Aviva Systems Biology

Conjugated Antibodies

Antibody	Species	Conjugate	Dilution	Source
α-CD3	Mouse	PE	1:20 (IF, Flow)	BD Biosciences
α-CD4	Mouse	PE	1:20 (Flow)	BD Biosciences
α-CD14	Mouse	PE	1:20 (IF, Flow)	BD Biosciences
α-CD19	Mouse	PE	1:20 (IF, Flow)	BD Biosciences
α-CD138	Mouse	PE	1:20 (Flow)	Miltenyi Biotech

α-BDCA2	Mouse	FITC	1:50 (Flow)	Miltenyi Biotech
α-mCD3	rat	APC	1:20 (Flow)	BD Biosciences
α-mCD19	rat	PE	1:20 (Flow)	BD Biosciences
α-mCD169	rat	PE	1:40 (Flow)	eBiosciences
α-mCD169	rat	Alexa 647	1:100 (IF)	Aviva Systems Biology, Invitrogen

Table 2. Secondary antibodies and detection conjugates used in this work.

Antibody/Reagent	**Species**	**Conjugate**	**Dilution**	**Source**
α-mouse IgG	donkey	Biotin	1:100 (IHC, IF)	Amersham
α-mouse IgG	sheep	Biotin	1:100 (IHC, IF)	Amersham
α-mouse IgG1	donkey	Cy2	1:50 (IF)	Jackson ImmunoResearch
α-rabbit IgG	donkey	Biotin	1:200 (IHC, IF)	Jackson ImmunoResearch
α-rabbit IgG	donkey		1:200 (IHC, IF)	Jackson ImmunoResearch
α-rabbit	goat	Alexa 660	1:200 (Flow, IF)	Invitrogen
α-rabbit	goat	Alexa 488	1:500 (IF)	Invitrogen
α-goat	donkey	Alexa 488	1:500 (IF)	Invitrogen
α-mouse	goat	Alexa 488	1:500 (IF)	Invitrogen
α-rat	donkey	Alexa 488	1:200 (Flow)	Invitrogen
Streptavidin		Cy3	1:1000 (IF)	Jackson ImmunoResearch
Streptavidin		Cy2	1:50 (IF)	Jackson ImmunoResearch
α-mouse IgG2a	goat		1:100 (IHC, IF)	Southern Biotech
α-mouse IgG1	rabbit	biotin	1:100 (IHC, IF)	Zymed
α-mouse IgG2a	rabbit	biotin	1:70 (IHC, IF)	Zymed
α-mouse IgG3	sheep		1:100 (IHC, IF)	Serotec
α-mouse IgG1	sheep		1:250 (IHC, IF)	Binding Site
α-mouse IgG2b	sheep		1:500 (IHC, IF)	Binding Site
α-rabbit IgG	goat	Biotin	1:200 (IHC, IF)	Jackson ImmunoResearch
α-mouse	goat	Atto 633	1:500 (IF)	Sigma-Aldrich
α-sheep	donkey	Cy2	1:50 (IF)	Jackson ImmunoResearch
α-sheep	donkey	Cy3	1:800 (IF)	Jackson ImmunoResearch

Flow, flow cytometry; IF, immunofuorescence; IHC, immunohistochemistry; WB, western blot

3.1.2 Kits

Table 3. Kits used in this work.

Name	**Source**
ABC-AP Kit	Vector Laboratories
Alexa Fluor Antibody Labeling Kit	Invitrogen
CD4 T cell isolation Kit (untouched)	Miltenyi Biotec
BDCA4 Microbead Kit	Miltenyi Biotec
Cytofix/ Cytoperm Kit	Beckton Dickinson

DNeasy Blood&Tissue Kit	Qiagen
Human/ mouse T cell Nucleofection Kit AMAXA	Lonza
Nucleobond Maxi prep Kit PC500	Macherey-Nagel

3.1.3 Chemicals and consumables

Table 4. Chemicals and consumables.

Name	**Source**
Acrylamide bis aqueous solution/Rotiphorese Gel 40	Roth
Ammoniumpersulfate (APS)	Roth
Ampicillin	Roth
AutoMACS column	Miltenyi Biotec
Blotting paper (Whatman 3MM)	Schleicher & Schuell
Bovine serum albumin (BSA), fraction V	Roth
Bovine serum albumin (BSA)-c	Aurion
BD Phosflow™ Fix Buffer I	BD Biosciences
BD Phosflow™ Perm Buffer III	BD Biosciences
Calcium chloride	Merck
p-Coumaric acid	Sigma-Aldrich
Cell strainer (40 µm/ 100 µm) nylon	BD Falcon
Cell culture consumables (flasks, plates, dishes)	BD Falcon
Citrate buffer (pH 6.1/9.0)	Dako
Citrate buffer pH 9 (Concentrate)	Dako
Coverslips 12 mm	Marienfeld
Di-methylsulfoxid (DMSO)	Merck
Di-potassiumhydrogenphosphate (K2HPO4)	Roth
Di-sodiumhydrogenphosphate (Na2HPO4)	Roth
EBSS (Earle`s balanced salt solution) 10x	Sigma-Aldrich
EBSS (Earle`s balanced salt solution) 10x	Gibco
ELISA plates Maxi sorb (96 well)	Nunc
Ethanol ROTIPURAN® ≥99,8 %, p.a.	Roth
Ethidium bromide	Merck
Fetal calf serum (FCS)	Biochrom
Ficoll	Biochrom
Fungizone	Invitrogen
Glycine	Roth
Hematoxylin	Sigma-Aldrich
Hematoxylin, Mayer's	Dako
Hoechst staining dye	Invitrogen
Human AB serum (Lot: 27240 #34005100)	Invitrogen
Hydrogen peroxide (H2O2)	Merck
Isopropanol	Sigma-Aldrich
Interferon α (6,000 IU/µl)	Roche
Interleukin 2 (IL2) human recombinant	Biomol
Interleukin 3 (IL3) human recombinant	Invitrogen

Immun-Blot® PVDF Membrane	Bio Rad
Kanamycin	Roth
Levamisol	Sigma-Aldrich
Luminol	Sigma-Aldrich
Lipopolysaccharides from *Escherichia coli* (LPS)	Sigma-Aldrich
β-Mercaptoethanol	Sigma-Aldrich
Midori Green DNA dye	Nippon Genetics
Milk powder	Roth
Mini-PROTEAN® TGX™ Precast Gels	Bio Rad
Harleco Mounting medium (Aquatex®)	Voigt Global Distribution
Fluoroshield™ with DAPI (histology mounting medium)	Dako
Mowiol	Calbiochem
N-actetyl-D-mannosamine	Sigma-Aldrich
N-actetyl-D-mannosamine	Werner Reutter
N-butanoyl-D-mannosamine	Werner Reutter
N-cyclopropylcarbamyl-D-mannosamine	Werner Reutter
N-isobutanoyl-D-mannosamine	Werner Reutter
N-pentanoyl-D-mannosamine	Werner Reutter
N-propanoyl-D-mannosamine	Werner Reutter
New Fuchsin	Sigma-Aldrich
Nitrocellulose membrane, Whatman	GE Healthcare
Non-essential amino acids, solution (100x)	Invitrogen
Paraformaldehyd (PFA)	Roth
Pancoll human density 1,077 g/l	PanBiotech
Biocoll	Biochrom
Penicillin/ Streptomycin	Sigma-Aldrich
peracetylated N-actetyl-D-mannosamine	Werner Reutter
peracetylated N-glycolyl-D-mannosamine	Ronald L Schnaar
peracetylated N-propanoyl-D-mannosamine	Werner Reutter
Lectin from *Phaseolus vulgaris* (PHA)	Sigma-Aldrich
Phorbol-12-Myristate-13-Acetate (PMA)	Merck
Poly-L-Lysin	Sigma-Aldrich
Potassiumchloride (KCl)	Merck
Potassium-di-hydrogenphosphate (KH2PO4)	Roth
Saponin	Roth
Saponin	Sigma-Aldrich
Sodium chloride	Sigma-Aldrich
Sodium dodecyl sulfate (SDS)	Serva Electrophoresis
Sodium pyruvate solution (100x)	Invitrogen
Sucrose	Sigma-Aldrich
Reagent reservoirs	Thermo Scientific
Target Retrieval Solution (Concentrate)	Dako
TaqMan Universal Master Mix; #4304437	Applied Biosystems
TEMED (N, N, N, N-Tetramethylethylendiamin)	Roth
Tris (Trishydroxymethylaminomethan)	Roth
Triton X-100	Pharmacia Biotech
Trypsin-EDTA (0.25%)	Biochrom

Trypan blue	Invitrogen
V-bottom plates	Corning
Vitamins solution (100x)	Invitrogen
X-ray films, CL-Xposure clear blue	Thermo Scientific
Xylene (isomers) >98 %, pure, for histology	Roth

3.1.4 Laboratory equipment

Table 5. Laboratory equipment.

Name	**Source**
Balance Ohaus Explorer	Ohaus, Nänikon
Blotter Fastblot B43/ B44	Biometra
Centrifuge Biofuge fresco	Heraeus
Centrifuge HERAEUS Megafuge 40R	Thermo-Scientific
Electrophoresis chamber Mini-PROTEAN® Tetra Cell	Bio Rad
ELISA reader multiscan EX	Thermo-Labsystems
Flow cytometer FACSCalibur	Beckton Dickinson
Flow cytometer FACSCanto	Beckton Dickinson
Flow cytometer FACSVerse	Beckton Dickinson
Fluorescence microscope IX70	Olympus
Fluorescence microscope Eclipse Ti-S	Nikon
Incubator HERAcell 150i	Thermo-Labsystems
LSM510 confocal microscope	Zeiss
MagNA pure LC nucleic acid extractor	Roche
Nanophotometer Pearl	Implen
Spectrophotometer GENESYS 10S UV-VIS	Thermo-Labsystems
Nucleofection device AMAXA	Lonza
Pipettes Biopette A	Labnet
PIPETBOY® acu Pipet Aid	INTEGRA Biosciences
Polyacrylamide Gel Elektrophoresis (Minigel)	Biometra
Power supply PowerPac™ Basic Power Supply	Bio Rad
Shaking incubator HT	Infors
Sterile hood SterilGard III Advance	The Baker Company
Sterile hood MSC-Advantage	Thermo-Scientific
Table centrifuge Multifuge 3S-R	Heraeus
Table centrifuge MicroSTAR	Thermo-Scientific
Trans-Blot® Turbo™ Transfer System	Bio Rad

3.1.5 Buffers and solutions

Table 6. Buffers and solutions recipes.

Blocking and antibody dilution buffer for fluorescence microscopy	
PBS 1x	
FCS	5 % (v/v)
BSA-c	0.1 % (v/v)
Horse serum	2-10 % (v/v)
Calcium chloride (CaCl2) 10x	
$CaCl_2$	2.5 mM
in H_2O	
sterile filtration	
EBSS washing buffer	
10x EBSS (Earle`s balanced salt solution)	100 mL
Hepes (1 M)	10 mL
add dH_2O	1 L
adjust to pH pH 7.4	
BSA (0.2%)	2 mL
EBSS saponin buffer	
EBSS washing buffer	
Saponin	0.1% (w/v)
Flow-stain buffer	
PBS 1x	
FCS	2 % (v/v)
HBS buffer (2x)	
NaCl	280 mM
Hepes	50 mM
Na_2HPO_4 x $2H_2O$	1.5 mM
in H_2O	
pH 7.1	
MACS running buffer	
PBS 1x	
Bovine serum albumin (BSA)	0.5% (w/v)
EDTA	2 mM
pH 7.2	
Orange G loading dye (5x)	
Orange G	20 mg
Sucrose	2 g
dH_2O	5 mL
10x PBS (Phosphate-buffered saline)	
NaCl	96 mM
Na_2HPO_4 x $2H_2O$	10 mM
$Na_2H_2PO_4$ x H_2O	2.3 mM
in H_2O	
pH 7.4	
PBS-Tween buffer	
PBS 1x	
Tween-20	0.1 % (v/v)
Paraformaldehyde (PFA) 4%	
Paraformaldehyde	4 % (w/v)
in 1x PBS	
pH 7.2	
SDS-PAGE sample buffer (2x)	
Tris/HCl pH 6.8	130 mM

SDS	6 % (w/v)
Glycerol	10 % (v/v)
β-Mercatoethanol	10 % (v/v)
Bromphenole blue	tip of spatula

SDS-PAGE running buffer

Tris/HCl	250 mM
SDS	0.1 % (w/v)
Glycin	200 mM

SDS-PAGE low separating gel buffer

Tris/HCl pH 8.0	1.88 M

SDS-PAGE stacking gel buffer

Tris/HCl pH 6.8	0.65 M

SG-PERT buffers

Preparation and storage of SG-PERT assay buffers: see Pizzato et al. 2009

TBS (Tris-buffered saline)

Tris	50 mM
NaCl	150 mM

Tris-EDTA (TE) buffer

Tris	10 mM
pH 8.0	
EDTA	1 mM

Tris-acetate-EDTA (TAE) buffer 50x

Tris	2 M
Acetic acid	2 M
EDTA	50 mM
pH 8.3	

Western Blot transfer buffer

Tris/HCl pH 8.8	25 mM
Glycin	192 mM
Methanol	20 % (v/v)
SDS	0.05 % (w/v)

3.1.6 Drugs and inhibitors

Table 7. Drugs and inhibitors used in this work.

Name	**Source**
ALLN	Calbiochem
Azidothymidine (AZT)	Sigma-Aldrich
Bafilomycin A1	Sigma-Aldrich
Brefeldin A	Sigma-Aldrich
Chloroquine	Sigma-Aldrich
Efavirenz (EFV), Sustiva 30 mg/ml	Bristol-Myers Squibb
Human interferon alpha	Roche
Murine interferon alpha	Pbl Interferon Source
Z-Leu-Leu-Leu-al (MG132)	Sigma-Aldrich

3.1.7 Markers and standards

Table 8. DNA and protein markers/standards used in this work.

Name	**Source**
DNA Smart Ladder	Eurogentec
Spectra™ Multicolor Broad Range Protein Ladder	MBI-Fermentas
Precision Plus Protein™ All Blue Standards	Bio Rad

3.1.8 Media

Table 9. Media for bacteria.

Lysogeny broth (LB) medium and agar	
NaCl	5 g/L
Yeast extract	5 g/L
Tryptone	10 g/L
add H_2O	
pH 7.2	
for plating: add Agar agar	12.5 g/L
Autoclave	
antibiotics were added to a final concentration of 0.1 mg/mL	

Terrific broth (TB) medium	
Yeast extract	24 g
Tryptone	12 g
Glycerol	4 mL
dH_2O	add 900 mL
autoclave and cool down to < 60°C, then mix with sterile:	
KH_2PO_4	2.31 g
K_2HPO_4	12.5 g
dH_2O	add 100 mL
antibiotics were added to a final concentration of 0.1 mg/mL	

Table 10. Media for eukaryote cells

Media for cell culture	
RPMI 1640+ GlutaMAX or DMEM high (4500 mg/l glucose) (Gibco) complemented with:	
FCS (heat inactivated)	10 % (v/v)
Penicillin	50 U/ml
Streptomycin	50 µg/ml

Human lymphoid aggregate culture (HLAC) medium	
RPMI 1640+ GlutaMAX complemented with	
FCS (heat inactivated)	15 % (v/v)

Fungizone	1 % (v/v)
Penicillin	50 U/ml
Streptomycin	50 µg/ml
Non-essential amino acids	1 % (v/v)
Sodium pyruvate	1 % (v/v)

Freezing medium

DMEM high (4500 mg/l glucose) complemented with	
FCS (heat-inactivated)	30 % (v/v)
DMSO	10 % (v/v)

Generation of L929 supernatant

Thaw and expand L929 cells for a week in RPMI (+FCS, +Penicillin/Streptomycin)

After one week: start collecting supernatant (collect at least 1 liter in total)

During collection: Split cells 1:2 every second day and havest supernatant

Discard cells after 4 weeks

Sterile filter collected supernatant (0.22 µM)

Titer activity and determine BMDM purity by flow cytometry

3.1.9 Bacterial strains

Table 11. Bacterial strains used in this work.

Strain	**Characteristics**	**Genotype**	**Utilized for**
Stable II (*E.coli*)	High transformation efficiencies; low recombination rates	F- mcrA Δ(mcrBChsdRMSmrr) recA1 endA1 lon gyrA 96 thi supE44 relA1 λ-Δ(lac-proAB)	Proviral plasmid transformation and amplification

3.1.10 Cell lines

Table 12. Cell lines used in this work.

Name	**Characteristics/ phenotype**	**Medium**
293T	Human embryonic kidney cell line expressing the large T antigen of SV40 (Pear et al., 1993); ATCC no.: CRL-11268	DMEM
ANA-1	Established from bone marrow cells of C57BL/6 (H-2b) mice (Blasi et al., 1985)	RPMI1640
Jurkat	Human T lymphocyte cell line derived from an acute T cell leukemia; ATCC no.: TIB-152	RPMI1640
L929	NCTC clone 929, subcutaneous areolar and adipose tissue of a 100-day-old male C3H/An mouse, secrete M-CSF	RPMI1640
S1A.TB	Balb/c strain derived mouse T lymphocyte cell line. Derived from the S1A lymphoma. ATCC No.: TIB-27	DMEM
TZM-bl	HeLa-derived indicator cell line (Wei et al., 2002)	DMEM

3.1.11 Plasmids

Table 13. Plasmids used in this work.

Plasmid name	**Reference**	**Received from/ Generated by**
pMoMLV-GFP	Diss. Volker Herrmann, Goffinet et al., 2007	H.-G. Kräusslich
FL-MLV-GagGFP pLRB303	Jin et al., 2011	W. Mothes

3.1.12 Primers

Table 14. Primers used for genotyping of wild-type and Siglec-1 knockout mice.

Name	**Sequence**
Neo	CGTTGGCTACCCGTGATATTGC
SND1F3	CACCACGGTCACTGTGACAA
SND2R2	GGCCATATGTAGGGTCGTCT

3.1.13 Computer software

Table 15. Computer software used in this work.

Software	**Source**
Accelrys Draw 4.2	Biovia
Adobe Illustrator CS6	Adobe
Adobe Photoshop CS6	Adobe
Aperio ImageScope software	Leica Biosystems
Ascent Software 2.6	Thermo Labsystems
CellquestPro	Beckton Dickinson
Endnote X5	ISI Research software
FACS SUITE software	Beckton Dickinson
FlowJo X	Tree Star, Inc.
LSM5 software	Zeiss
Microsoft Office 2010	Microsoft Cor.
Odyssey 2.1	Li-cor Biosciences
GraphPad Prism version 6.00 for Windows	GraphPad software
Image Lab software	Bio Rad
Bio Rad CFX Manager Software	Bio Rad
Nikon NIS Elements software	Nikon

3.2 METHODS

3.2.1 Molecular biology

3.2.1.1 Transformation of bacteria

25 µl of competent bacteria (Stable II cells) were transformed by addition of 1 µg plasmid DNA. After 20 minutes of incubation on ice, bacteria were subjected to heat shock at 42 °C for 1 minute and then cooled down on ice for 2 minutes. After 30 minutes to 1 hour incubation in 1 ml LB-medium at 37 °C, bacteria were plated on LB-agar plates containing ampicillin overnight at 37 °C.

3.2.1.2 Large scale DNA preparation "maxi-prep"

200 mL of overnight-cultured *E. coli* was pelleted by centrifugation (10 min, 4000 rpm, 4°C) and plasmid DNA was then isolated and purified according to the principle of anion exchange chromatography, using the NucleoBond MaxiPrep PC500 kit (Macherey Nagel) according to the manufacturer's description. Plasmid DNA was then precipitated with isopropanol and washed with 70% EtOH. Finally, DNA pellets were resuspended in 100-200 µl TE buffer.

3.2.1.3 Quantification of DNA using spectrophotometry

DNA concentrations were measured by UV-absorption spectrophotometry at a wavelength of 260 nm. Since the absorption is highest for proteins at 280 nm, the ratio of absorbance at 260 and 280 nm (A260/A280) can be used as an indicator of nucleic acid purity. This ratio will hence be reduced the more contaminating protein the sample contains. DNA was considered as pure at A260/A280 ratios ranging between 1.8 and 2.0. DNA solutions were generally adjusted to a concentration of 1 µg/µl and stored at -20°C or at 4°C.

3.2.1.4 Agarose gel electrophoresis

DNA fragments can be separated according to their size by agarose gel electrophoresis. For gel preparation, the agarose (1-2%) was dissolved in 1xTAE buffer by boiling for 2-5 minutes. After cooling down to below 60°C, the DNA dye Midori Green (Nippon Genetics) was added to the gel mix. Typically, before loading samples onto a gel, 20 µl DNA solution was mixed with 5 µl 5x Orange G loading dye. Samples were then loaded into the pockets of the gel that was placed in 1xTAE running buffer. Standard running conditions for a gel of the size 10x10 cm was 80 – 100 V. For size determination of DNA fragments, the DNA molecular weight marker "SmartLadder" (Eurogentec) was used. DNA band patterns were detected and documented by a BioRad ChemiDoc device equipped with UV- light (302 nm).

3.2.1.5 Genotyping of wild-type and Siglec-1 -/- mice

DNA was prepared from tail cuts of newborn or infant (up to 3 weeks) mice using the DNeasy blood and tissue kit (Qiagen) according to manufacturer's protocol for rodent tails. Following DNA extraction, a PCR reaction (3.2.1.6) was performed in order to amplify the DNA regions of interest.

3.2.1.6 Polymerase chain reaction (PCR)

For selective amplification of fragments from genomic mouse tail DNA, Taq polymerase was used according to the manufacturer's protocol. PCR reactions were carried out in a final volume of 50 µl and contained the following components: autoclaved MilliQ water, x10 NEB buffer, 1.5 mM MgCl2, 0.2 mM dNTPs, 1 µM of each sense and antisense primer, 0.025 U/µl NEB Taq and 1µl of the extracted template DNA. Amplification was performed using an Eppendorf thermocycler with the following settings:

1. 95°C: 2 min
2. 95°C: 30 sec (denaturation)
3. 55°C: 30 sec (annealing)
4. 72°C: 45 sec (elongation)
5. Step 2 – 4 repeat x29
6. 72°C: 5 min

PCR products were separated and visualized by agarose gel electrophoresis.

3.2.2 Cell biology

3.2.2.1 Culturing and passaging of eukaryotic cell lines

Cells were grown either in suspension or as monolayer cultures in culture flasks or on cell culture dishes in DMEM or RPMI (Gibco) complemented with supplements indicated in table 10. All cells were grown at 37°C, in 5% CO2 and 95% relative humidity in an incubator. Passaging was routinely performed 1-3 times a week (depending on the growth rate and confluence of the cell line) at a split ratio of 1:3 to 1:10. For adherent cells, the culture medium was aspirated and cells were rinsed once with sterile PBS. Cells were then incubated with a small volume of trypsin-EDTA for 5-10 minutes at room temperature or at 37°C. Medium containing FCS was used to resuspend dislodged cells, and a fraction of the cell suspension was transferred to a fresh cell culture flask or plate. Non-adherent suspension cells were generally cultivated at a density around $5x10^5$ cells/mL, in cell culture flasks standing in an upright position.

3.2.2.2 Long-term storage and thawing of cells

For long-term storage, cells were cryo-preserved in liquid nitrogen. Around $1x10^7$ cells were pelleted by centrifugation and resuspended in 500 µl freezing medium in cryotubes (Nunc). Cells were first

frozen and stored for 24 hours at -80 °C, before transfer to liquid nitrogen. For thawing, an aliquot of cells was thawed rapidly, washed once in cell cultivation medium and resuspended in an appropriate volume of fresh medium.

3.2.2.3 Human peripheral blood

Fresh human blood was obtained from healthy donors with informed consent and was approved by the Local Ethics committee of the Medical Faculty of the University of Heidelberg (approval no. 157/2006). Peripheral mononuclear cells (PBMC) were separated from whole blood by density gradient centrifugation (Biocoll, Biochrom). For lymphocyte and T cell cultures, cells were maintained in complete RPMI, at a density of $2x10^6$ cells/mL. In case of T cell activation, PHA-P (5 µg/mL) or PHA-L (2 µg/mL) (both from Sigma-Aldrich) were added to the culture medium for 2-3 days together with IL-2 (20 or 100 IU/mL) (Biomol).

3.2.2.4 Human tonsil tissue

Fresh tonsil tissue was obtained from routine tonsillectomies performed at the department of Otolaryngology, Head and Neck Surgery, University of Heidelberg. The use of anonymous surgical waste was approved by Heidelberg University's ethics committee (approval no. 077/2005). Immediately after tonsillectomy, tonsils were cut in 1-3 mm pieces and gently passed through a 100 µm cell strainer (BD) into a cell culture dish filled with HLAC medium. Cells were separated on a Ficoll gradient. Lymphocytes were collected and washed twice in PBS and thereafter either stained for analysis by flow cytometry or cultivated in 96-well round-bottom plates, seeded at $1x10^6$ cells per well in 200 µl of HLAC medium.

3.2.2.5 Primary mouse cells

Bone marrow derived macrophages (BMDM) were prepared from C57BL/6 mice. After sacrifice using CO_2, femur and tibia were extracted and bone marrow cells collected by centrifugation. Cells were seeded in a 15 cm tissue-culture dish containing complete RPMI and incubated at 37°C over-night. The following day, suspension cells were pelleted, resuspended and counted. $10x10^6$ cells per 10 cm bacterial petri dish were then seeded in L929-containing BMDM-differentiation medium. 3 days later, L929 supernatant was added to the cultures. Cells were typically harvested and reseeded for experiments 6 days after preparation. For some experiments, IFNα (pbl Interferon source) was added, either to the differentiation cultures at day 4 of differentiation or at day 6 when reseeding the cells for an experiment.

Spleen and lymph nodes were collected from euthanized C57BL/6 mice. Organs were collected in cold RPMI and gently passed through a 100 µm cell strainer. Cell suspensions were then washed once in PBS, resuspended in complete RPMI, counted and seeded either in a tissue-culture flask or plate for the appropriate volume. Cells were typically seeded at a density of $2\text{-}5x10^6$ cells/mL. In case of B- or

T cell activation 7.5 µg/mL LPS (Sigma-Aldrich) or 10 nM phorbol myristate acetate (PMA, Calbiochem) respectively, was added to the cultures.

3.2.3 Virological methods

3.2.3.1 Calcium phosphate precipitation for MLV production

293T cells were transfected by calcium phosphate precipitation. For virus production 4-6x10^6 cells were seeded in a 15 cm dish the day before transfection. 40-70 µg DNA was used per dish. DNA was mixed with H_2O (Braun) and then 0.1 mL $CaCl_2$ was added to the mixture. After vortexing, 1 mL HBS buffer was added dropwise. The solution was vortexed again and then incubated at room temperature before dropwise addition to the 293T cells seeded the day before. Medium was exchanged 4-6 hours post transfection and around 40 hours later, supernatants were collected and used for concentration and purification.

3.2.3.2 Production of MLV under treatment with ManN-analogs

293T cells were seeded for virus production in the presence or absence of ManN analogs at sub-toxic concentrations (5 mM ManNAc, -Prop, -But, -iBut, -Pent, -Cyclo or 0.3 mM peracetylated (–PA) ManNGc, -Ac, -Prop). After 5 days, cells were re-seeded and transfected with MLV-GFP plasmid using the calcium phosphate precipitation method (3.2.3.1). 4-6 hours post transfection the medium was changed and new ManN analogs added. 48 hours post transfection, MLV particles were harvested by ultracentrifugation through a 20% sucrose cushion. After freezing at -80°C, viral titers were determined by direct infection of S1A.TB cells.

3.2.3.3 Determination of viral infectivity

The infectivity of MLV-GFP stocks encoding a gene for GFP expression was generally analyzed by flow cytometry. Thus, the cell line S1AT.B (which was typically used as MLV target cells in the experiments in this thesis) was infected with serial dilutions of the generated virus stocks and incubated for 48 hours. Cells were then analyzed by flow cytometry for GFP expression. The infectious titer (IU/ml) of the respective virus stock was calculated using the percentage of GFP-positive cells.

3.2.3.4 MLV capture and transfer assays

To assess Siglec1-dependent MLV transfer from macrophages to lymphocytes, L929-differentiated BMDM were exposed to – i.e. pulsed with – MLV-GFP for 4 hours at 37°C, and then washed extensively in PBS (in case of antibody blocking, BMDM were treated with 10 µg/mL anti-mSiglec1 or isotype control antibody for 30 minutes at 4°C before virus pulse). The mouse T cell line S1A.TB was then added and co-cultured with the macrophages for 48 hours. T cells were harvested and analyzed for GFP-expression on a flow cytometer. MLV capture experiments were performed

acording to the description above, with the difference that the pulsed BMDM were harvested immediately after the extensive post pulse wash. BMDM from MLV capture assay were either subjected to flow cytometry or to RT-PCR.

3.2.3.5 SYBR Green-based Product Enhanced Reverse Transcriptase (SG-PERT) assay

SG-Pert is an assay for quantitation of retroviruses in cell culture supernatants and has been described by M. Pizzato and colleagues (162). Briefly, the enzymatic activity of Reverse Transcriptase (RT), present in all retroviruses, is measured using an RNA template derived from the bacteriophage MS2, which is reverse transcribed *in vitro* by the retroviral enzyme. The resulting DNA product (cDNA) is then amplified by PCR and quantified using the signal obtained from the intercalating fluorescent dye SYBRGreen, as a measure of the amount of virions present in the sample. The linear logarithmic relationship between virus concentration and CQ (crossing point) value, where an increase in virus concentration of 1 log corresponds to a difference of 3.3 in CQ values, is described by Pizzato et al (162).

In short, the reaction was carried out as follows: 10 µl of the diluted cell/virus lysate samples were mixed immediately with 10 µl of 2× reaction mix already aliquoted into a white shell clear well plate with a seal (BioRad). The plate was briefly centrifuged to sediment the reaction components and then applied to the BioRad real-time platform. Thermal cycler conditions used were: 20 minutes RT reaction at 42°C, 2 minutes hot-start Taq activation at 95°C and 40 cycles of amplification. Each amplification cycle was composed of 5 seconds denaturation at 95°C, 5 seconds annealing at 60°C, 15 seconds of elongation at 72°C and 7 seconds of acquisition at 80°C.

Biological triplicate samples were run in technical triplicates (in total 3x3 replicates). The relative RT activity was calculated by normalizing samples to the positive control sample within each data set.

3.2.4 Standard laboratory methods

3.2.4.1 Flow Cytometry

For all flow cytometry experiments, at least $2x10^5$ cells/sample were used. For GFP readout, cells were washed once in PBS, followed by flow cytometric analysis (FACS Calibur or FACS Verse, BD Bioscience). Data was analyzed with FlowJo software (TreeStar). Cells were gated on forward scatter / side scatter characteristics. For surface antigen labeling, cells were transferred to a 96-well V-bottom plate, washed once in flow-stain buffer and incubated with primary antibodies or directly labeled antibodies diluted in flow-stain buffer for 30 minutes at 4°C. Washing was followed by flow cytometric analysis. For intracellular labeling, cells were surface labelled, fixed, permeabilized and stained either according to the BD Cytofix/Cytoperm protocol or to the BD Phosflow protocol for staining of nuclear antigens.

3.2.4.2 Immunofluorescence and microscopy of adherent or suspension cells

Adherent cells were seeded onto glass coverslips (12 mm) one day before the experiment (e.g. virus pulse), while suspension cells were seeded on coverslips that were either coated with Poly-L-lysine or left uncoated, for 20-30 minutes at 37°C. Prior to staining, cells were fixed in 4% paraformaldehyde (PFA) for 15-30 minutes, permeabilized either with 0.1% Triton X-100/PBS for 2-4 minutes (BMDM) or with PBS supplemented with 0.5% saponin (Sigma-Aldrich). Cells were then blocked for 20 minutes in PBS containing 5% FCS, 0.1% BSA-c (Aurion), and 2-10% horse serum (Sigma-Aldrich). Cells were incubated with primary antibodies diluted in blocking buffer for 60 minutes at room temperature, then fluorescently conjugated secondary antibodies for 60 minutes, with washes in blocking buffer in between. Coverslips were mounted onto glass slides using DAPI mounting medium (Sigma). Epifluorescence images were taken on an inverted Nikon eclipse Ti-S microscope using the Nikon software program, on an Olympus IX71 inverted microscope and confocal images on a Leica SP5. The final presented images were prepared using ImageJ or/and Adobe Photoshop CS5.

3.2.4.3 Real-Time Polymerase chain reaction (RT-PCR)

To normalize the data obtained with the SG-PERT assay for cell numbers, a quantitative PCR of genomic DNA was performed, using a probe for the murine GAPDH housekeeping gene. After DNA extraction from BMDM cell pellets using an automated MagNAPure LC nucleic acid extraction instrument (Roche), a commercial 20x mix containing primers and probe (6-carboxyfluorescein (FAM)- labelled) was used to detect GAPDH DNA. After preparation of a master mix containing (per sample) 1.25 µl commercial GAPDH mix, 8.75 µl H_2O and 12.5 µl TaqMan Mix, this mix was aliquoted into an optical plastic 96-well microtiter plate (Applied Biosciences) in a volume of 22.5 µl/sample. 2.5 µl of sample DNA was then added to each well.

The PCR was performed at an ABI7500 under the following conditions:

1. 50°C: 2 min
2. 95°C: 10 min
3. 95°C: 15 sec (denaturation)
4. 60°C: 1 min (annealing)
5. Step 1 – 4 repeat x39

Data was analyzed using the ABI7500 v.2.0.1 software.

3.2.4.4 SDS-Polyacrylamide-Gel electrophoresis (SDS-PAGE)

For protein analysis, samples were mixed with 2x SDS-PAGE sample buffer and denaturated at 95°C for 5 minutes and loaded onto precast 10-12% polyacrylamide gels (BioRad). Gels were typically run at 80 mA per gel for around 30 minutes. For estimation of the molecular weight of the samples, a

prestained protein marker was used as reference. Proteins were then further processed for western-blot analysis.

3.2.4.5 Immunoblot analysis

After separation by SDS-PAGE, proteins were electro-transferred onto polyvinylidene difluorid (PVD) membranes. After 30 minutes membrane blocking in 5% non-fat milk, membranes were incubated with primary antibodies diluted in a 2% BSA/TBS buffer over-night at 4°C. After extensive washing in TBS, secondary horse radish peroxidase-conjugated antibodies were added and incubated with the membranes for 1 hour at room temperature. Membranes were developed using the Clarity western ECL development kit (BioRad) and chemiluminescent bands were visualized and documented with a BioRad ChemiDoc device.

3.2.4.6 Immunohistochemistry and microscopy of tissue sections and tissue micro array (TMA)

Paraffin-embedded tissue sections, anonymously obtained from routine diagnostics (Institute for Pathology Heidelberg and the Senckenberg Institute of Pathology, Frankfurt), were immunohistochemically stained according to the following description: After deparaffinization in xylene (2 x 5 minutes), and hydration in ethanol (100% 2 x 5 minutes, 96% 3 minutes, 70% 3 minutes), sections were first rinsed in dH_2O and then steam cooked for antigen retrieval in pre-heated 10 mM citrate buffer (pH 6.1, DAKO) for 30 minutes. Slides were then removed from the steamer and cooled down on ice for 15-30 minutes. After washing slides in dH_2O (2 x 2 minutes) and in a pH 7.4 washing buffer containing H_2O with 10% Earle's balanced salt solution, 1% Hepes and 0.2% bovine serum albumin (EBSS/H/BSA) (3 x 2 minutes), sections were permeabilized for 15 minutes in EBSS/H/BSA washing buffer with 0.1% saponin added (EBSS/H/BSA/SAPONIN). Tissue sections were then incubated with a total volume of 100 µl/slide of primary antibody solutions (antibody dilutions were prepared in EBSS/H/BSA/SAPONIN buffer) at room temperature for one hour and then overnight at 4°C. The following day, sections were washed in EBSS/H/BSA/SAPONIN (3 x 2 minutes) and blocked by incubation for 20 minutes at room temperature with sheep or donkey serum (dilution 1:6), depending on which species the secondary antibody was from. A secondary, biotinylated antibody (also diluted in EBSS/H/BSA/SAPONIN buffer) was then added, and after incubation for 30 minutes at room temperature, tissue secions were washed three times and incubated with an avidin-biotin alkaline phosphatase solution (ABC-AP-kit) (Vectastain) for 30 minutes. Finally, slides were washed three times in EBSS/H/BSA/SAPONIN, twice in EBSS/H/BSA and another two times in TBS and thereafter developed with New Fuchsin (Sigma) in the presence of levamisole (Sigma) for 1-20 minutes. The reaction was judged by eye and stopped with tap water. Slides were mounted with Harleco Aquatex mounting medium and analyzed with an Olympus BX45 or a Nikon eclipse Ti-S microscope.

The TMA was originally assembled by Dr. Judith Lehmann-Koch from the Department of Pathology, University of Heidelberg, and is courtesy of the Nationales Zentrum für Tumorerkrankungen (NCT Heidelberg). The array contained tissue sections from 250 patients with assessable clinical records. 10-30 postmortem and biopsy tissues from each of 20 different organs had been paraffinized and mounted on glass slides. After immunohistochemical staining for detection of CD317 according to the above description, slides were scanned for image acquisition by John Moyers from the Department of Pathology, Heidelberg University. CD317 expression in different tissues was then evaluated together with Dr. Felix Lastischka, Department of Pathology, Heidelberg University, and rated according to its expression as – (negative), + (low), ++ (medium) or +++ (high). Images were acquired with Aperio ImageScope software.

3.2.4.7 Immunofluorescence and microscopy of tissue sections

Paraffin-embedded tissue sections were treated as described in section 3.2.4.7 on the first day of the staining procedure. The following day the primary antibody was washed off with EBSS/H/BSA/SAPONIN buffer three times, before the secondary antibody was applied and incubated with the tissue sections for 30 minutes (diluted in EBSS/H/BSA/SAPONIN buffer). After three more washing steps with EBSS/H/BSA/SAPONIN buffer, fluorochrome-coupled antibodies or conjugates were added to the slides (diluted in EBSS/H/BSA/SAPONIN buffer). Slides were incubated for 20-30 minutes at room temperature in the dark and thereafter washed twice in EBSS/H/BSA/SAPONIN buffer, twice in EBSS/H/BSA buffer and twice in H_2O. Slides were mounted with DAPI mounting medium (Sigma-Aldrich) and analyses were performed on an Olympus MT20 fluorescence microscope, a Leica AF6000 confocal microscope or a Nikon eclipse Ti-S microscope.

3.2.4.8 Statistical analyses

Plotting of graphs and general statistical analyses were performed using either Microsoft Excel or GraphPad Prism 5 software package (GraphPad Software Inc., La Jolla, CA). These two programs were also used to calculate significance values by applying the two-tailed, unpaired Student's *t*-test.

4. RESULTS

4.1 EXPRESSION PROFILE OF THE ANTIVIRAL RESTRICTION FACTOR AND TUMOR-TARGETING ANTIGEN CD317/TETHERIN/HM1.24 IN HUMANS

Many restriction factors including A3G, TRIM5α, SAMHD1 and MX2 act at early stages of HIV-1 replication, whereas CD317/tetherin acts at a later stage. The importance of restriction factor activity in human cells can be seen by the fact that viruses have evolved countermeasures to overcome these barriers. The implications in disease progression and viral replication *in vivo* are often only poorly understood. To understand these, a detailed analysis of the expression profile is required, and was undertaken for CD317/tetherin in the present study. We perfomed microarray-based CD317 expression profiling in nontransformed tissues to provide a framework for studies of its biological functions in humans, with a focus on its potential importance as an antiviral factor and on therapeutic strategies proposing CD317 as a target for immunotherapy of B-cell malignancies and solid tumors.

The following chapter has been published during the course of this thesis and is modified from (**I**).

CD317 Is Expressed on Specialized Cells in a Variety of Human Tissues

As a methodological basis for a comprehensive evaluation of CD317 expression *in vivo*, we developed an immunohistochemical staining protocol for formalin-fixed, paraffin-embedded tissue sections, given that standard protocols yielded only low-level staining in tonsil (Fig. 4.1). The mouse anti-HM1.24 mAb, specific for an epitope in the extracellular domain of CD317 (114), was used as primary detection reagent. The specificity and sensitivity of this immunohistochemical staining protocol was validated on patient-derived multiple myeloma (71), tonsil tissue, and human cell lines expressing high endogenous CD317 levels (67) or no CD317 (153) (Figs. 4.2 and 4.3A).

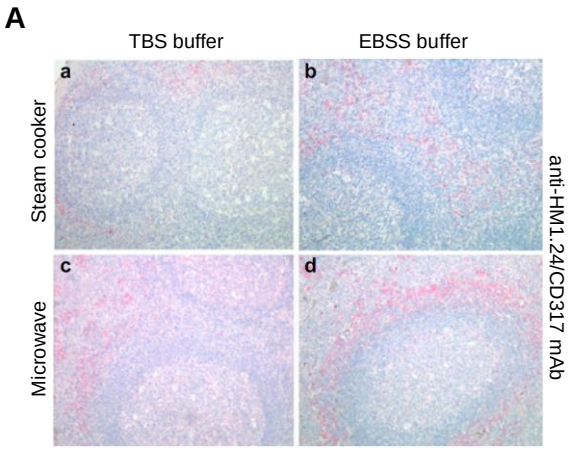

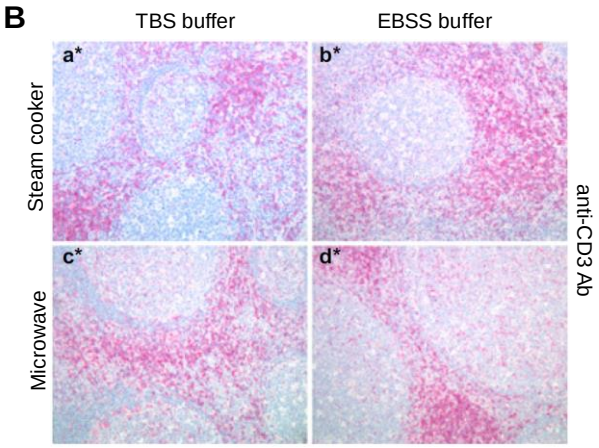

Fig. 4.1 Optimization of an anti-CD317 immunohistochemistry protocol on human tonsil. Before immunostaining, sections from the formalin-fixed, paraffin embedded tonsil from one donor underwent various antigen retrieval protocols (a–d and a*–d*), details of which are reported in Materials and Methods. (a and a*) microwave and TBS buffer; (b and b*) microwave and EBSS buffer; (c and c*) steam cooker and TBS buffer; (d and d*) steam cooker and EBSS buffer. Subsequently, sections were stained with either the anti-HM1.24/CD317 mAb (IgG2a) (A) or a polyclonal rabbit anti-CD3 antiserum (clone SP7) (B), followed by a biotinylated sheep α-mouse secondary antibody or donkey α-rabbit secondary antibody, respectively. Sections were then exposed to the avidin-containing ABC-AP Kit, followed by substrate development with New Fuchsin. Nuclei were counterstained with Hematoxylin. From (**I**).

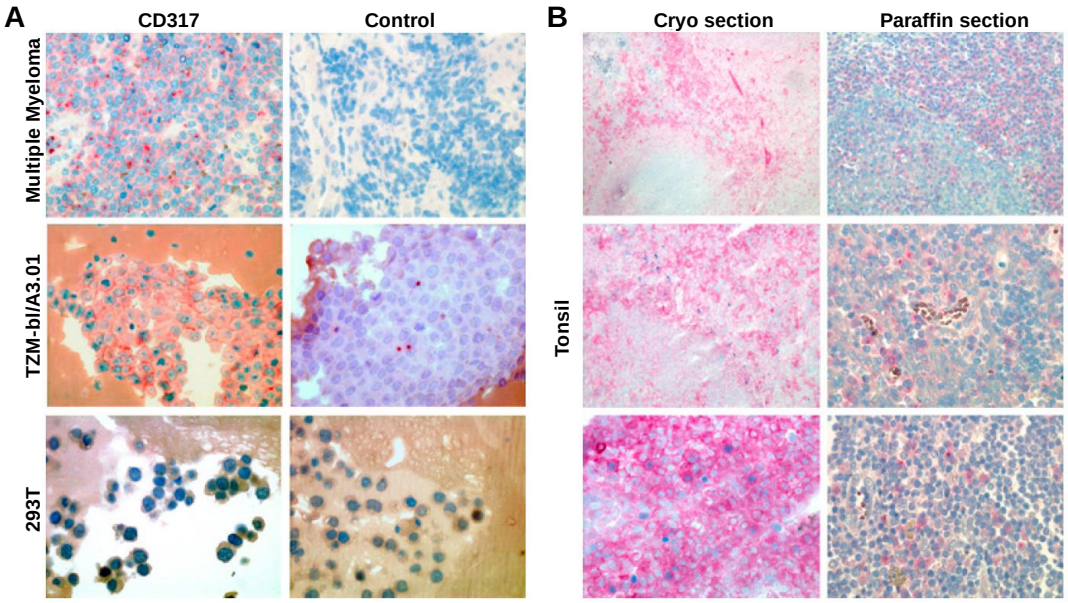

Fig. 4.2 Validation of the anti-CD317 immunohistochemistry protocol. (A) Patient-derived multiple myeloma and human cell lines, expressing either high levels of endogenous CD317 (mixture of TZM-bl and A3.01 cells) or no endogenous CD317 (293T cells), were formalin-fixed and paraffin-embedded. Sections were stained with the anti-HM1.24 mAb (Left) or an IgG2a isotype control mAb (Right) using the optimized immunohistochemistry protocol, followed by a biotinylated sheep α-mouse secondary antibody. Subsequently, sections were exposed to the avidin-containing ABC-AP Kit, followed by substrate development with New Fuchsin. Nuclei were counterstained with Hematoxylin. (B) Immediately after tonsillectomy, tonsil tissue was divided and either (i) snap-frozen in liquid nitrogen, cut on a cryotome, and fixed in ice-cold acetone (cryo section) or (ii) fixed in formalin and paraffin-embedded, sections of which underwent the antigen retrieval protocol (paraffin section). Staining of all sections was performed as described above. (Original magnifications, 10×–40×.) From (**I**).

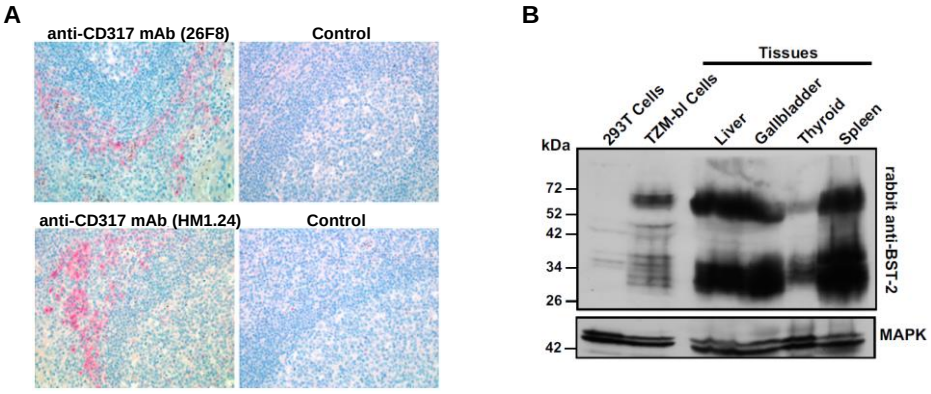

Fig. 4.3 Detection of CD317 expression by three different antibodies. (A) Immunohistochemical detection of CD317 in tonsil. Sections from a paraffin block were stained either with the mouse anti-CD317 mAb clone 26F8 (IgG1; eBioscience), mouse anti-CD317 mAb clone HM1.24 (IgG2a; Chugai Pharmaceuticals), or corresponding isotype control mAbs (control, Right) using the optimized antigen retrieval protocol. (B) Western blot analysis of CD317 in homogenates from selected human tissues (liver, gallbladder, thyroid, and spleen) and cell lines with low (293T cells) or high (TZM-bl cells) endogenous CD317 expression. Cell lysates were separated by SDS/PAGE, and nitrocellulose membranes were probed with a polyclonal rabbit anti-BST-2 antiserum (provided by Klaus Strebel). From (**I**).

In a cross-sectional CD317 expression analysis, we used a tissue microarray (TMA) containing 468 individual sections derived from 25 paraffinized nontransformed tissue samples from more than 210 patients. CD317 expression was rated based on a combined proportion and intensity scoring system reported by Allred et al (2). Remarkably, CD317 was expressed in more than 40% of patient samples in 21 of the tissues analyzed (Figs. 4.4 and 4.5A). The expression scores varied considerably among tissues; the highest scores were seen in spleen, gallbladder, and stomach (>70% medium or high expression scores), whereas more moderate expression scores were seen in pancreas, adrenal gland, small intestine, liver, and salivary gland (40–70% medium or high expression scores) (Fig. 4.5B). More than half of the cases analyzed for heart, ovary, uterus, kidney, testis, and bladder tissues received low or medium scores. CD317 expression in lung, appendix, skin, tonsil, fat, and thyroid samples of the TMA was low or negative (Figs. 4.4B, 4.4C and 4.5B).

In a complementary approach, Western blot analyses of snap-frozen samples of tissues with high (liver, gallbladder, spleen) or low (thyroid) CD317 expression on immunohistochemistry (Figs. 4.4 and 4.5) were confirmatory (Fig. 4.3B). Based on histological criteria, CD317 expression in organ sections of the TMA was identified on type I and type II pneumocytes in the lung, intercalated and striated ducts of major salivary glands, squamous epithelium of the esophagus, gastric fundic epithelium and glands, Paneth cells of the small intestine, mononuclear cells in the lamina propria of the large intestine, acinar cells of the exocrine pancreas, hepatocytes, gallbladder epithelium, cells in the adrenal zona reticularis, collecting ducts of the kidney, Leydig cells in the testis, endometrial

glands, and vasculature (Fig. 4A and 4.4C). Thus, in contrast to previous work (71), we found CD317 to be widely expressed and exposed on a number of specialized cell types.

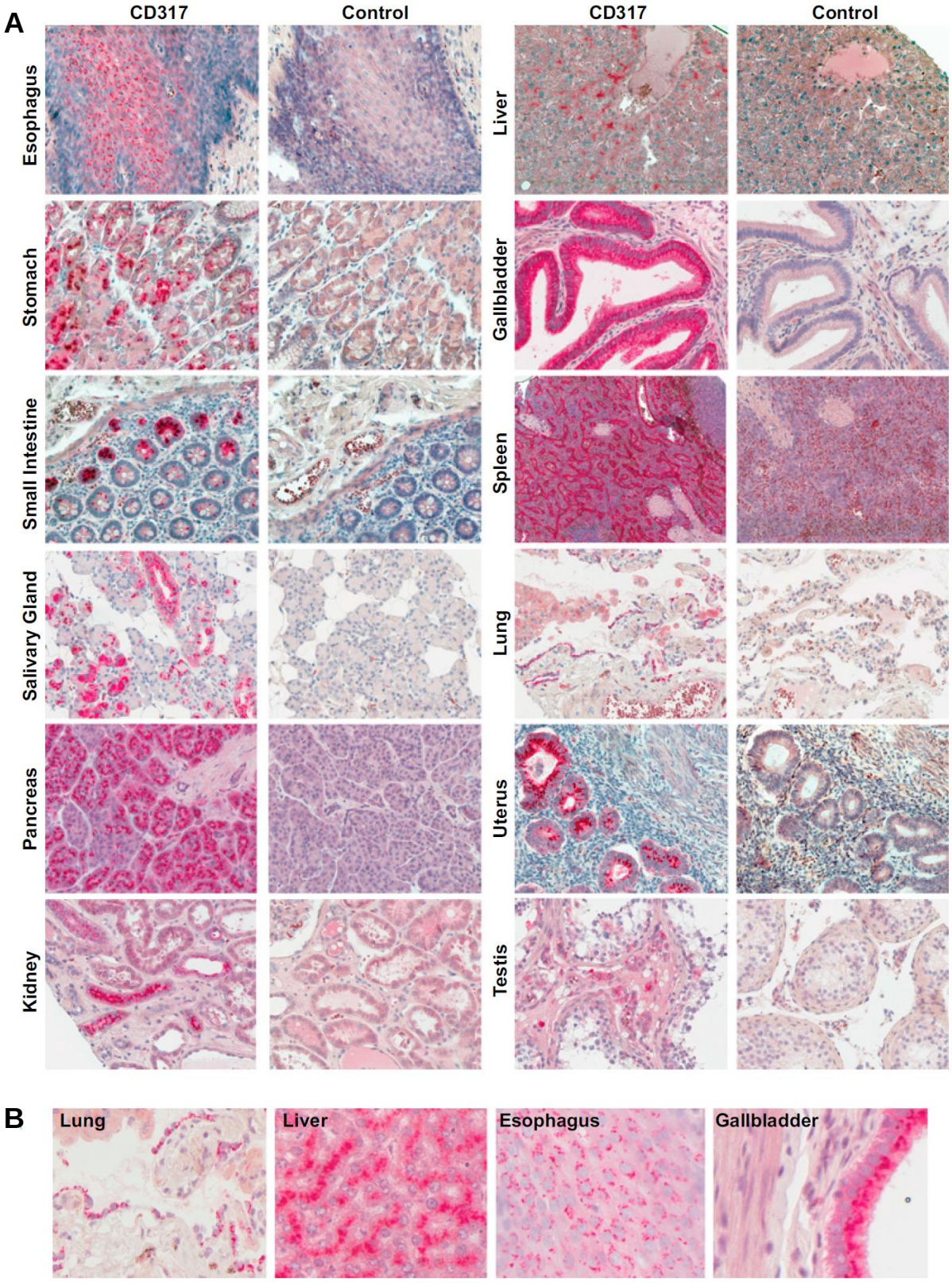

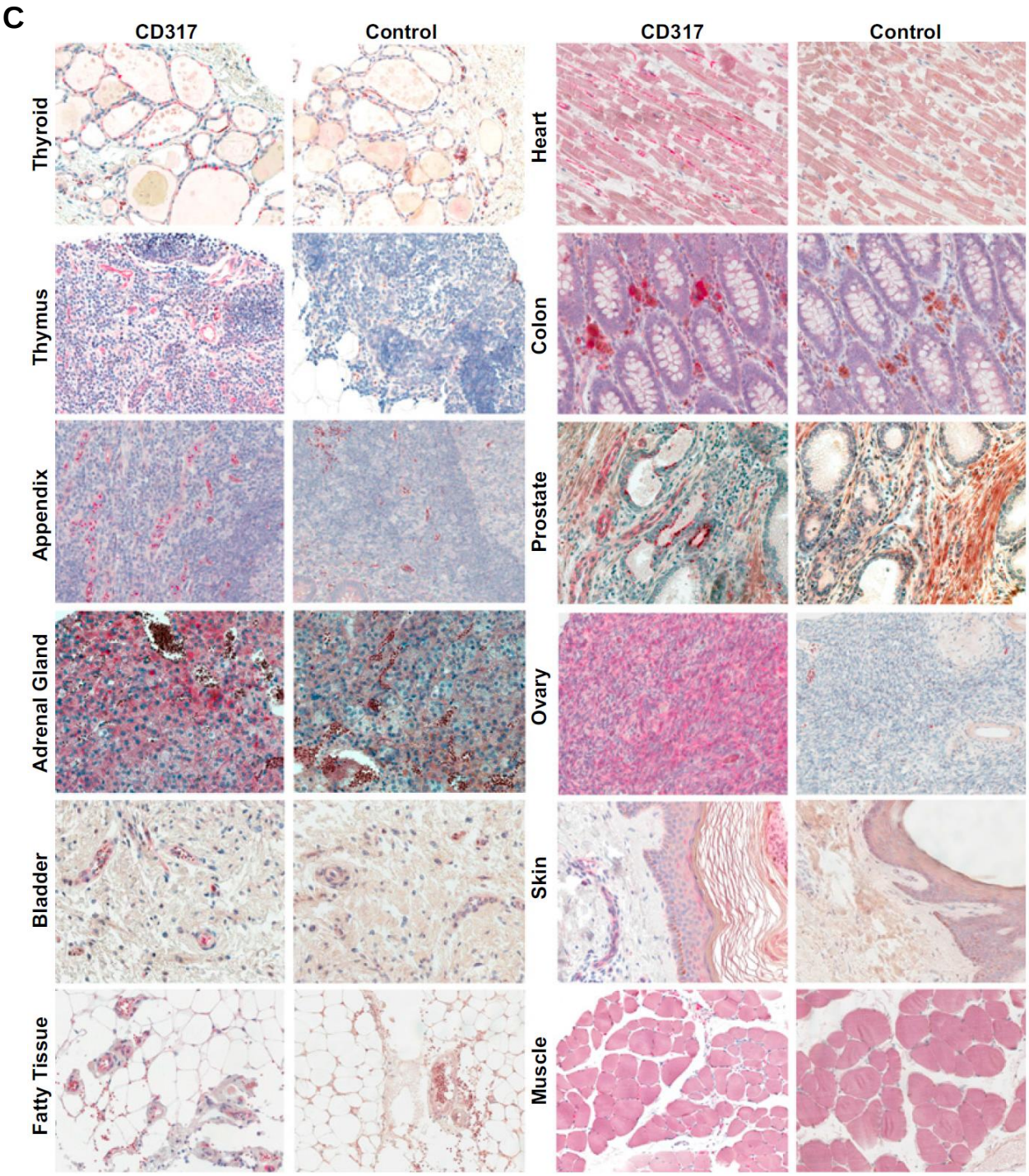

Fig. 4.4 CD317 is expressed in a variety of human tissues. (A, C) 20× magnification. (B) 40× magnification. TMA slides were stained with the anti-HM1.24/CD317 mAb (Left) or an isotype control mAb (Right), followed by a biotinylated sheep α-mouse secondary antibody. Subsequently, sections were exposed to the avidin-containing ABC-AP Kit, followed by substrate development with New Fuchsin. Nuclei were counterstained with Hematoxylin. From (**I**).

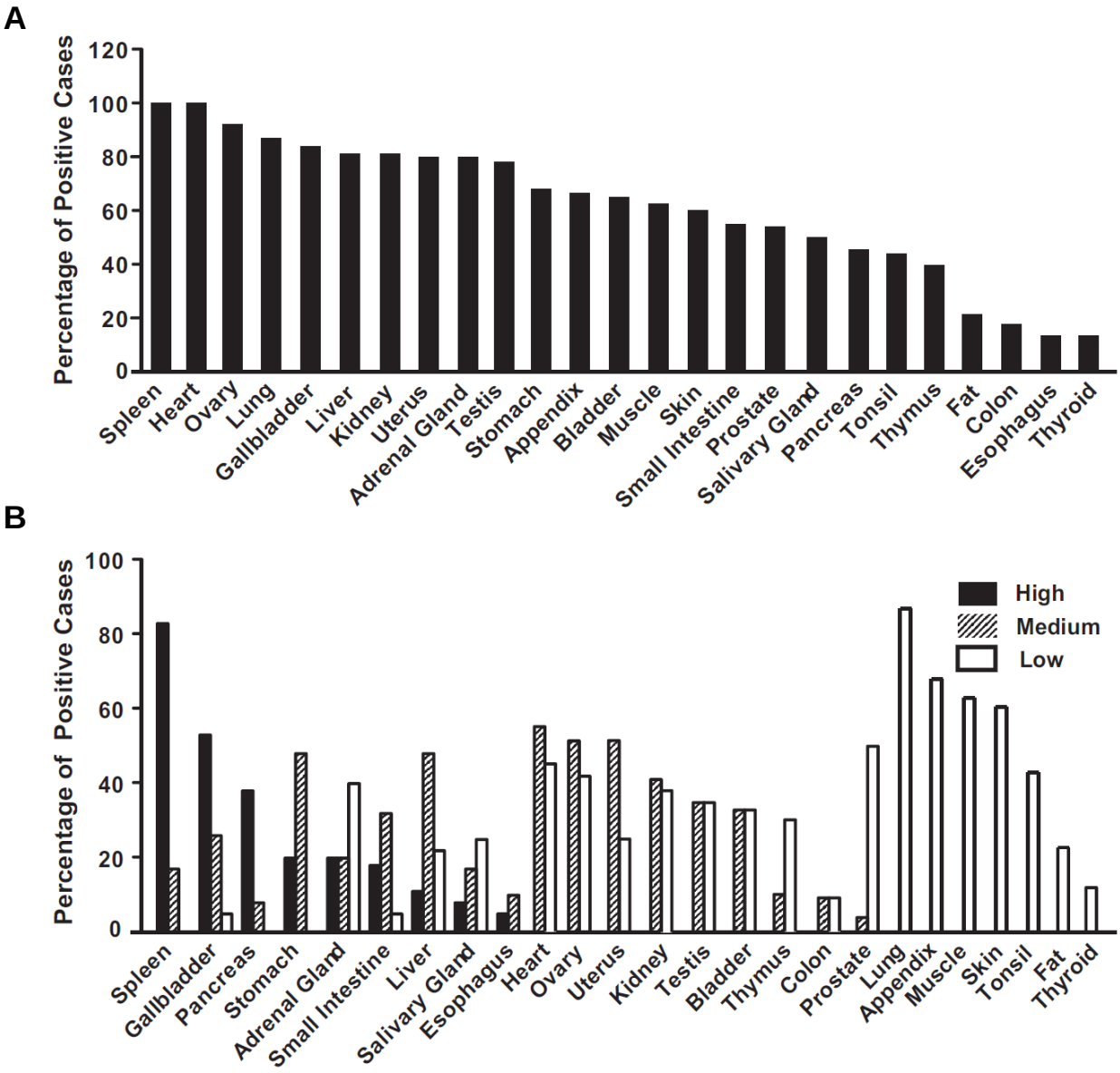

Fig. 4.5 Rating of CD317 expression in human tissues. The expression of CD317 detected in tissues of the TMA by immunohistochemistry was rated based on a proportion and intensity scoring system (22). (A) Histogram bars depict the percentage of samples (n = 6–34 per tissue), in which the indicated tissue section scored positive. (B) Histogram bars depict the percentage of samples with high (solid), medium (hatched), or low (open) expression ratings. The percentage of samples with negative ratings is not shown. From (**I**).

CD317 Is Ubiquitously Expressed on Blood Vessels

We next focused on the CD317 expression on vasculature. Blood vessels in all tissues represented in the TMA demonstrated CD317 staining in the lumen-oriented endothelial lining. In highly vascularized organs, such as spleen, the majority of CD317 expression was on blood vessels (Fig. 4.4 and 4.6A), but prominent vessel staining was observed in sections from gastrointestinal tract, muscular tissue of the heart (Fig. 4.6C), liver, pancreas, and bladder as well (Fig. 4.6A). In line with these immunohistological findings, CD317 expression co-localized with expression of the blood vessel endothelial cell marker CD31 (platelet endothelial cell adhesion molecule, PECAM-1) in the

endothelium of larger arteries such as coronary arteries and the aorta, as well as in smaller, organ associated blood vessels such as those found in tonsil (Fig. 4.6B and D). We conclude that CD317 is highly expressed on blood vessels throughout the body.

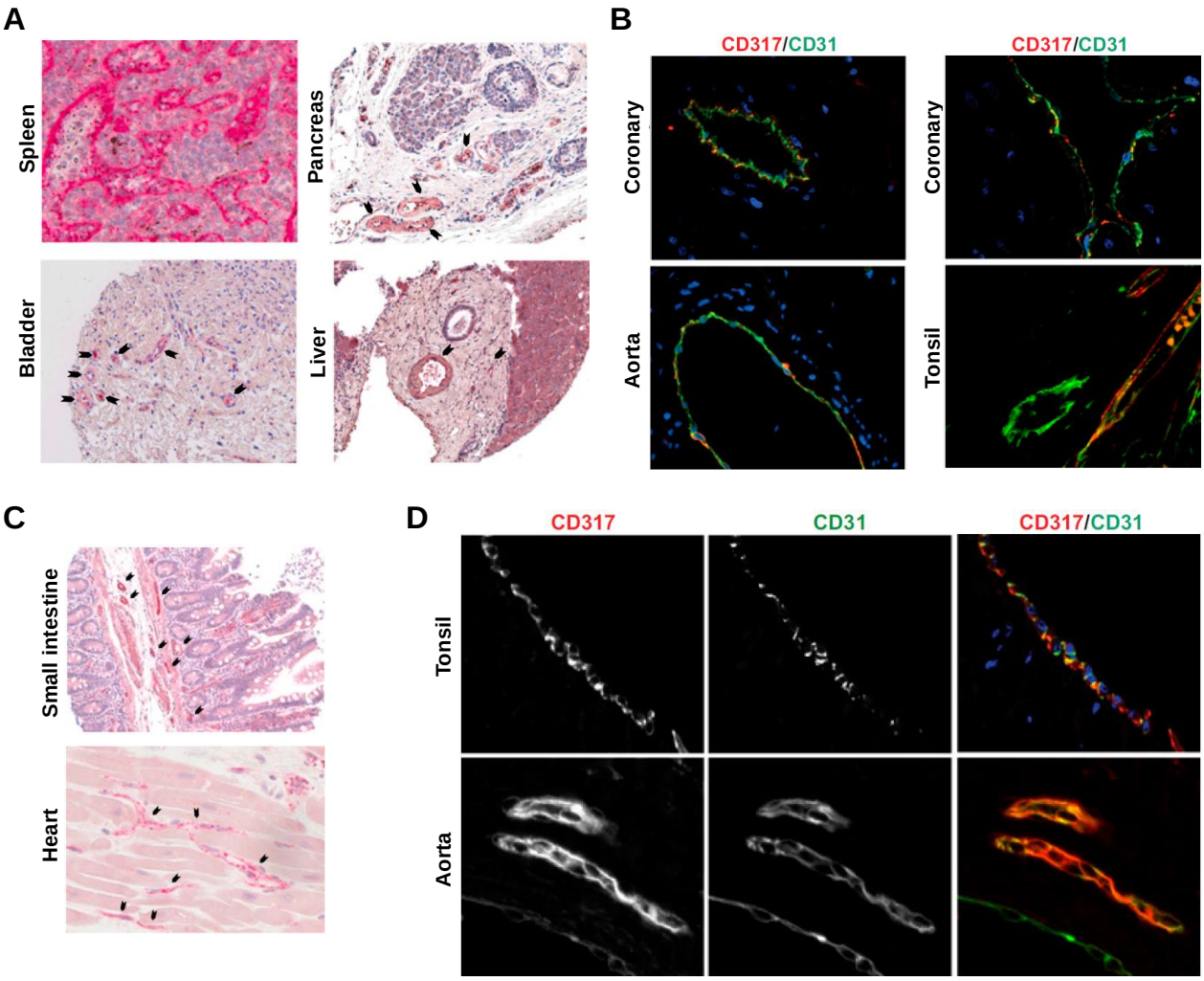

Fig. 4.6 CD317 is expressed on CD31+ blood vessel endothelium. (A, C) Immunohistochemical analysis of CD317 expression on blood vessels in liver, bladder, pancreas, spleen, heart musculature and small intestine. Black arrows indicate blood vessels with CD317+ endothelium. (B, D) Co-expression analysis of the vascular endothelial cell marker CD31 (PECAM-1) and CD317 in coronary artery, aorta, and tonsil tissue (two donors/organ). Tissue sections were labeled with the anti-CD31 mAb JC70A (IgG1) and the anti-HM1.24 mAb (IgG2a), followed by appropriate secondary reagents. Merged three-/two-color images for CD317 (red staining), CD31 (green staining), and nuclei (blue staining) are shown in B and in C, Right panel. Left and Middle panels show individual fluorescence channels. Fluorescent images were acquired at 10–60× magnification. Modified from (**I**).

Cell Type–Specific CD317 Expression in Hematopoietic Compartments and Intestinal Lamina Propria

We next characterized CD317 expression in tonsil, peripheral blood mononuclear cells (PBMCs), and bone marrow. Based on documented CD317 expression on B cell malignancies, including multiple myeloma, plasma cell leukemia, and Waldenström's macroglobulinemia (71) (Fig. 4.2A), we first focused on cells of the B-cell lineage. In tonsil, little or no expression of CD317 was found on naïve and immature B cells (soluble IgD+, CD21+), mature CD23+ B cells, or cells expressing the pan B-cell marker CD19 (Fig. 4.7A). A considerable fraction of terminally differentiated CD138+ B cells, which localized primarily to the perifollicular region, stained positive for CD317 (Fig. 4.7A, white arrows). In tonsil, no CD317 expression was detected on T cells, tissue-resident macrophages, dendritic cells (Fig. 4.7B), or CD66b+ granulocytes. Expression analysis on PBMCs demonstrated that CD3+ T cells did not express CD317, whereas CD19+ B cells expressed low levels on their surfaces (Fig. 4.7C). CD14+ monocytes were the only cell type in peripheral blood that expressed high levels of CD317 (Fig. 4.7C). An initial expression analysis in a previous study (96) indicated preferential expression of CD317 on cell lines with characteristics of bone marrow stroma; based on this, the surface protein was termed bone marrow stromal antigen 2 (BST-2). In the present study, we assessed CD317 expression in bone marrow aspirates from healthy donors. A considerable fraction of nucleated bone marrow cells stained positive for CD317 by immunohistochemistry (Fig. 4.7D, Left). In Ficoll gradient–purified bone marrow, the majority of cells that expressed the stromal cell marker CD106 (VCAM-1) (177) co-expressed CD317 on the surface (Fig. 4.7D).

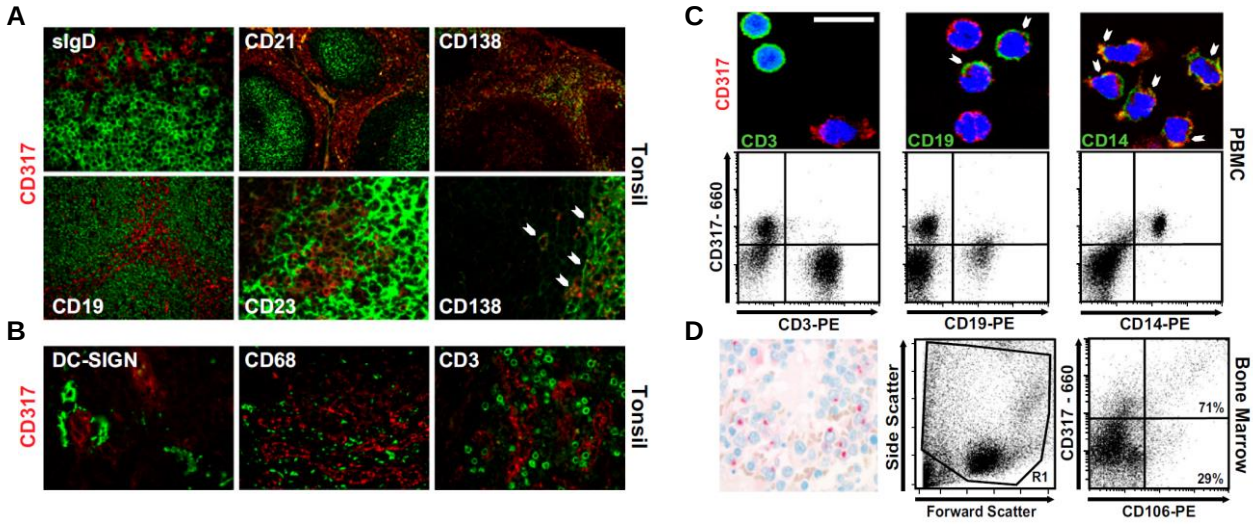

Fig. 4.7 Characterization of CD317 expression in tonsil, PBMCs, and bone marrow. (A) Co-expression analysis of CD317 and several markers of the B-cell lineage in human tonsil sections. (B) Co-expression analysis of CD317 (red staining) on dendritic cells, macrophages, and T cells (green stainings) in tonsil. (C) CD317 co-expression analysis on T cells, B cells, and monocytes in PBMCs by immunofluorescence microscopy of cells that had been seeded on coverslips, fixed, and permeabilized (Upper) or by flow cytometry of unfixed cells (Lower). FACS plots shown were gated on viable lymphocytes and monocytes. For microscopy, cells were stained with the anti-HM1.24 mAb, Alexa Fluor 660– labeled secondary Ab, and PE-conjugated Abs to the respective lineage markers. (Scale bar: 10 μm.) White arrows indicate double-

positive cells. (D) CD317 immunohistochemistry of bone marrow. (Original magnification, 40×.) (Left) Co-expression analysis of the bone marrow stromal cell marker CD106 and CD317 in a bone marrow aspirate. Shown is the forward scatterplot/side scatterplot with the R1 live gate indicated and a FACS dot plot of CD106 and CD317. (Right) Relative percentages of CD317+ and CD317− cells among CD106+ cells. Data are representative of the results from two donors. From (**I**).

Furthermore, co-labeling analyses of the lamina propria of the large intestine with cell type–specific markers identified CD138+ plasma cells, but not HIV target cells (i.e., CD4+ T cells, macrophages, DC), as the major CD317+ cell type (Fig. 4.8). These findings indicate that, along with terminally differentiated B cells (71), monocytes and primary bone marrow stromal cells express high levels of CD317 within the hematopoietic lineage.

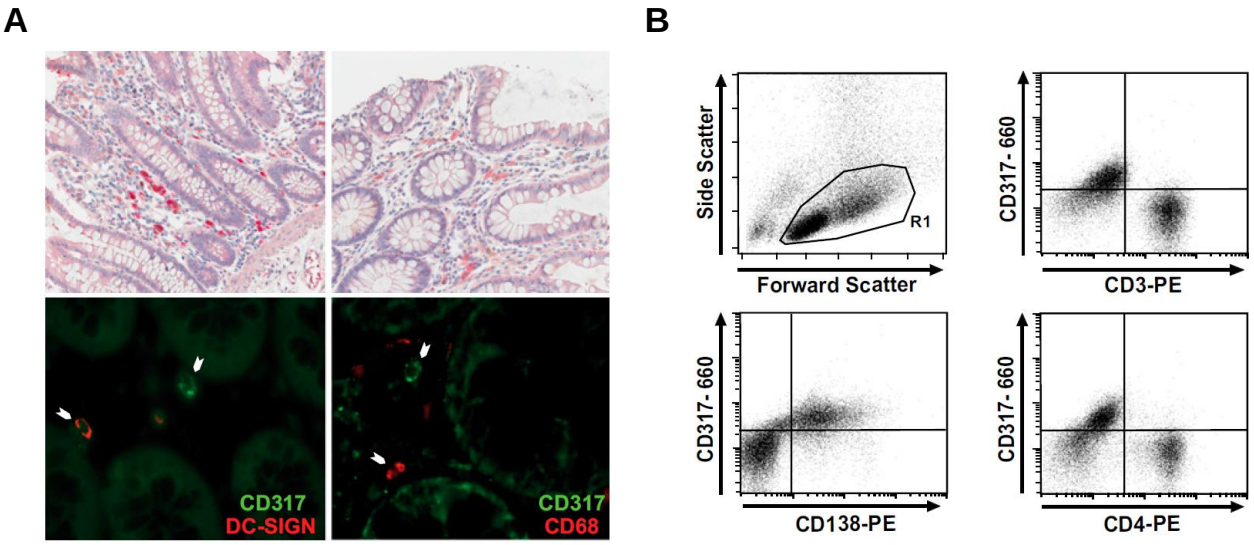

Fig. 4.8 Plasma cells, but not HIV target cells, in the lamina propria of the large intestine are CD317+. (A) Immunohistochemical analysis of CD317 expression in colon sections. (B) Co-expression analysis of CD317 (green staining) on DC-SIGN+ dendritic cells or CD68+ macrophages (red staining). White arrows indicate cells that express either CD317 or the cell type–specific marker. (C) CD317 co-expression analyses on CD3+ T cells, CD4+ cells, and CD138+ plasma cells on freshly isolated lamina propria lymphocytes by flow cytometry. Gate R1 defines the viable lymphocyte population. From (**I**).

Expression of CD317 on Human Plasmacytoid Dendritic Cells Is Not Constitutive

In mice, CD317 is a constitutively expressed surface antigen on plasmacytoid dendritic cells (pDC) (188) and a frequently used marker for positive selection of pDC from lymphatic organs. In human tonsil, BDCA2+ pDC were found predominantly in the T cell–rich lymphocyte wall and to a lesser extent in the perifollicular region (Fig. 4.9A, Left). Co-expression analysis of CD317 and BDCA2 by in situ immunofluorescence microscopy (Fig. 4.9A, Right) and flow cytometry (Fig. 4.9B) found no evidence of significant CD317 expression on pDC from human tonsil. Similarly, CD317 was not expressed on BDCA2+ pDC from Ficoll gradient–purified PBMCs, in line with a recent report (25). In isolated pDC, stimulation with type I IFNs upregulated CD317 mRNA levels by twofold to fivefold (Fig. 4.9C) and CD317 surface levels by threefold to fivefold (Fig. 4.9D). Collectively, these results

demonstrate a species-specific expression pattern of CD317 on pDC. In contrast to mice, CD317 is not constitutively expressed on pDC in human blood and tonsil, but can be up-regulated by type I IFNs, at least on isolated cells.

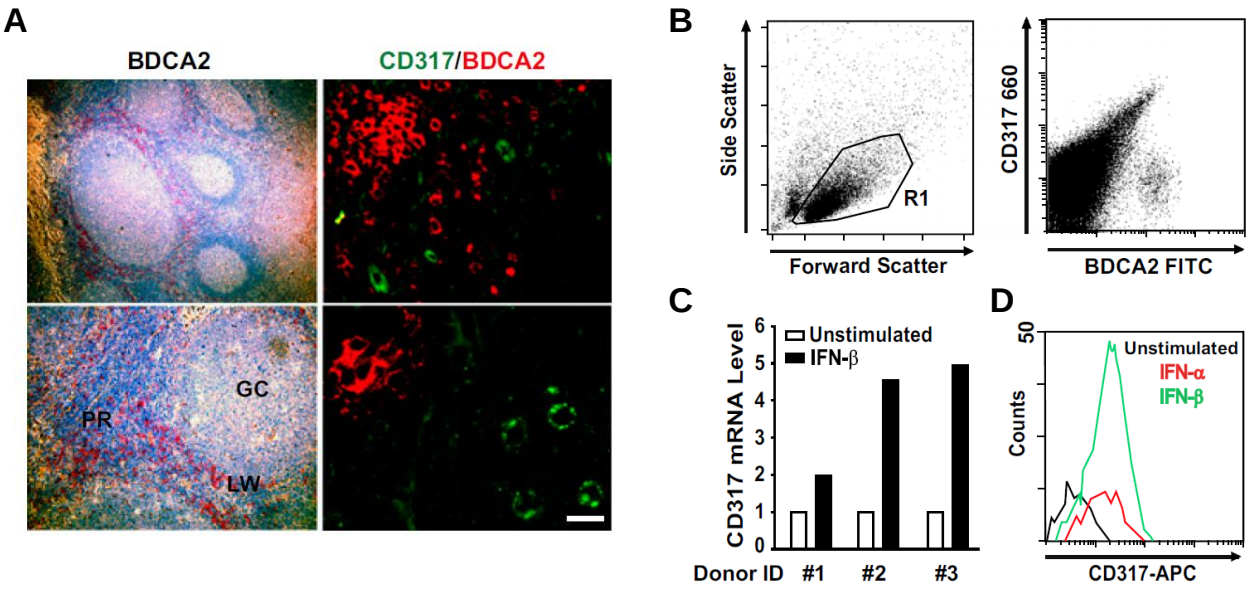

Fig. 4.9 Expression of CD317 on pDC is not constitutive but can be stimulated in vitro by IFN-α or IFN-β. (A) Detection of BDCA2+ pDC in tonsil sections. GC, germinal center; LW, lymphocyte wall; PR, perifollicular region. Co-expression analysis of CD317 on BDCA2+ pDC by (A, Right) in situ-double-immunofluoresence microscopy (A, Right) or flow cytometry of dispersed organs (B). (Scale bar in A: 10 μM.) In B, viable cells were identified by gating on the live lymphocyte population (gate R1) and analyzed for BDCA2 and CD317 expression (Right). (C) Relative CD317 mRNA levels in purified pDC from three donors were quantified by RT-PCR in unstimulated cells after exposure to IFN-β for 4 h. RNaseP-normalized CD317 mRNA levels in unstimulated pDC were set to 1. (D) pDC from peripheral blood were stimulated with IFN-α or IFN-β for 24 h and analyzed for surface CD317 expression on pDC by flow cytometry. From (**I**).

Type I IFNs May Only Partially Regulate CD317 Expression *In Vivo*

On various types of cultured cells, CD317 is up-regulated after exposure to type I IFNs (145, 198), consistent with its function as an antiviral restriction factor and the presence of IFN-response elements in the CD317 promoter (156). We examined the degree to which the prominent CD317 expression in certain cell types and tissues *in vivo* was induced by IFN. We began by performing co-labeling studies with the myxomavirus resistance protein A (MxA). The expression of MxA, which restricts the replication of orthomyxoviruses and other RNA viruses (85), is strictly dependent on stimulation by type I or type III IFNs, classifying MxA as a convenient marker for IFN bioactivity (202). Individual expression analyses of each restriction factor showed that the majority of MxA-expressing cells in tonsil were located within germinal centers, with additional cells staining positive in the lymphocyte wall and perifollicular region (Fig. 4.10A). In contrast, the majority of CD317+ cells were found in the perifollicular region, and few cells within germinal centers expressed CD317. Most importantly, double-immunofluorescence microscopy demonstrated that cells in tonsil typically expressed either

MxA or CD317 (Fig. 4.10A, Lower and Fig. 4.11A), and that co-expression was a rare event (Fig. 4.10A, Lower Right, white arrow). Similarly, CD317+ pneumocytes did not express the IFN biomarker MxA, and macrophages found in the lung were MxA+CD317− (Fig. 4.10B, Left and Fig. 4.11B). In contrast, frequent co-expression of both restriction factors was found on vessel endothelium, as exemplified in aorta samples from several patients (Fig. 4.10B, Right and Fig. 4.11C).

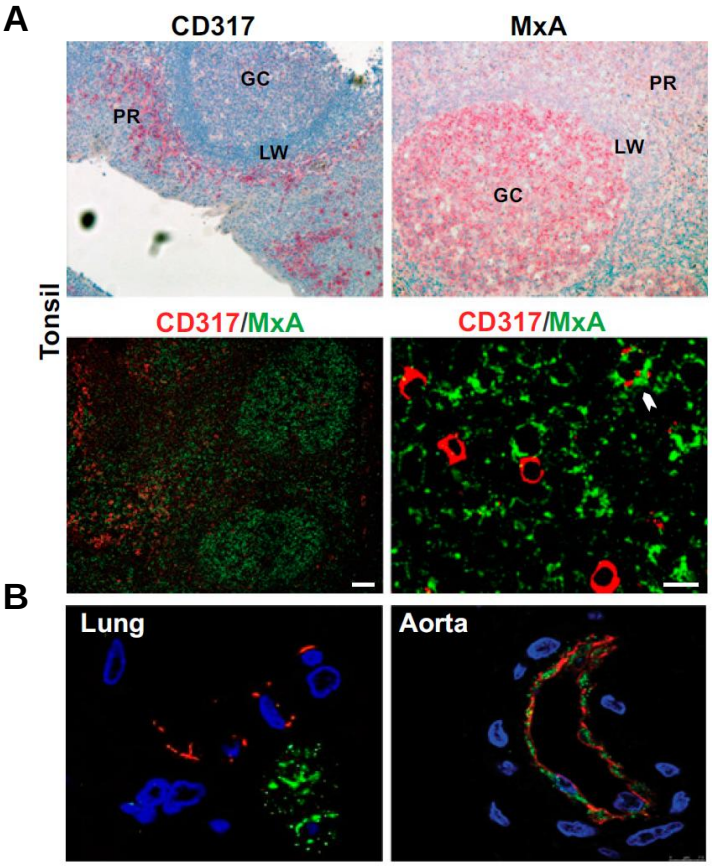

Fig. 4.10 Cell type–dependent coexpression of CD317 and the IFN biomarker MxA. (A) (Upper) Immunohistochemical detection of CD317 and MxA in tonsil. GC, germinal center; LW, lymphocyte wall; PR, perifollicular region. (Original magnification, 10×.) (Lower) Coexpression analysis of CD317 (red staining) and MxA (green staining) in tonsil by immunofluoresence microscopy. (Scale bars: Left, 100 μm; Right, 10 μm.) The white arrow indicates a coexpressing cell. (B) Coexpression analysis in lung tissue and aorta. Merged three-color images for CD317 (red staining), MxA (green staining), and nuclei (blue staining) are shown. Images from additional donors [tonsil (n = 2), aorta (n = 3), and lung tissue (n = 2)] are shown in Fig. 4.11. From (**I**).

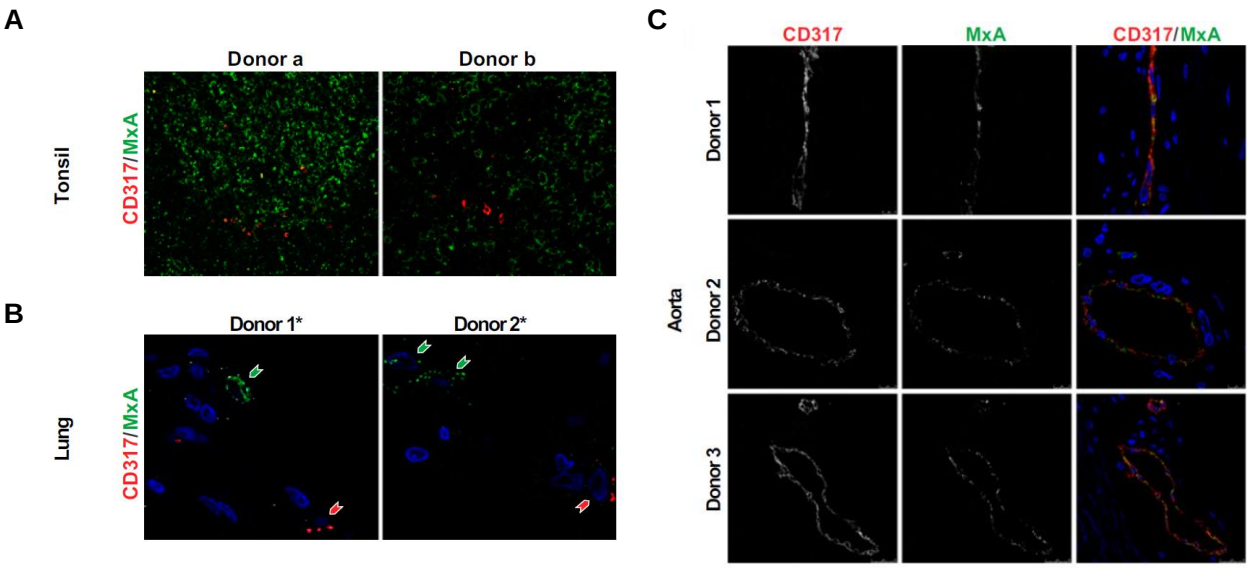

Fig. 4.11 Coexpression analysis of CD317 and the IFN biomarker MxA in different human tissues from different donors by in situ immunofluorescence microscopy: tonsil (A), lung (B), and aorta (C). In B, arrows indicate MxA+ cells (green) or CD317+ cells (red). (C) (Right) Merged three-color images for CD317 (red staining), MxA (green staining), and nuclei (blue staining). (Left and Middle) Individual fluorescence channels from the identical image. Images from other donors are shown in Fig. 4.10. From (**I**).

To explore whether exogenous IFN stimulation can trigger CD317 expression in tonsil explants, we exposed dispersed human lymphoid aggregate cultures (tonsil-HLAC;(104)) to IFN-α for 24 h. This *ex vivo* stimulation enhanced CD317 expression on tonsillar lymphocytes only marginally, whereas a strong and concentration-dependent increase of MxA expression was seen (Fig. 4.12A). As a reference, IFN-α also readily triggered surface expression of CD317 on Jurkat-TAg cells (Fig. 4.12B).

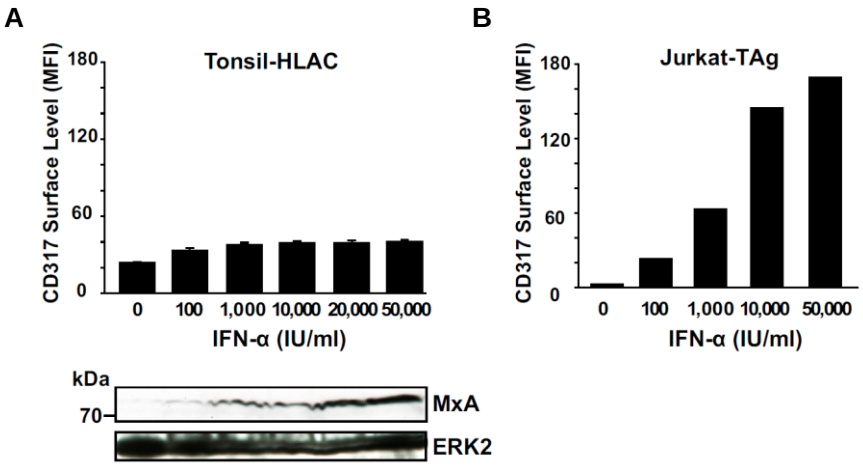

Fig. 4.12 Primary lymphocytes from tonsil are largely refractory to IFN-α induction of CD317. *Ex vivo* HLAC cultures from tonsil (tonsil-HLAC) (A) and the T cell line Jurkat-TAg (B) were cultivated for 24 h in the absence or presence of the indicated concentrations of IFN-α and then analyzed for CD317 surface expression by flow cytometry. The mean

fluorescence intensity (MFI) of CD317 expression on viable lymphocytes from five donors was quantified; values are arithmetic mean ± SEM. (A, Lower) In parallel, lysates from IFN-α–stimulated HLAC were separated by SDS/PAGE and blotted for MxA. ERK levels served as a loading control. Shown are Western blots from one representative donor. From (**I**).

Collectively, these results suggest a cell type– and/or tissue related IFN dependence of CD317 expression. Whereas marked CD317–MxA coexpression was found in vessel endothelium, their nearly mutually exclusive expression pattern in lymphoid and pulmonary tissue and insensitivity to exogenous IFN stimulation suggest that type I IFNs may only partially regulate CD317 levels *in vivo*.

4.2 INVESTIGATING THE ANTIVIRAL ACTIVITY OF SAMHD1 IN RESTING T CELLS BY FLOW CYTOMETRY

Resting CD4+ T cells are unlike activated CD4+ T cells refractory to productive HIV-1 infection and only become permissive upon activation (185, 214). Briefly, the activation process that resting T cells undergo – leading to proliferation – involves first a transition from the quiescent G0 state of the cell cycle into the G1 phase, which occurs after stimulation through the T cell receptor (TCR) (33). This event leads to production and secretion of interleukin-2 (IL-2) and the expression of IL-2-receptors on the cell surface. Binding of IL-2 to the IL-2 receptors then induces progression of G1 cells into S phase and mitosis (24, 182). The non-permissivity of resting CD4+ T cells has been attributed to blocks at different post-entry steps in the viral life cycle, one of the early blocks being the inefficient reverse transcription where the viral genomic RNA is copied into cDNA (163, 214). Because the original papers (92, 131) describing the antiviral activity of SAMHD1 did not detect SAMHD1 expression in T cell lines, they assumed that this protein was not effective in T cells. To determine whether SAMHD1 imposes a restriction of HIV-1 infection in resting CD4+ T cells, a method for SAMHD1 detection by flow cytometry was first established, and was followed up with functional experiments focussing on infections with HIV-1 or HIV-2 into which viral Vpx was artificially or naturally packaged, respectively.

The results in this chapter have been published during the course of this thesis and the figures and text are modified from (**II**) and (**III**).

SAMHD1 Is Expressed in Human CD4+ T cells

SAMHD1 is expressed in dendritic cells, monocytes and macrophages, but not in T cell lines (e.g Jurkat, SupT1 and human peripheral blood acute lymphoid leukemia (HPB-ALL), and it has been reported to act as a lineage-specific infection barrier for HIV-1 (92, 131). After establishing a staining protocol including a permeabilization procedure suitable for detection of SAMHD1 in primary leukocytes by flow cytometry (Fig. 4.13A), we examined expression levels of the protein in PBMC and tonsil cells. Using a methanol-based permeabilization protocol, in spite of the proposed lineage specificity, we detected endogenous SAMHD1 protein in all nucleated hematopoietic cells among PBMCs and in tonsil tissue (Fig. 4.13B). This analysis included resting CD4+ T cells from peripheral blood, where we found high levels of SAMHD1 mRNA (not shown) and protein expressed (Fig. 4.13C). SAMHD1 was also abundantly expressed in explants of human tonsil, a lymphoid tissue targeted by HIV-1 *in vivo*, where the majority of SAMHD1-expressing cells localized to the perifollicular region (Fig. 4.13D).

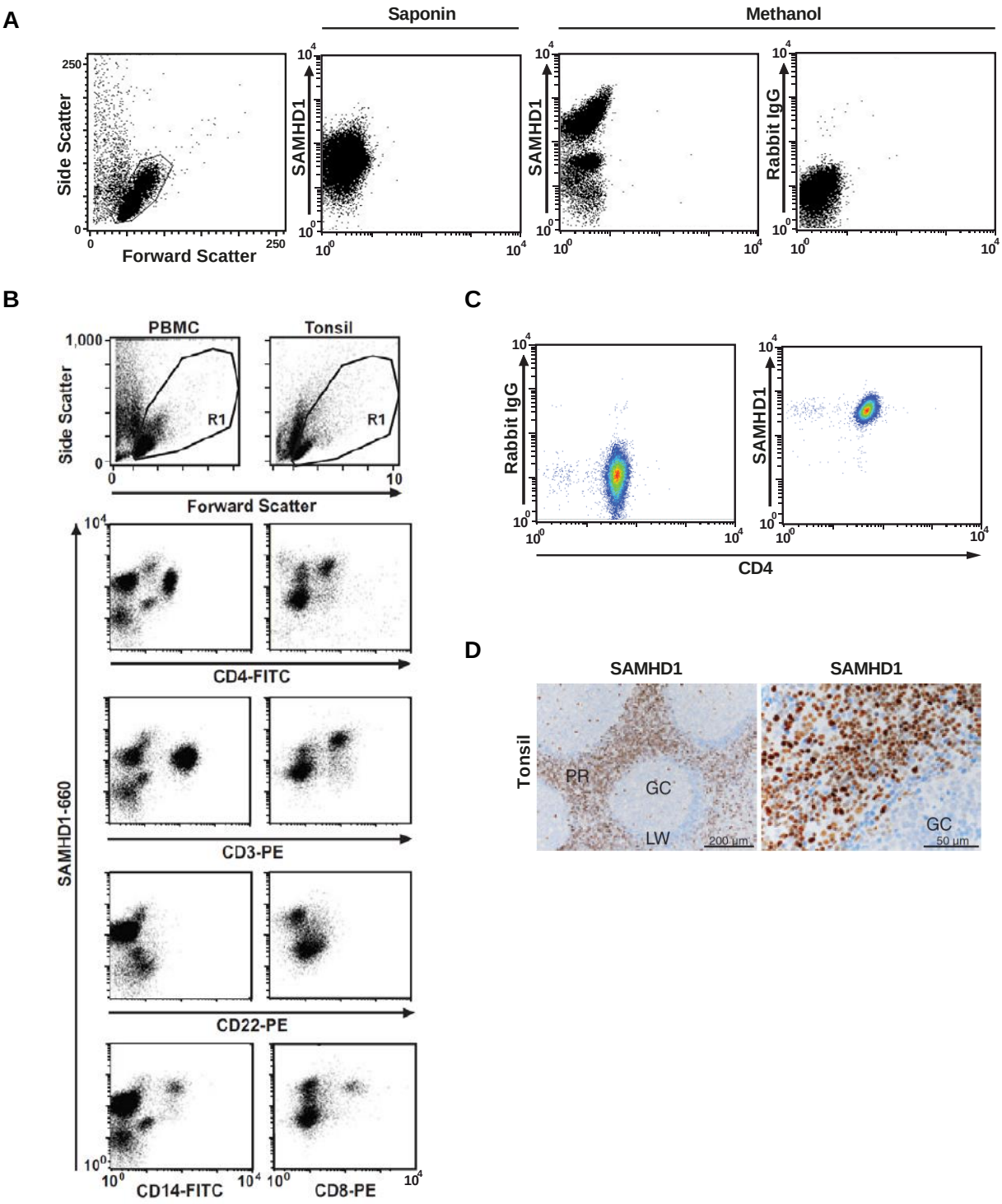

Fig. 4.13 Specific detection of SAMHD1 by flow cytometry and immunohistochemistry. (A) Freshly isolated PBMC or tonsil cells were fixed, permeabilized using either a saponin- or methanol-based protocol and stained with a rabbit polyclonal SAMHD1 antibody or rabbit IgG as a control. A secondary Alexa660-conjugated goat anti-rabbit antibody was used as a detection reagent, and cells were analyzed on a FACSCalibur. (B) Freshly isolated PBMC or tonsil cells were fixed, permeabilized and stained for SAMHD1 in combination with the respective lineage markers and analyzed by flow cytometry. (C) Resting CD4+ T cells were fixed and permeabilized as described in Materials and Methods and stained either with a rabbit control serum (left panel) or a rabbit anti-SAMHD1 serum (right panel). After co-staining with a secondary Alexa660-conjugated goat anti-rabbit antibody and an anti-CD4-FITC mAb, cells were analyzed by flow cytometry. (D) *In situ* expression of SAMHD1 in explants of human tonsil. Left and center, immunohistochemical detection of SAMHD1. Nuclei

were counterstained with hematoxylin. GC, germinal center; LW, lymphocyte wall; PR, perifollicular region. Modified from reference (**II**) and (**III**).

Vpx Degrades Endogenous SAMHD1 in Resting CD4+ T cells

Several studies have demonstrated that SAMHD1 is targeted by Vpx for CRL4/DCAF1 ubiquitin ligase-mediated proteasomal degradation (12, 92, 131). To assess the ability of Vpx to degrade endogenous SAMHD1 in resting CD4+ T cells from healthy donors, we co-expressed SIVmac239 Vpx (WT Vpx) or the DCAF1 interaction-deficient mutant Q76A (Q76A) with GFP. Upon Vpx co-expression, we detected a potent and Q76-dependent reduction of SAMHD1 levels by intracellular flow cytometry. Low levels of co-expressed GFP and WT Vpx were sufficient to maximally degrade SAMHD1 and diminished intracellular SAMHD1 levels by more than 90% (Fig. 4.14).

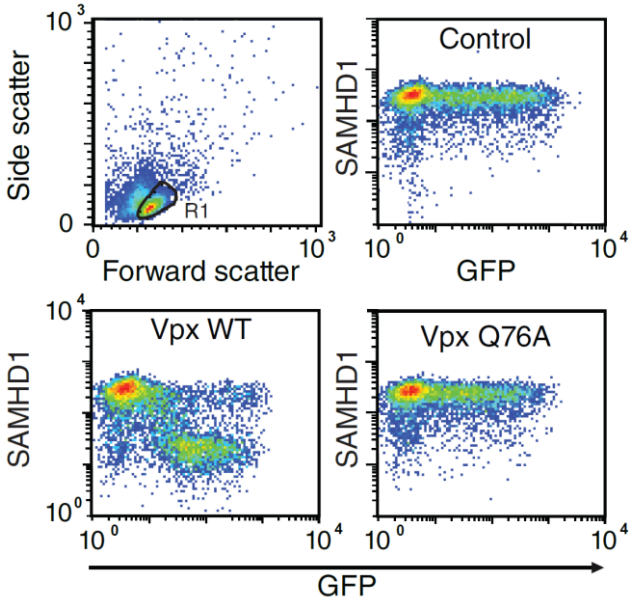

Fig. 4.14 Vpx mediates SAMHD1 depletion in resting CD4+ T cells. Quantification of intracellular SAMHD1 levels in nucleofected resting CD4+ T cells. Cells were nucleofected to co-express GFP in combination with WT Vpx, Vpx Q76A or an empty control and 16 h later analyzed for SAMHD1 expression in relation to GFP expression by flow cytometry. Modified from (**II**).

SAMHD1 Depletion is Specific for HIV-1 Virions with Incorporated Vpx WT or for HIV-2 WT Virions

To address the question whether Vpx would allow HIV-1 to infect resting human CD4+ T cells, we generated a replication-competent HIV-1 GFP reporter virus (HIV-1* GFP), into which we incorporated Vpx by adding a Vpx-interaction motif into the Gag p6 domain of the CXCR4-tropic HIV-1 strain NL4-3. When resting CD4+ T cells were infected with wild-type Vpx-carrying HIV-1 or its mutant variant (Vpx Q76A) incorporated (Fig. 4.15A), massive depletion of the cellular SAMHD1 pools were observed for wild-type Vpx-incorporated HIV-1 but not for the Vpx Q76A mutant

derivative (Fig. 4.15B). The Q76A-dependent SAMHD1 depletion correlated with enhanced infectivity (not shown). Similarly, successful HIV-2 infection correlated with Vpx-dependent degradation of SAMHD1 (Fig. 4.15C).

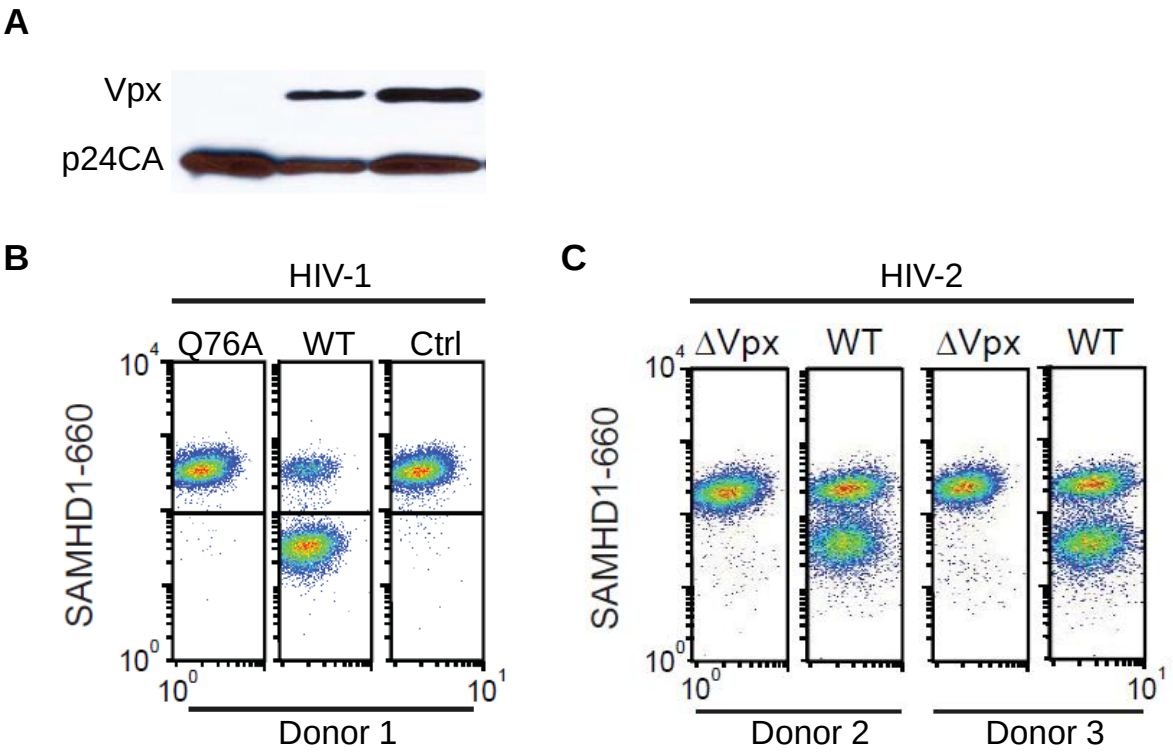

Fig. 4.15 SAMHD1 depletion is specific for HIV-1 virions with incorporated Vpx WT or for HIV-2 WT virions. (A) Immunoblot analysis of HIV-1* GFP virions carrying no Vpx (Control), Vpx WT or Q76A. (B) Resting CD4+ T cells were challenged with identical infectious units of the HIV-1 virions in Fig.4.15A and analyzed for intracellular SAMHD1 levels 1 day post infection. (C) SAMHD1 levels in resting CD4+ T cells were monitored by flow cytometry 3 days post-challenge with either HIV-2ROD9 (WT) or the Vpx-defective, isogenic counterpart (ΔVpx). Modified from (**II**).

Susceptibility of Resting CD4+ T Cells to Vpx-Carrying HIV-1 Is Paralleled by Proteasomal Degradation of SAMHD1

To explore the relationship between Vpx-mediated degradation of SAMHD1 and permissivity to HIV-1 in resting CD4+ T cells, we followed both parameters over time at a single-cell level. Whereas infection with HIV-1* GFP had no effect, SAMHD1 was massively depleted in 20–80% of cells 1 day after challenge with HIV-1* GFP plus SIVmac239 Vpx (Fig. 4.16A). This degree of depletion was constant until day 3 after infection, when GFP reporter expression indicated proviral integration and early viral gene expression (4.3% of cells in Fig. 4.16A). SAMHD1 degradation in resting CD4+ T cells was specific to HIV-1* GFP virions containing Vpx; it was observed as early as 6 hours after virion challenge and correlated in magnitude with the percentage of GFP+ cells (Fig. 4.16A,B). The peptidic virion fusion inhibitor T20 or the CXCR4 antagonist AMD3100 inhibited Vpx-dependent

depletion of SAMHD1 (Fig. 4.16C), demonstrating that this process strictly depends on virus entry and subsequent release of Vpx. Furthermore, the depletion of SAMHD1 and the enhancement of resting T cell infection by virion-packaged Vpx was abrogated by treatment of cells with the proteasome inhibitors MG132 (Fig. 4.16C) or ALLN (not shown).

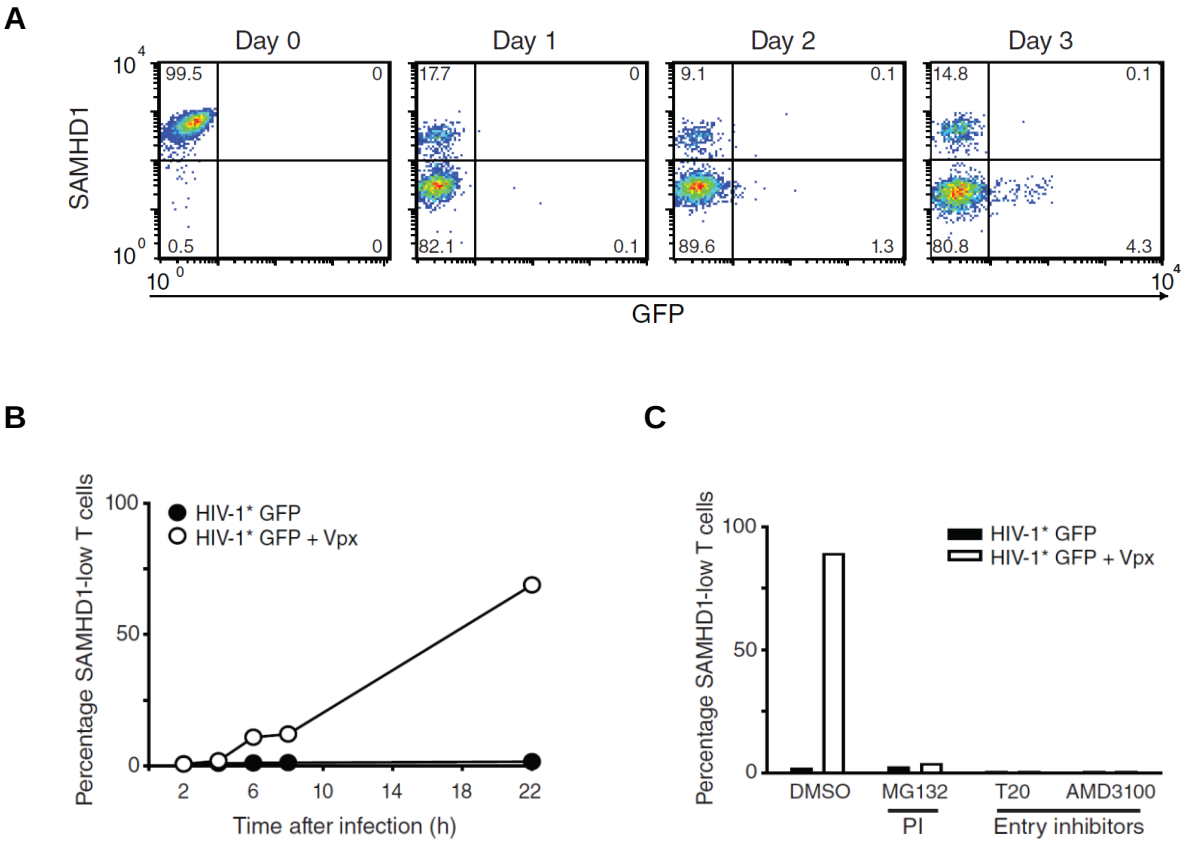

Fig. 4.16 Susceptibility of resting CD4+ T cells to Vpx-carrying HIV-1 is paralleled by proteasomal degradation of SAMHD1. (A) Time course of SAMHD1 and GFP expression in resting CD4+ T cells after challenge with HIV-1* GFP + Vpx (SIVmac239). The percentages of cells in the respective quadrants are shown. (B) Quantification of SAMHD1 expression in resting CD4+ T cells within the first 22 hours after exposure to HIV-1* GFP with (+ Vpx) or without (Control) incorporated Vpx. Data points mark the percentages for cells with low SAMHD1 levels (corresponding to the bottom left quadrants in FACS panels shown in A). (C) Effect of proteasome or HIV-1 entry inhibitors on SAMHD1 levels in resting CD4+ T cells after exposure to HIV-1* GFP ± Vpx. Resting CD4+ T cells were pretreated for 1 hour with either the proteasome inhibitor (PI) MG132 (10 µM), the fusion inhibitor T20 (50 µM) or the CXCR4 antagonist AMD3100 (5 µM) before infection with HIV-1* GFP with or without virion-packaged Vpx. Drugs were removed 20 hours later. Shown are the percentages of resting CD4+ T cells with low levels of SAMHD1 24 hours after infection for one of three donors. Modified from (**II**).

4.3 MOUSE SIGLEC-1 MEDIATES *TRANS*-INFECTION OF MURINE LEUKEMIA VIRUS IN A SIALIC ACID N-ACYL SIDE CHAIN-DEPENDENT MANNER

The Ig-type lectin Siglec-1 expressed on monocyte-derived DC has been demonstrated to bind to glycolipids in the HIV-1 membrane, thereby being able to capture viral particles as well as mediating their transfer to permissive CD4+ T cells (100, 168). This process, referred to as *trans*-infection, occurs by a two-step process in which the Siglec-1-expressing cell – which is usually itself non-permissive to the virus – first captures virus particles and can retain these viruses for a certain period of time. Transmission of viral particles is then mediated to permissive neighboring target cells, promoting viral dissemination and spread (99). In mice, Siglec-1 is highly expressed on specific macrophage subsets in the secondary lymphoid organs (122), and these cells have been described as critical for the clearance of viruses from the lymph, and also for initiating humoral immune responses (108). In this context, we investigated the role of mouse Siglec-1 in mediating *trans*-infection of MLV. We also studied the interaction between the Siglec-1 receptor and the virus particles, and how this interaction depends on the N-acyl side chain of the sialic acids that are exposed in the viral membrane gangliosides.

The following chapter is in preparation for publication and is modified from (**IV**).

Mouse Siglec-1 is Expressed on Macrophages, Upregulated by IFNα Treatment and Mediates MLV Trans-Infection of Lymphocytes

To explore the expression of Siglec-1 on the cell surface of mouse macrophages, cell line ANA-1 and L929-differentiated primary bone marrow-derived macrophages (BMDM) were stained with either rat anti-mouse Siglec-1 mAb 3D6.112 or an isotype control mAb and processed for flow cytometry. Cells, which had either been left untreated or exposed to mouse IFNα for 48 hours, were analyzed. ANA-1 cells exposed low constitutive levels of Siglec-1 on the surface, the expression of which could be induced 3- to 5-fold by IFNα stimulation (Fig. 4.17). BMDM expressed markedly higher constitutive, but also INFα-responsive levels of the sialic acid-binding Ig-like receptor on their cell surface.

For direct infection or *trans*-infection studies we employed a replication-competent ecotropic Moloney MLV carrying an IRES-*egfp* element (MLV-GFP) (68). The GFP reporter encoded by this recombinant retrovirus is expressed only upon productive infection of target cells. We first characterized the susceptibility of the cell lines and primary cells used in this study for direct, productive MLV-GFP infection. Virus exposure of the S1A.TB.4.8.2 (S1A.TB) T-cell lymphoma or LPS-activated primary mouse splenocytes demonstrated their high-level susceptibility (Fig. 4.18A), while neither BMDM (Fig. 4.18A) nor ANA-1 cells (data not shown) were permissive.

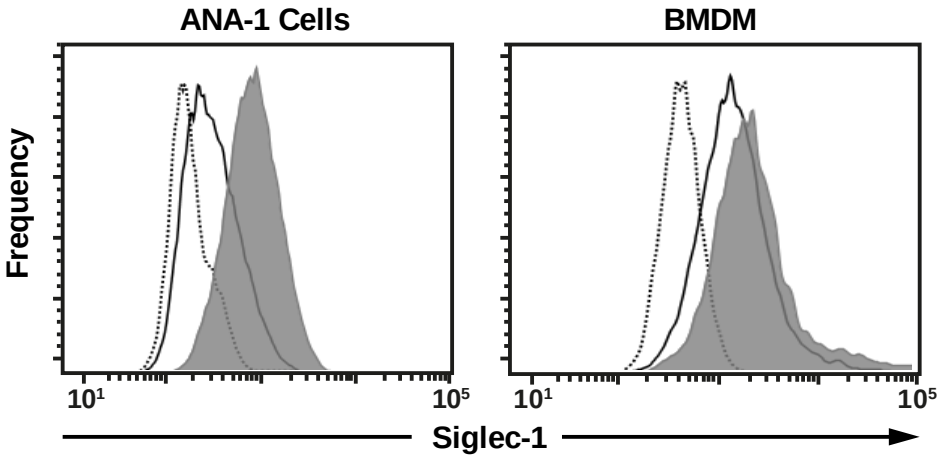

Fig. 4.17 Siglec-1 is expressed on mouse macrophages in an INFα-responsive manner. ANA-1 cells or L929-differentiated BMDM were stimulated with 500 U/mL mouse IFNα for 48 hours or left untreated. Mechanically detached cells were stained using a PE-conjugated anti-mSiglec-1 mAb or an isotype control mAb and analyzed by flow cytometry. Shown are untreated cells (black lines) or IFNα-treated cells (shaded histograms) stained for mSiglec-1 and untreated cells (dotted line) stained with the isotype mAb. Modified from (**IV**).

The inability of MLV to infect non-cycling macrophages is well established (135, 172) and an important characteristic to unambiguously assess their role as a virus donor in MLV *trans*-infection of lymphocytes in the current study. To explore the ability of mouse macrophages to capture and *trans*-infect MLV-GFP in a Siglec-1-dependent manner, BMDM or ANA-1 cells were first pretreated for 30 min at 4°C with blocking anti-Siglec-1 or isotype control mAbs, then exposed to MLV-GFP particles for 4 hours at 37°C, washed extensively, and subsequently co-cultured with target S1A.TB lymphocytes (Fig. 4.18B). Two days later the percentage of GFP-positive S1A.TB cells was analyzed by flow cytometry as a quantitative readout for the efficiency of *trans*-infection. ANA-1 cells and BMDM pretreated with the isotype control mAb mediated a robust MLV-GFP *trans*-infection (Fig. 4.18C). Their capacity for *trans*-infection was increased by IFNα pretreatment and this effect correlated with their Siglec-1 surface levels (Fig. 4.17 and data not shown). Importantly, MLV *trans*-infection was efficiently and specifically blocked when macrophages were pretreated with the anti-mouse Siglec-1 mAb. Thus, Siglec-1 on the cell surface of BMDM is constitutively expressed, IFNα-responsive and appears to have the capacity to mediate *trans*-infection of the simple retroviral pathogen MLV to permissive lymphocytes.

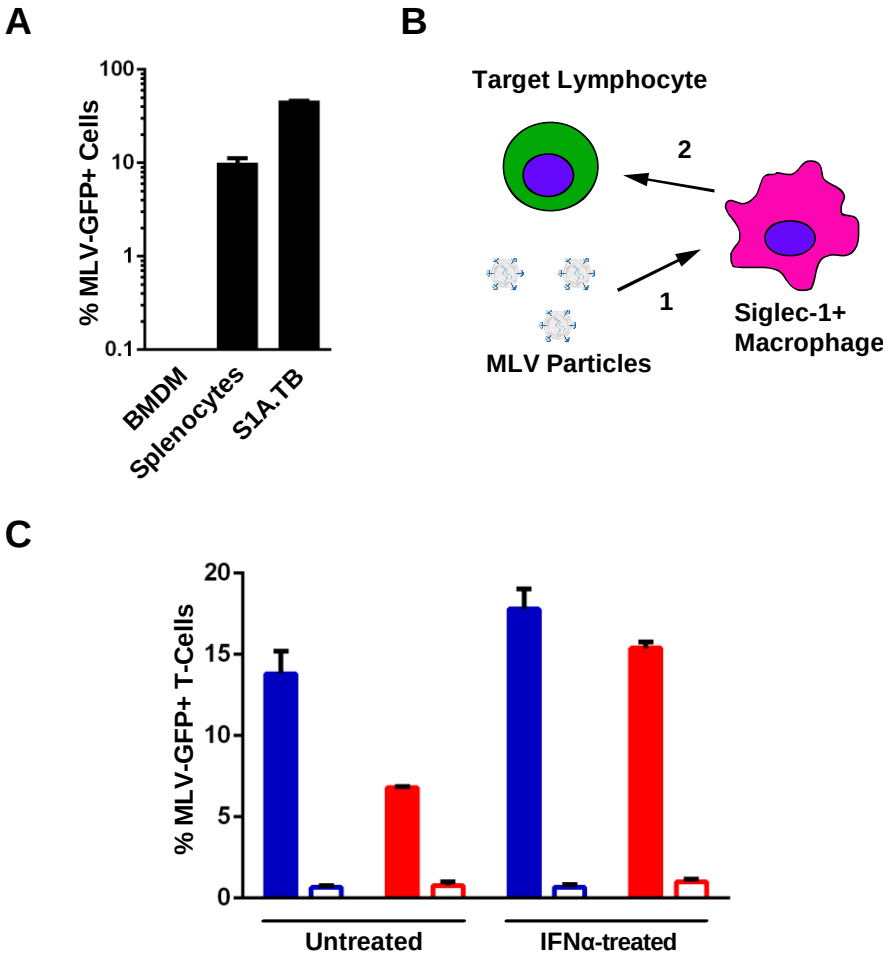

Fig. 4.18 Siglec-1 supports MLV *Trans*-Infection. (A) Each of the indicated cell types was infected with MLV-GFP (MOI 0.1) and two days later analyzed for GFP expression by flow cytometry. (B) Experimental set-up used for the experiments depicted in panel D for *trans*-infection. (C) L929-differentiated BMDM or ANA-1 cells were stimulated with 500 U/mL mouse IFNα for 48 hours or left untreated. Cells were pre-incubated with 10 µg/mL of an anti-Siglec-1 mAb or an isotype control mAb at 4°C, exposed to MLV-GFP (MOI 0.1) for 4 hours at 37°C and washed three times in PBS. S1A.TB cells were then added in a 1:1 ratio to the virus-pulsed macrophage cultures for 48 hours and then analyzed for GFP expression by flow cytometry. Data are expressed as the arithmetic means + S.D. (*standard deviation*) of triplicate samples from one mouse and are representative of at least two experiments each performed using 2-3 mice. Modified from (**IV**).

BMDM From Wild-type, But Not From Siglec-1 Knockout Mice Support MLV Capture and Trans-Infection

To further corroborate the role of mouse Siglec-1 in MLV *trans*-infection we employed Siglec-1 knockout (KO) mice, the generation and characterization of which has been reported (155). The genotype of mice was determined using an allele-specific PCR (Fig. 4.19A). The absence of Siglec-1 expression in KO mice carrying the homozygous (-/-) deletion was demonstrated in cultured BMDM (Fig. 4.19B) and mCD11b-positive cells of the monocyte/macrophage lineage in a freshly isolated lymph node suspension (Fig. 4.19C), in line with previous characterizations (127).

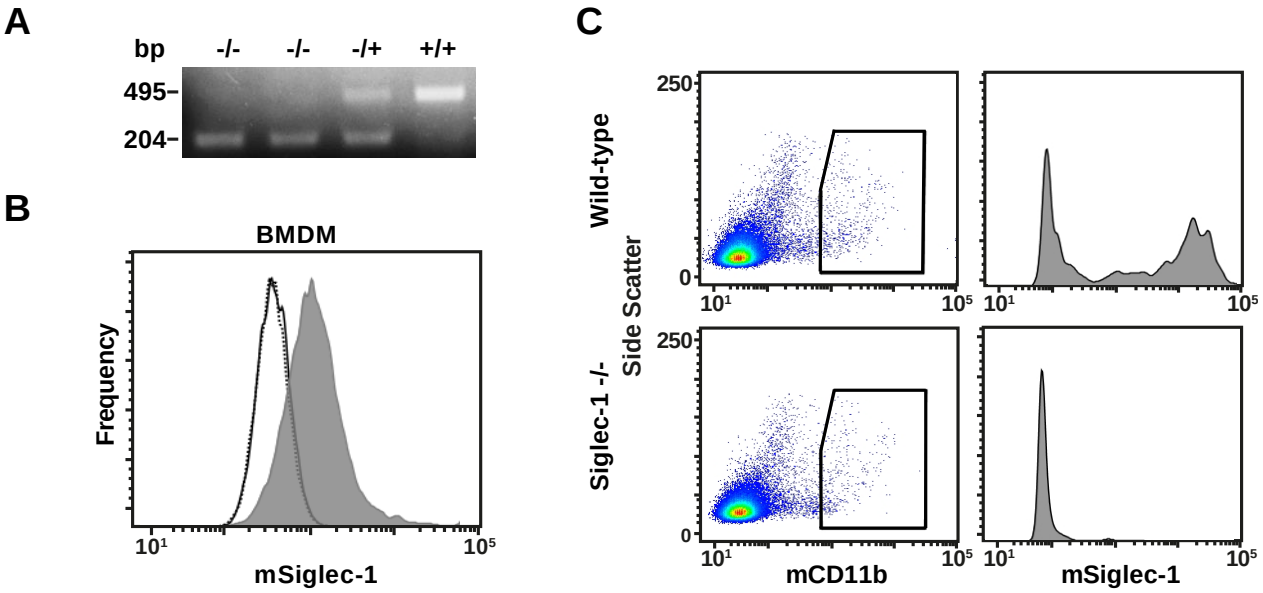

Fig. 4.19 Charachterization of Siglec-1 -/- mice. (A) Genotyping of Siglec-1$^{-/-}$ mice (KO mice) by PCR. DNA extracted from mouse tails was amplified using an allele-specific PCR. Product sizes of 495 bp or 204 bp are diagnostic for the wild-type (WT) and knockout (KO) allele, respectively. (B, C) Selected Siglec-1 phenotyping of KO and WT mice: (B) L929-differentiated BMDM and (C) freshly isolated, mechanically disrupted inguinal lymph nodes were stained for mSiglec-1 surface expression (in (C) co-stained for mCD11b) and analyzed by flow cytometry. (B) Shown are WT-BMDM (shaded histogram) or KO-BMDM (black line) stained for mSiglec-1 and WT-BMDM (dotted line) stained with the isotype mAb. From (**IV**) .

In a comparative assessment of Siglec-1-deficient KO and wild-type (+/+, WT) mice we explored whether Siglec-1-dependent capture of MLV particles could be quantified in BMDM. Two experimental approaches were taken: BMDM from WT and KO mice were incubated with MLV for 4 hours at 37°C, washed with PBS, detached by gentle scraping and processed for detection of either cell-associated MLV p30^{Gag} structural protein or cell-associated reverse transcriptase (RT) activity. For the first approach BMDM were fixed, permeabilized and stained using a rat anti-p30^{Gag} mAb. While flow cytometric analysis of MLV-exposed BMDM from KO mice showed only background staining (gate R2, Fig. 4.20A and Fig. 4.20B), BMDM from WT-littermates, which had been exposed to MLV particles for 4 hours, revealed a robust signal for the p30^{Gag} capsid staining (gate R2, Fig. 4.20A and Fig. 4.20B). For the second approach BMDM were lysed and processed for a SYBR Green I-based product-enhanced RT assay, a method previously developed for the quantitation of retroviruses in culture supernatants (162). MLV exposure of WT-BMDM, but not of KO-BMDM, resulted in a significant cell-associated RT activity (Fig. 4.20C). Next, BMDM derived from WT and KO mice were analyzed side-by-side for their capacity to mediate MLV *trans*-infection. In line with the above antibody-blocking studies (Fig. 4.18C), WT-BMDM efficiently *trans*-infected S1A.TB T-lymphocytes and LPS-stimulated splenocytes (Fig. 4.20D). In contrast, KO-BMDM were unable to

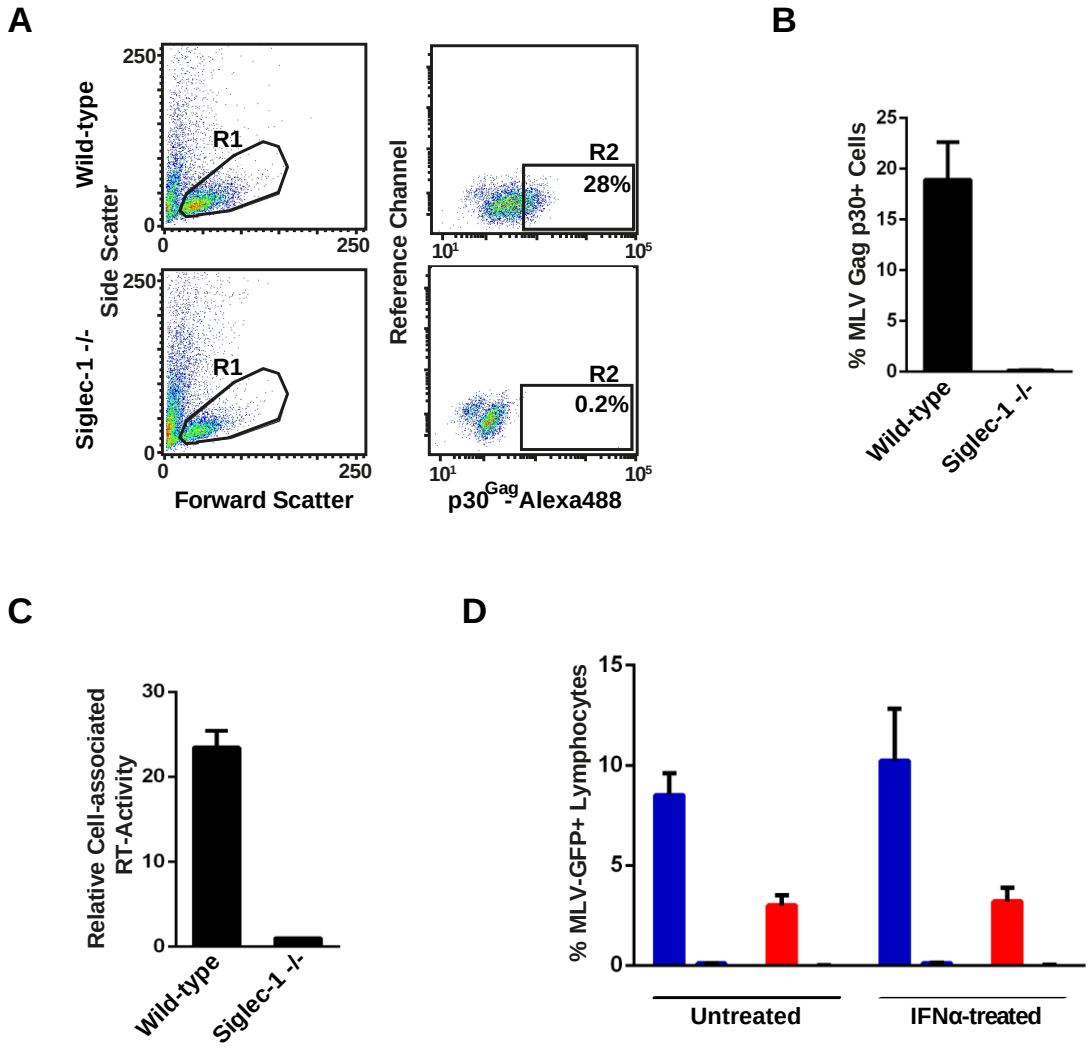

Fig. 4.20 BMDM from wild-type, but not from Siglec-1 knockout mice support MLV capture and *trans*-infection. (A-D) L929-differentiated BMDM from WT and KO mice were exposed to MLV-GFP for 4 hours at 37°C and subsequently washed three times with PBS. (A-C) MLV-GFP-pulsed BMDM were detached and analyzed for MLV capture by two methods: (A, B) First, pulsed cells (MOI 0.5) were fixed, permeabilized and stained with rat anti-$p30^{Gag}$ mAb followed by an Alexa488-conjugated secondary antibody. (A) Flow cytometric dot plots depicting (left panels) the forward- and side scattering of light (FSC/SSC) to identify live cells (gate R1) and (right panels) Alexa488 staining to identify cell-associated MLV $p30^{Gag}$ (gate R2). The percentage of viable cells within R2 is indicated. (B) Histogram bars depict the arithmetic mean + S.D. of the percentage of $p30^{Gag}$-positive cells from triplicates. (C) Second, pulsed cells (MOI 0.1) were detached, lysed and analyzed for cell-associated RT activity. (D) MLV-GFP-pulsed BMDM were co-cultivated with LPS-activated splenocytes at a 1:1 ratio. 48 hours later lymphocytes were analysed for GFP expression by flow cytometry. Data are expressed as the arithmetic means + S.D. (*standard deviation*) of triplicate samples from one KO and one WT mouse and are representative of at least two experiments each performed using 2-3 mice. From (**IV**).

support MLV *trans*-infection and IFNα stimulation could not overcome this limitation. Together, these results demonstrate that primary macrophages from mice are capable of capturing infectious MLV particles and of mediating a subsequent *trans*-infection of lymphocytes in a Siglec-1-dependent manner.

MLV-GFP Trans-Infection Is an Efficient Process That Preferentially Targets Activated Primary B-Cells

Next, we sought to assess the relative contribution of direct infection and *trans*-infection to the overall infection of cultured primary lymphocytes in the context of a constant multiplicity of infection. Furthermore, we tested the impact of two activation protocols for splenocyte cultures, i.e. treatment with either LPS and ConA/IL-2, which preferentially stimulate the proliferation of B-cells and T-cells, respectively (32, 47) on lymphocytes MLV-GFP susceptibility. WT-splenocyte cultures following LPS activation for three days consisted of 64% CD19-positive and 31% CD3-positive cells, expressed as fractions within the viable lymphocyte gate. In contrast, stimulation with ConA/IL-2 resulted in 97% CD3-positive T-cells (Fig. 4.21C).

Two interesting observations were made: First, in the absence of BMDM only LPS activation allowed for a robust direct infection of WT-splenocytes (4 ± 0.80%, Fig. 4.21A), the vast majority of which were blasted CD19-positive B cells (99.8%, data not shown). In comparison, the low-level infection of the ConA/IL-2-stimulated culture (0.2 ± 0.08%, Fig. 4.21A) represented both T cells (30%) and B cells (60%) (data not shown). Second, the experimental set-up in which WT-splenocytes (targets for both direct and *trans*-infection) and BMDM (donor cells for *trans*-infection), the latter derived from either WT or KO mice, were present in the culture at the time of virus addition, revealed that WT-BMDM were able to markedly boost the overall infection level of lymphocytes (Fig. 4.21A). For LPS-stimulated splenocytes, the co-culture with WT-BMDM raised the percentage of GFP-positive lymphocytes to 14 ± 1.30%, representing a 3- to 5-fold increase over the conditions with splenocytes alone or co-culture with Siglec-1-deficient BMDM (Fig. 4.21A). Virtually all infected cells were CD19-positive B-cells (Fig. 4.21B).

Remarkably, co-culture with WT-BMDM resulted also in a notable infection of ConA/IL-2-activated splenocytes translating to a 15-fold enhancement over the reference conditions (Fig. 4.21A) with both T-cells and B-cells being infected (Fig. 4.21C). Collectively these results indicate that Siglec-1-dependent *trans*-infection via macrophages may contribute to a more efficient infection process of lymphocytes in the context of a limited number of infectious MLV particles. Moreover, activated primary B-cells appear to be a preferential target of direct infection as well as *trans*-infection of MLV.

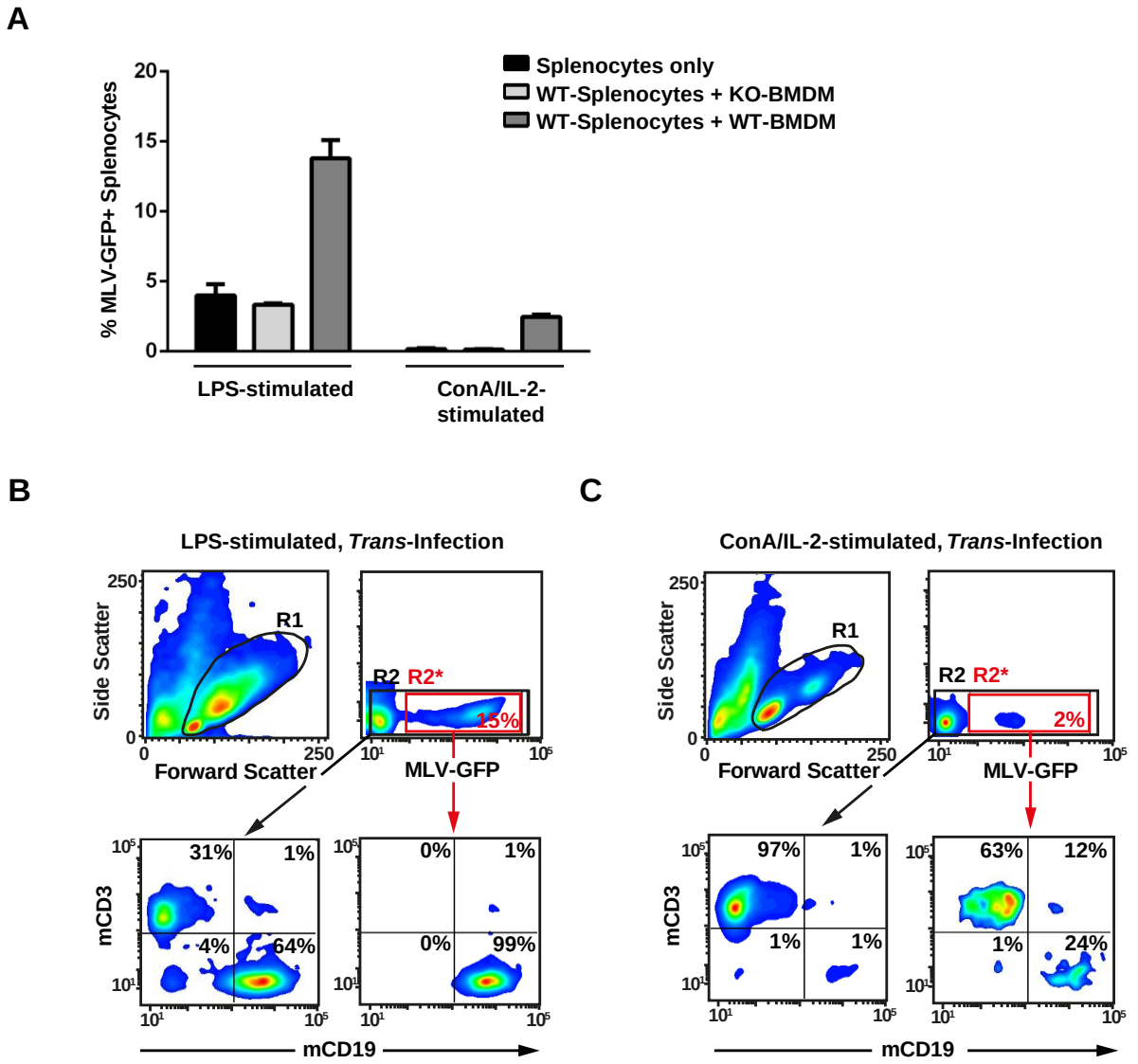

Fig. 4.21 BMDM-mediated *trans*-infection of MLV-GFP efficiently targets activated primary B-cells. Splenocytes from WT mice were activated with either LPS or ConA/IL-2 for 3 days and then seeded either alone or onto BMDM from WT or KO mice in a ratio of 1:1. Cultures were challenged with MLV-GFP (MOI 0.2) and splenocytes analyzed for GFP expression 48 hours later by flow cytometry. (A) Histogram bars depict the arithmetic means + S.D. (*standard deviation*) of the percentage of GFP-positive, viable cells from triplicates. Experiments were performed using 2-3 KO or WT mice and repeated at least twice showing similar results. (B, C) The identity of the MLV-GFP-infected splenocytes was determined by co-staining for the lineage markers CD3 (T-cells) and CD19 (B-cells). R1 identifies the viable cells. R2* (red box) identifies the MLV-GFP-positive cells and R2 (black box) all viable cells. Dot plots in the lower panels depict the respective mCD3/mCD19 stainings. Modified from (**IV**) .

Mouse Siglec-1 and MLV Gag Partially Co-localize in Intracellular Compartments Early After Virus Exposure

Next, we investigated the fate of Siglec-1 and MLV in BMDM early and late after virus exposure by co-immunofluorescence microscopy and *trans*-infection analysis. BMDM derived from WT or KO mice were pulsed with either MLV-GFP or MLV-Gag-GFP, for 4 hours at 37°C and then extensively washed. The latter virus carries Gag-GFP fusion proteins within the particle. BMDM grown on cover slips were either fixed immediately after pulse ("4 hours") or cultivated for another 20 hours ("24 hours") and stained with antibodies to mSiglec-1. At the 4-hour time point, mSiglec-1 and Gag-GFP partially co-localized in distinct punctae in WT-BMDM (Fig. 4.22B, upper and middle panels). Two phenotypes were frequently observed: A dominant single accumulation of the mSiglec-1 receptor and the viral structural protein was observed in 69 % of cells (Fig. 4.22B, upper panels), resembling the sac-like compartment reported for human Siglec-1 and HIV $p24^{Gag}$ in myeloid dendritic cells (100). In 31% of BMDM a more scattered cytoplasmic localization of Siglec-1 and Gag-GFP was noted with up to 100 distinct punctae, in which signals for both proteins partially overlapped (Fig.4.22B, middle panels). No colocalization of the mSiglec-1/ Gag-GFP-positive punctae with a marker for acidic lysosomes was observed (Fig. 4.22E). BMDM from KO mice displayed only background staining for mSiglec-1 and at most a few small Gag-GFP signals consistent with their inability to capture and *trans*-infect MLV (Fig. 4.22B, lower panels, Fig. 4.22A). Interestingly, at 24 hours, the frequency and intensity of the punctae for both mSiglec-1 and Gag-GFP in WT-BMDM were strongly diminished (Fig. 4.22C).

In parallel to the microscopic analyses we assessed the ability of BMDM to *trans*-infect S1A.TB cells immediately after the virus pulse ("4 hours") and after the prolonged storage period. Remarkably, delayed addition of target T-cells at only 24 hours resulted in a drastic drop in the efficiency of *trans*-infection, levels of 2% compared to the condition in which the S1A.TB cells had been added to the BMDM at the 4-hour time point (Fig. 4.22A). Neither the loss of capsid signal in immunofluorescence nor the drop in *trans*-infection could be rescued by pre-treating the BMDM with proteasomal or lysosomal inhibitors (data not shown). In conclusion, mSiglec-1 and MLV Gag partially co-localize in intracellular compartments in BMDM early after virus exposure. Within 24 hours the detection of the viral structural protein is greatly diminished coinciding with a marked reduction in the ability of pulsed BMDM to *trans*-infect.

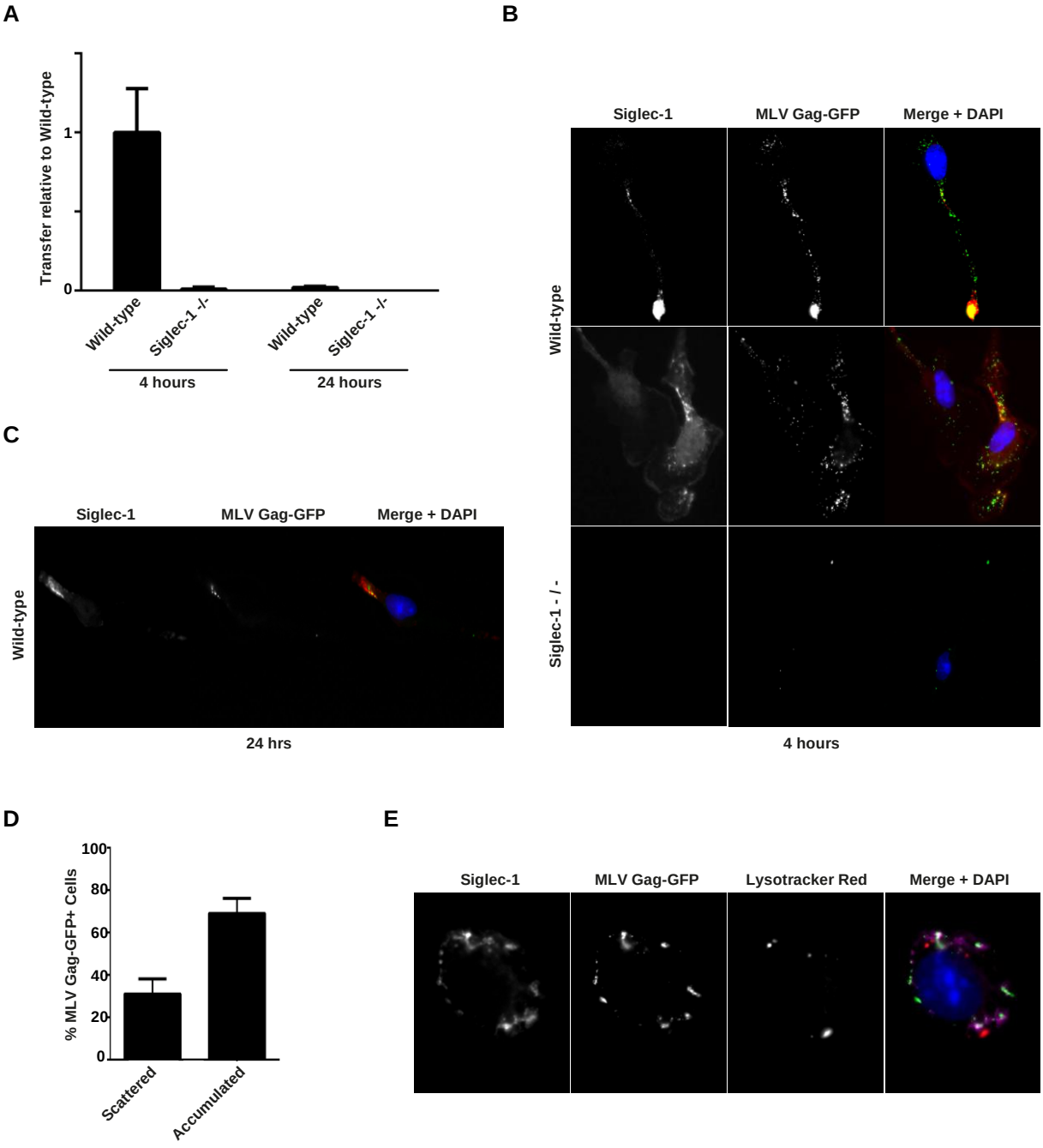

Fig. 4.22 Captured MLV particles partially co-localize with Siglec-1 in BMDM early after virus exposure. BMDM derived from either WT or KO mice were pulsed with (A) MLV-GFP or (B-E) MLV Gag-GFP, which carries a Gag-GFP fusion protein, for 4 hours at 37°C. PBS-washed BMDM were either (A) co-cultivated with S1A.TB-cells added either immediately after washing (4 hours) or 20 hours later (24 hours) or (B, C, E) fixed, permeabilised and stained using an Alexa647-conjugated anti-Siglec-1 mAb. Representative images for (B, upper panels, 4h) a dominant single accumlated MLV Gag/Siglec-1 signal or (B, middle panels, 4h) multiple scattered punctae from WT-BMDM are shown. (B, bottom panel) Images of MLV-Gag-GFP-pulsed KO-BMDM stained for mSiglec-1. (D) The MLV Gag pattern (”scattered” or ”accumulated”) and frequency of WT-BMDM displaying this phenotype were quantified. At least 70 cells from each of three mice were analysed. (E) The lysosomal marker Lysotracker Red was added to BMDM 30 minutes before fixation. Modified from (**IV**).

Biosynthetic Modulation of the N-Acyl Side Chain of Sialic Acid in Virus Producer Cells Affects the Ability of MLV Particles for Siglec-1-Dependent Capture and *Trans*-Infection

We then sought to functionally explore the role of the sialic acid for the Siglec-1-dependent *trans*-infection of MLV at a submolecular level in living cells by employing metabolic oligosaccharide engineering (117, 138). This experimental approach is based on the established ability of synthetic N-substituted D-mannosamine (ManN) derivatives to act as metabolic precursors for sialic acids with structurally altered N-acyl side chains incorporated into cellular glycoconjugates, including sialylated gangliosides that are incorporated into budding retroviruses (19, 27). We first pretreated 293T cells with six different synthetic N-acyl-modified ManN analogs (Fig. 4.23) or the most common physiological precursor, N-Acetyl ManN (ManNAc), for five days at non-toxic concentrations.

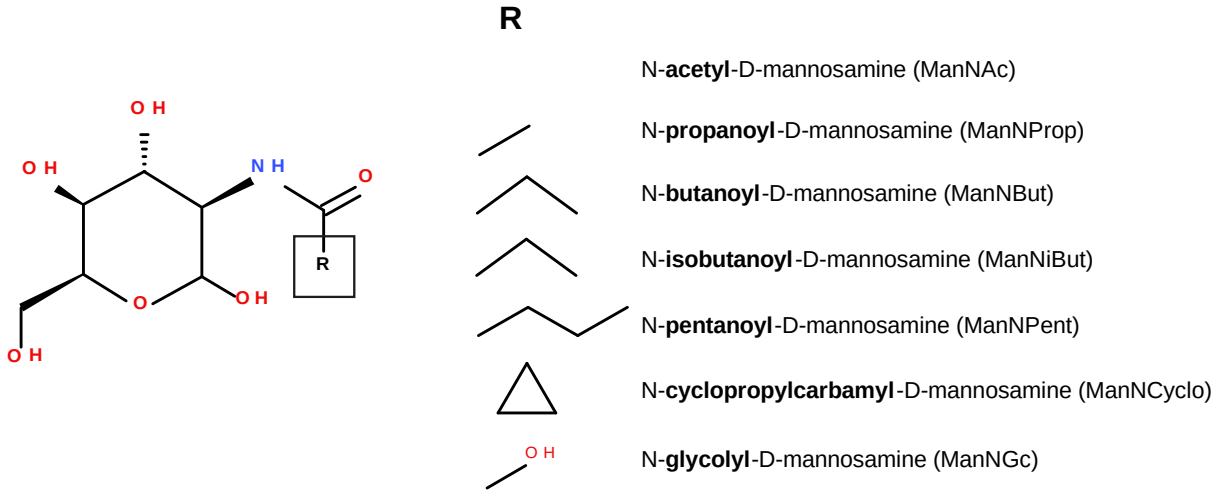

Fig. 4.23 N-acyl side chain modifications in ManN derivatives added to virus producer cells. (A) Schematic representation of ManNAc and the applied N-substituted ManNs with R indicating the modified N-acyl group. From (**IV**).

Subsequently, re-seeded cells were transfected with MLV-GFP proviral DNA and cultivated in the presence of the respective ManN derivatives for two more days. Released MLV-GFP particles were concentrated and purified by ultracentrifugation through a 20% sucrose cushion and cell pellets frozen for biochemical characterization. The preparations of MLV-GFP particles released from ManN analog-pretreated 293T cells were first titered on S1A.TB T-cells, the binding and infection process of which is believed to be mediated by the mCAT receptor in a sialic acid-independent manner (174). Next, employing the standard experimental set-up, the MLV-GFP particle preparations were assessed for their functionality to be captured by Siglec-1-positive WT-BMDM and to *trans*-infect S1A.TB T-cells. In parallel, the inocula of the different MLV-GFP stocks were used to infect S1A.TB T-cells directly (Fig. 4.24A), confirming that comparable infectious titers had indeed been applied. Striking functional differences were however observed for capture and *trans*-infection: MLV-GFP particles released from 293T cells pretreated with N-butanoyl, N-isobutanoyl, N-glycolyl, or N-pentanoyl-

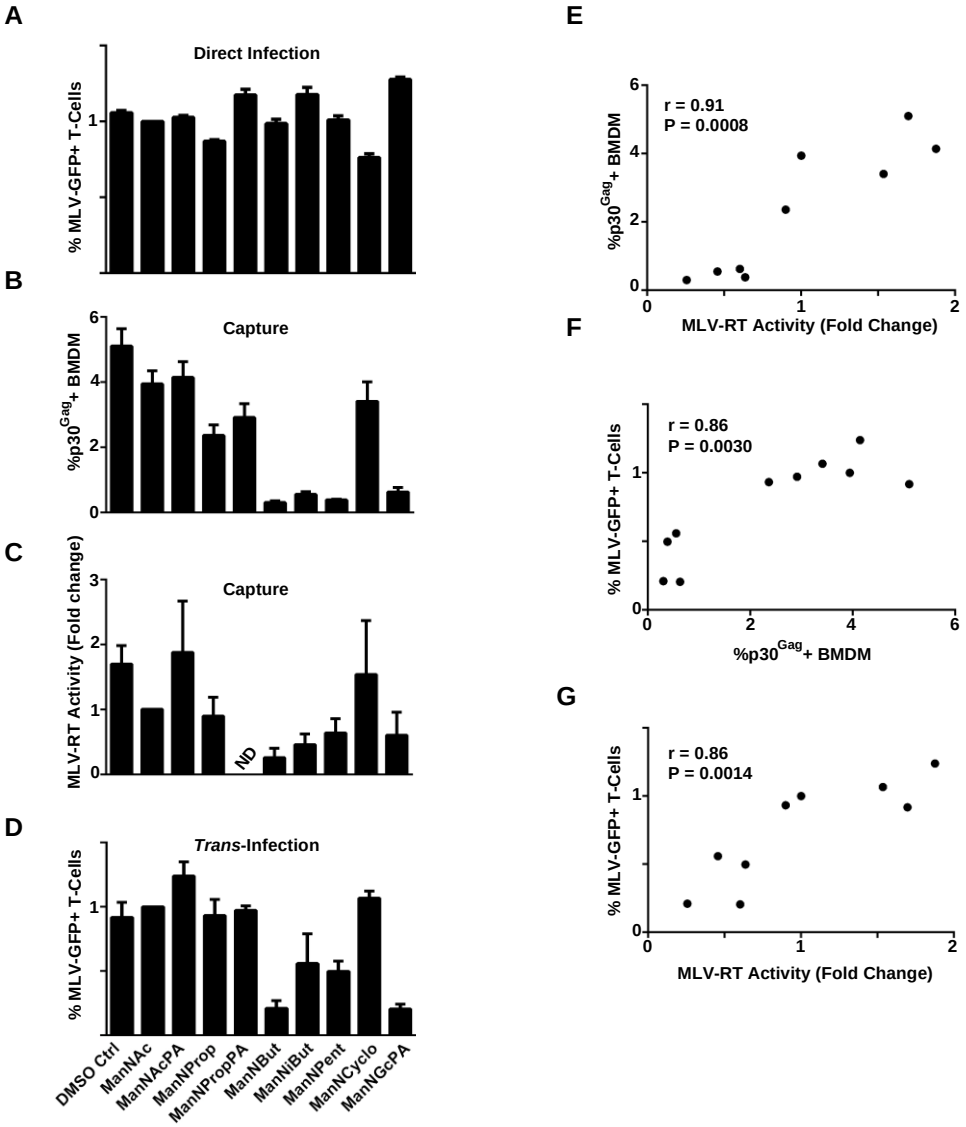

Fig. 4.24 Diminished capture and transfer of MLV particles derived from producer cells carrying certain N-acyl-substituted sialic acids. (A) S1A.TB cells were directly infected with MLV-GFP stocks (MOI 0.1) produced in the absence or presence of the indicated ManN analogs and analyzed two days later for GFP expression. (B-D) WT-BMDM were pulsed with MLV-GFP stocks (B: MOI 0.5; C, D: MOI 0.1) produced in the absence or presence of the indicated ManN analogs for 4 hours at 37°C. Washed cells were then either analyzed for MLV capture by (B) quantification of $p30^{Gag}$-positive cells by flow cytometry or (C) cell-associated RT activity, in principle as reported in the legend to Fig. 4.20, or (D) used for *trans*-infection of S1A.TB cells. Data are expressed as the arithmetic means + S.D. (*standard deviation*) of triplicate samples from one mouse and are representative of at least two experiments each performed using 2-3 mice. (E) Correlation between the relative efficiency of virus capture (data depicted in panels B, C) and *trans*-infection (panel D) for the 10 different MLV-GFP stocks. Pearson correlation coefficients and significance values were calculated by applying the two-tailed, unpaired Student's *t*-test. Modified from (**IV**).

modified sialic acid precursor analogs were only inefficiently captured by BMDM, while N-propanoyl or N-cyclopropylcarbamyl ManN treatments had no or only slight effects (Fig. 4.24B-D). Levels of cell-associated MLV $p30^{Gag}$ staining and cell-associated RT activity were reduced by up to 92% (Fig. 4.24B, C) and these capture readouts strongly correlated (Fig. 4.24E, r=0.91, p=0.0008). In support of

a cardinal role of virus capture for the efficiency of subsequent *trans*-infection, levels of MLV-GFP infection in S1A.TB cells were markedly reduced for viruses derived from producer cells exposed to the N-butanoyl, N-isobutanoyl, N-glycolyl, or N-pentanoyl ManNs (Fig. 4.24D) and these infection levels correlated with both readouts for virus capture (Fig. 4.24E-G). Collectively, these results suggest that biosynthetic engineering of glycoconjugates in virus-producer cells is a feasible strategy to alter the composition of sialylated glycolipids and glycoproteins within the envelope of viruses that bud from the plasma membrane allowing their functional characterization. Specifically, this approach allowed us to identify the N-acyl side chain of sialic acid as a critical determinant for the mSiglec-1-MLV particle interaction.

5. DISCUSSION

5.1 WIDESPREAD CD317-EXPRESSION IN HUMAN TISSUES – BUT NOT IN HIV-1 TARGET CELLS

This chapter has been published during the course of this thesis and is modified from (**I**).

Our *in vivo* expression profiling of the antiviral restriction factor and potential tumor-targeting antigen CD317 in nontransformed human organs documented widespread tissue expression on a number of specialized cell types. This stands in contrast to a previous report suggesting selective expression of CD317 on the surface of nontransformed, terminally differentiated B cells (71). Explicitly, that earlier study described a lack of CD317 expression on PBMCs, lymph nodes, liver, spleen, kidney, and heart, applying the identical anti-HM1.24 mAb. Although we can confirm CD317 expression on plasma cells, our study identified many additional CD317+ cell types and tissues throughout the body, greatly expanding the expression profile of this protein. We suspect that differences in the sensitivity of immunodetection might underlie this discrepancy. Our findings refute the widely held belief that the constitutive expression of CD317 in humans is highly restricted, a misperception that has spurred antibody-based immunotherapy strategies for multiple myeloma and certain solid human tumors (28, 71, 103, 114, 158), (8, 22, 113, 181, 201). In line with our findings, a previous Northern blot analysis documented CD317 mRNA in several tissues, including pancreas, liver, lung, and heart (96).

5.1.1 CD317 is expressed on cell types targeted *in vivo* by enveloped viruses

The role of CD317 in the control of virus replication *in vivo* is not completely understood; however, several lines of evidence point to an important antiviral capacity of CD317 in mammals. First, various completely unrelated viruses (i.e., lentiviruses, herpes viruses, filoviruses, orthomyxoviruses) encode CD317 antagonists with distinct modes of action to overcome the restriction imposed by CD317 (48). Second, anti-CD317 activities have evolved in three different lentiviral genes (nef, env, and vpu) (120), implying a critical role of CD317 in the lentivirus–host adaption and cross-species transmission. In support of this notion, a nef-deleted simian immunodeficiency virus rapidly acquired compensatory changes in gp41 in infected rhesus macaques that restored resistance to CD317/tetherin (178). Third, CD317 proteins from different species show evidence of positive selection, consistent with adaptations in response to invading viruses (120). The present study establishes that CD317 is expressed on a variety of specialized cell types known to be *in vivo* targets for enveloped viruses. For example, vascular endothelial cells, identified as high CD317 expressers, are major replication sites of hemorrhagic fever viruses (e.g., Lassa virus, Ebola virus, Hantaan virus), as well as KSHV, vesicular stomatitis virus, and herpes simplex virus (197). In the lung, CD317+ type I and II alveolar pneumocytes are targeted by various respiratory pathogens, including influenza viruses (79), severe acute respiratory syndrome coronavirus (81), and respiratory syncytial virus (107). Remarkably, cell culture experiments have already demonstrated that CD317 can exert antiviral activity against some of

these pathogens, including Lassa virus, vesicular stomatitis virus, influenza A virus, Ebola virus, and KSHV (48, 210). Intriguingly, the latter three viruses encode CD317 antagonists, indicating evolutionary adaptation of these pathogens. In addition, hepatocytes, monocytes, epithelial cells, terminally differentiated B cells, and bone marrow stromal cells, which express CD317 *in vivo*, are sites of replication for diverse viruses. The insights provided by the current expression profiling underscore CD317's *in vivo* relevance as an antiviral factor and suggest the possibility of future studies to investigate whether some of these other viruses are affected by this restriction factor and/or have evolved antagonists.

5.1.2 Origin of Vpu's function to antagonize CD317

Although HIV encodes potent CD317 antagonists, namely Vpu and Env, it remains unclear where the virus actually encounters CD317 *in vivo*. In secondary lymphoid organs and gut epithelium, major cell types for productive infection (i.e., CD4 T cells, macrophages, dendritic cells, and pDC) did not express significant levels of CD317. Although the subset of CD16+ monocytes might serve as an HIV-1 reservoir (31), it seems unlikely that this minor population of infected, CD317+ cells exerts sufficient selection pressure for HIV to preserve CD317 antagonistic activities. It is conceivable that systemic responses in HIV-infected individuals enhance CD317 expression in CD4 T cells, or that susceptible cells in other anatomic compartments, such as genital mucosa, show a different profile of constitutive expression and regulation. In support of the former notion, a previous study found that CD4 T cells in blood and lymph nodes from African green monkeys and rhesus macaques rapidly up-regulated CD317 mRNA after simian immunodeficiency virus infection (101).

5.1.3 *In vivo* regulation of CD317 expression

Secretion of type I IFNs from virus-infected cells is a hallmark of antiviral immunity. Potential target cells of infection that receive these signals increase expression of IFN-stimulated genes, many of which are linked to antiviral functions (69, 105, 191). The IFN responsiveness of CD317 in cultured primary cells is subtle; monocyte-derived macrophages up-regulated CD317 mRNA levels by less than twofold (78), and protein levels were elevated only slightly (145). Moreover, in the present study, type I IFN stimulation increased CD317 levels on isolated pDC only moderately, and CD317 expression on lymphocytes in tonsil was largely unresponsive to IFN. In line with the latter observation, virtually no co-expression of CD317 and the strictly IFN-induced restriction factor MxA was observed in tonsillar and pulmonary tissue. In contrast, the abundant MxA–CD317 co-expression in vascular endothelial cells is consistent with an IFN-mediated co-stimulation. Taken together, these findings suggest that type I IFNs may be a key regulator of CD317 expression only in certain cell types and tissues. Conceivably, other cytokines (e.g., TNF-α, IL-1, IL-6) secreted by the host in response to a viral insult may possibly trigger CD317 expression *in vivo* (156).

Along with antiviral activity, other functions of CD317 are starting to emerge for which knowledge of CD317's *in vivo* expression profile is of interest, including its proposed capacity as a negative *trans* regulator of pDC responses (25) and as an organizer of the subapical actin cytoskeleton in polarized epithelial cells (173). In support of the relevance of the latter function, gallbladder epithelial cells, which express high levels of CD317 in situ (Figs. 4.4A and 4.5), are characterized by a particularly pronounced structural polarization (157). From a therapeutic perspective, the widespread expression of human CD317, in particular its presence on a number of vital cell types, calls into question the proposed development of tumor-selective, CD317-based targeting strategies.

5.2 SAMHD1 EXERTS ANTIVIRAL ACTIVITY IN RESTING CD4+ T CELLS

SAMHD1 has been reported to potently restrict productive HIV-1 infection at an early stage of the viral replication cycle in monocytes and DC (92, 131), but was assumed not to be effective in T cells due to its absence in several transformed T cell lines. Previous immunofluorescence analyses of SAMHD1-expressing cells demonstrated a clear nuclear localization of the protein (17). We could show that SAMHD1 is abundantly expressed in resting CD4+ T cells circulating in peripheral blood and residing in lymphoid organs, and the protein could be found both in the nuclear and in the cytoplasmic compartment (**II**).

5.2.1 Monitoring restriction factor activity and regulation by flow cytometry

To monitor SAMHD1 levels during the course of an infection with a GFP-encoding virus, and to investigate its *in vivo* expression levels in specific cell types, it was important to establish a staining protocol for flow cytometry for this mainly nuclear protein. Depending on the protein's location inside the cell, different staining strategies work differently well. Saponin-based permeabilization methods are commonly used to detect intracellular antigens such as cytokines, but nuclear antigens usually require stronger permeabilization conditions that allow the antibody to enter the nucleus and access the epitope(s). For this purpose, we employed a methanol-based permeabilization protocol normally used for phosphoepitope detection by flow cytometry (126). This permeabilization strategy was required to enable detection of a distinct SAMHD1+ population, whereas a saponin-based method yielded only dim staining. Recent findings demonstrate SAMHD1 antiviral activity to be determined by its phosphorylation status, where phosphorylation at residue T592 renders SAMHD1 incapable of blocking retroviral infection (34, 204). This phosphorylation was suggested to be induced upon T cell activation, whereas treatment with type-I IFN resulted in reduced phosphorylation (34). Detection of phospho-SAMHD1 by flow cytometry could be a useful tool for monitoring – at a single cell level – phosphorylation status and antiretroviral activity of SAMHD1 in primary cells, although this would require further optimization and establishment of activation and/or inhibition protocols.

5.2.2 SAMHD1 restricts HIV-1 infection in resting CD4+ T cells and is depleted by Vpx

The data showing that Vpx, delivered to primary resting CD4+ T cells either by transfection or by infection using HIV-1 or HIV-2 virions into which viral Vpx was artificially or naturally packaged, respectively, was able to deplete endogenous SAMHD1 and in the latter case overcome the restriction, suggest that HIV-1 reverse transcription is actively suppressed in resting human CD4+ T cells, and that SAMHD1 is a cellular factor that is responsible for this restriction. When primary resting CD4+ cells were infected with a Vpx-carrying HIV-1* GFP virus and followed over a 3 days' time course, GFP+ cells were detected exclusively within the population of cells containing low amounts of SAMHD1, whereas the residual cell population expressing high amounts of SAMHD1 remained refractory to HIV-1 infection. Virion-incorporated Vpx seemed insufficient to render all resting CD4+ T cells permissive for HIV-1 infection, suggesting either additional blocks insensitive to Vpx-mediated counteraction (60, 74, 111, 185, 209), or SAMHD1 depletion by defective virions still carrying Vpx.

5.2.3 SAMHD1's antiviral action

SAMHD1 was first characterized as a deoxyribonucleotide triphosphate (dNTP) triphosphohydrolase, an activity that localized to the HD-domain of the protein (70, 166). Accordingly, alleviating the SAMHD1 block of HIV-1 infection by depletion of SAMHD1 correlated with a loss of dNTPase activity and increased dNTP pools in myeloid cells (132). More recently, a second enzymatic function of SAMHD1 has been identified; apart from cleaving monomeric dNTPs, the HD-domain also exhibits exonuclease activity against single-stranded DNA and RNA and can thus degrade poly(ribo)nucleotides (10). Interestingly, recent studies claim that phosphorylation of T592 in SAMHD1, relieving the anti-HIV restriction, has no impact on dNTPase activity (204). This argues against a mechanistic role of dNTP depletion in HIV-1 restriction which is consistent with the relatively moderate changes of dNTP levels observed in our work (**II**). It would be interesting to investigate whether phosphorylation of this residue affects (decreases) the exonuclease activity, because that would open up for the possibility that SAMHD1 restricts HIV-1 replication by degrading the viral genetic components. Interestingly, an even more recent study suggests that the RNase function of SAMHD1 may be primarily responsible for its restriction activity. This study also demonstrated that phosphorylation of SAMHD1 at T592 decreases the RNase activity of the protein, this correlating with impaired HIV-1 restriction (175). More research is necessary to identify and characterize the possible HIV-1 polynucleotide intermediates (RNA, DNA or RNA-DNA hybrids) that are recognized and cleaved by SAMHD1. Resting CD4+ T cells constitute a large pool of noncycling cells in secondary lymphoid organs. In HIV-1 infection, these cells are "bystanders" that only become abortively infected – something that SAMHD1 might be partly responsible for. After infection is aborted in these cells they undergo cell death, causing massive T cell depletion, destruction of the lymphoid tissue, and eventually AIDS (53). Recent studies (44, 45, 146) describe how HIV-1 DNA products generated during this abortive infection can be sensed by the

cytoplasmic DNA sensor IFI16 (see section 1.1.2.2), this triggering CD4+ T cell death through an inflammatory cell death pathway called pyroptosis. More research is also needed to investigate whether additional sensors of nucleic acids are involved in mediating T cell immunopathology and AIDS pathogenesis.

5.3 SIGLEC-1+ MACROPHAGES MEDIATE MLV *TRANS*-INFECTION

This chapter is in preparation for publication and is modified from (**IV**).

In the current study we demonstrate that Siglec-1 is a key receptor on primary mouse macrophages for capture of the enveloped retrovirus and mouse pathogen MLV and its efficient trans-infection of interacting lymphocytes. Terminal sialic acid residues on plasma membrane-derived sialyllactose-containing gangliosides that are incorporated into the envelope of budding retroviral particles are the key interaction moiety with the lectin receptor Siglec-1. Using metabolic engineering we introduced various N-acyl modified sialic acids into glycoconjugates of virus producer cells and demonstrate that for some substitutions newly produced MLV particles were functionally impaired for Siglec-1-dependent capture and trans-infection. This highlights the use of sialic acid precursor analogs as a feasible approach to study in a native environment the impact of submolecular modifications in glycoconjugates incorporated into enveloped viruses and identifies the N-acyl side chain as a critical determinant for the mSiglec-1-MLV interaction. Collectively, mSiglec-1 is an important receptor for the sialic acid-dependent macrophage/lymphocyte trans-infection of MLV ex vivo.

5.3.1 Virus capture: enforcing or restricting viral spread?

Macrophages and dendritic cells patrol peripheral mucosal sites recognizing, capturing and processing potential pathogens into antigenic peptides for MHC class II presentation to CD4 T-cells in lymphoid tissue (5). Landmark studies by Geijtenbeek and colleagues proposed that HIV-1 usurps this natural DC function in the newly infected host by "hiding" inside DC, which traffic to lymphoid organs, probably taking advantage of the formation of DC-/T-cell conjugates to promote its replication and spread (64, 65, 130). Today it is widely believed that human DC capture and internalize infectious HIV particles into clustered "storage" compartments and subsequently transfer these virions to neighboring T-cells at virological synapses (63, 99). In contrast to the virus-promoting scenario proposed for HIV, Siglec-1-positive sinus macrophages residing underneath the lymph node capsule were shown to act as gatekeepers at the lymph-tissue interface capturing and trans-presenting lymph-borne viruses, including vesicular stomatitis virus (VSV), to migrating B-cells in the underlying follicles leading to activation of effective antiviral humoral immune responses (108). Furthermore, these macrophages also appear to prevent VSV spread and fatal neuroinvasion by additional innate mechanisms (93). Of note, Siglec-1 in these studies was used as a marker for this subset of macrophages and not explored as a bona fide virus-binding receptor.

5.3.2 Siglec-1 transfers MLV efficiently via a short-term storage compartment

In contrast to the notion of an intracellular storage compartment for captured viruses that may be capable of efficient trans-infection of HIV-1 for up to 4 days (64, 130), Cavrois and colleagues provided evidence that virions bound to the surface of monocyte-derived DC or CD34-derived Langerhans cells, and not internalized HIV-1, was the major source of infectious virions transmitted in *trans* (26). While these authors also detected large amounts of internalized HIV-1 particles by confocal microscopy, they suggest that this may be a dead end for *trans*-infection. These authors also reported a marked drop of HIV-1 *trans*-infection efficiency of MDDC within a few hours, resembling our observations with MLV. From another perspective, given the unique subanatomical localization of Siglec-1-positive mouse macrophages in the subcapsular sinus a long-term storage of captured infectious virus may not be critical for interaction and virus transmission to closely adjacent B-lymphocytes in the lymph follicles, which appear to be the preferential target cell of MLV, at least in vitro. A central question for the process of trans-infection is the relative efficiency of this process compared to direct infection. For HIV-1 MDDC-trans-infection has been suggested to be particularly effective for minimal virus doses that alone may not be sufficient for productive infection of CD4 T-cells by direct infection (64). Our results for MLV support this notion: The Siglec-1-dependent *trans*-infection of activated primary lymphocytes via BMDM, compared to direct infection, was 4- to 15-fold more efficient. Together, it will be fascinating to compare WT and Siglec-1 KO mice for the ability to support MLV replication and pathogenesis via lymphatic and intravenous challenge routes.

5.3.3 Pretreatment of MLV producer cells with synthetic sialic acid precursors modified in the N-Acyl side chain alters Siglec-1 mediated capture and *trans*-infection

To our knowledge the current study for the first time investigated the functional impact of metabolically modified sialic acids in virus producer cells on newly produced viruses, supposedly carrying cell-derived glycoconjugates. To determine up to which degree the synthetic sialic acids had been incorporated into the 293T producer cell membrane, a quantification of the N-substituted sialic acids in glycolipids and glycoproteins by LC-MS/MS is currently being undertaken. Unfortunately, these analyses could not be sufficiently up-scaled to quantify the abundance of modified sialic acids also in highly purified MLV particles. Analysis of the lipid content of HIV-1 and MLV particles indicated that the overall lipid content of these retroviruses mostly matched that of the plasma membrane, with some lipids being enriched including cholesterol, ceramide, and GM3 (19, 27). Notably, a single HIV-1 virion was estimated to contain ~12,000 sialylactose-containing GM3 molecules which may constitute the primary interactor with the lectin receptor (99). The only micromolar affinity of Siglec-1 for different sialylated ligands was postulate to result in high-avidity binding by receptor and ligand clustering (38). This may also be true for the interaction with viruses: HIV-1, bound initially over the entire plasma membrane, subsequently accumulated in many instances at one pole of the cell (97). Several lines of evidence suggest that the metabolically engineered

gangliosides carrying N-acyl modified sialic acids were indeed incorporated into MLV particles: First, the sialic acid-independent mCAT-mediated direct infection of lymphocytes was comparable for all MLV preparations, while particles derived from N-butanoyl, N-isobutanoyl, N-glycolyl, or N-pentanoyl ManN-treated cells displayed grossly reduced capacities for the sialic acid-dependent mSiglec-1-mediated capture and *trans*-infection. Second, in agreement with these functional analyses, both *in vitro*-interaction studies of sialylated ligands with Siglec-1 (115, 116, 122) and molecular modeling studies of mSiglec-1 in complex with sialic acid derivatives (Fig. 5.3) indicated reduced binding affinity for the N-glycoyl but not for N-propanoyl substitution. Three-dimensional models of mSiglec-1 in complex with Neu5Ac, Neu5Gc, Neu5Prop and Neu5But were generated and, notably, all ligands could be accommodated in the binding site without steric clashes (Fig. 5.3A). Based on these structures two different computational methods were applied to model an influence of the N-acyl side chain modifications on the binding affinity. In a molecular dynamics (MD)-based approach the relative binding strength of the ligands was estimated by calculation of the average potential interaction energy (Fig. 5.3B).

As an alternative method to predict the relative binding affinities a 'docking and post-scoring' approach was applied. Post-scoring of the docked poses was performed using the modeling software SeeSAR. The values of the estimated affinity (Fig. 5.3B) showed a similar trend as found in the MD-based approach. Neu5Gc and Neu5But were predicted to have the lowest affinity for mSiglec-1 by both methods. According to this prediction Neu5Ac and Neu5Prop have most likely similar binding affinity. Thus, in agreement with the functional analyses, these crystal structure-based molecular modeling studies suggest reduced binding affinities for N-butanoyl and N-glycoyl, but not for N-propanoyl sialic acid side chain modifications for the interaction with mSiglec-1.

MLV particles that were captured and *trans*-infected lymphocytes to a significantly lower extent than control particles were all released from cells pretreated with ManN derivatives in which the N-acyl side-chain was elongated with more than one carbon, this suggesting that bulkiness of this side-chain might affect the affinity for Siglec-1. However, pretreatment with N-cyclopropylcarbamyl ManN – that contains a cyclopropyl group – notably, did not result in reduced capture or *trans*-infection. A potential reason for this is that treatment with this precursor analog might not have resulted in sufficient incorporation of the modified sialic acid in the virus producer cell membrane. The current LC-MS/MS analysis will hopefully provide answers to this question. Further, molecular modeling and *in vitro*-interaction studies of sialylated ligands with Siglec-1 could also be employed to investigate the Neu5Cyclopropylcarbamyl-Siglec-1 interaction.

A

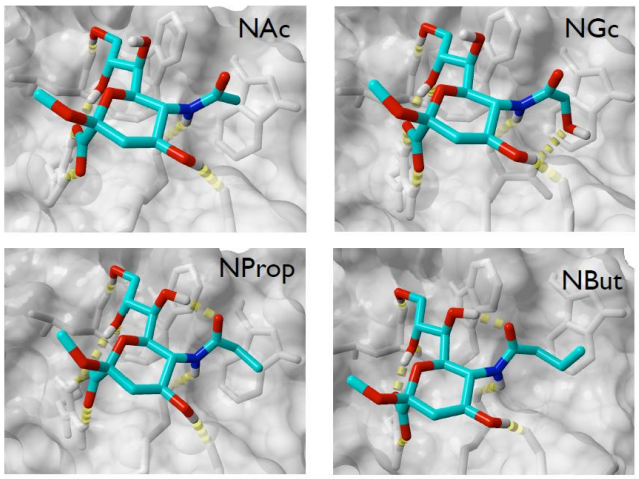

B

Relative Potential Interaction Energies and SeeSAR Affinity Scores

Ligand	Relative Potential Interaction Energy [kcal/mol]	SeeSAR Affinity Score [mM]
Neu5Ac	0	5
Neu5Prop	5.5	12
Neu5But	-6.2	26
Neu5Gc	-5.8	33

The relative average potential interaction energies were calculated from 50 ns MD simulations in water (higher values means better binding) and the average estimated affinity values calculated by SeeSAR (lower values means better binding).

Fig. 5.3 Molecular modeling of structural interaction, interaction potentials and binding affinities of mSiglec-1 in complex with sialic acid derivatives. (A) Three-dimensional models of mSiglec-1 in complex with Neu5Ac, Neu5Gc, Neu5Prop and Neu5But were generated. (B) Relative potential interaction energies and SeeSAR affinity scores. Data generated by Martin Frank, Biognos, Gothenburg, Sweden. From (**IV**).

Neu5Gc naturally occurs in mice, but not in humans (18). Interestingly, while both resting T-cells and B-cells preferentially carry Neu5Gc in α-2,6-linkage, activation results in marked changes in glycosylation including a shift to Neu5Ac in α-2,3-linkage (150, 151). As a result, expression of Siglec-1 and Siglec-F ligands is enhanced on these lymphocytes. These changes may of course also be highly relevant for MLV: On one hand, the surface expression of selective ligands fosters the interaction of activated lymphocytes with Siglec-1-positive macrophages, increasing the likelihood for trans-infection. On the other hand, MLV replicates in these Neu5Ac-containing proliferating B- and T cells, leading to the release of Siglec-1-interaction-competent virions.

Collectively, results from the current study and the availability of Siglec-1-knockout mice provide the basis to explore the role of Siglec-1 and the process of trans-infection in general for spread and pathogenesis of MLV in vivo.

6 CONCLUDING REMARKS

Viruses are intracellular parasites, and the viral genome must therefore enter a cell in order to sucessfully replicate. This process starts with adherence of the virus particles to the plasma membrane of the cell and this occurs through binding to receptor molecules on the cell surface. After the virus enters the cell, its infectious cycle continues with replication of the genome followed by assembly of new infectious particles. Throughout this process, host factors can alter the efficiency of the different steps required for productive infection. By use of different experimental approaches, the work presented in this thesis has focused on characterizing the expression and function of three host proteins which have shown potential to modulate retroviral infection; CD317, SAMHD1 and Siglec-1.

Using a tissue microarray-based method for in situ-detection of CD317 protein, this work identified several previously unknown possible interaction sites of enveloped viruses with this antiviral restriction factor (**I**). An important previously unknown interaction site between virus and host factor was also found for the early restriction factor SAMHD1. Its abundant expression in resting CD4+ T cells prompted further investigations of SAMHD1's antiviral activity in these cells and we could demonstrate that HIV-1 replication is restricted, at least partly, by SAMHD1 in this cell type (**II**). Our study on the sialic acid-binding surface receptor Siglec-1 confirmed that this protein is an important mediator of retroviral *trans*-infection. MLV released from cells treated with synthetic sialic acid precursor analogs showed different capacities for Siglec-1 mediated capture and *trans*-infection, and the N-acyl side chain of sialic acid was demonstated to be important for the mouse Siglec-1-MLV interaction (**IV**).

The findings described here give rise to several important questions. The widespread tissue-expression of CD317, and – at the same time – lack of its expression on CD4+ HIV-1 target cells, first of all motivate further studies to re-evaluate CD317's suitability as a selective target for immunotherapy in B-cell cancers, but also raise questions about Vpu and its presupposed evolutionary arms race with CD317. Thus far it remains unclear where the virus actually encounters CD317, yet HIV-1 encodes this CD317 antagonist, suggesting that evolutionary pressure has been exerted by the restriction factor *in vivo*. To investigate where such an encounter might have occurred, a more detailed analysis of HIV-target cells in other tissues than the already examined, including the genital mucosa, should be performed. The mechanistic details on how SAMHD1 imposes retroviral restriction are still not fully understood. However, our results demonstrating that SAMHD1 restricts HIV-1 replication in resting CD4+ T cells contribute to the active field of research focused on elucidating the mechanisms for detection and restriction of incoming viral genomes. Our findings that mouse Siglec-1 is an important receptor for mediating *trans*-infection of MLV, strengthens the notion that this receptor, has the capability to influence viral spread. Further studies using Siglec-1-/- mice will likely investigate whether these results transfer to also having an impact on tissue dissemination and pathogenesis *in vivo*.

Collectively, the work presented in this thesis characterizes the expression and function of three host factors that can act as modulators of retroviral infection. The findings described here thereby contribute to the overall understanding of how virus attachment receptors and anti-viral restriction factors influence the chances for viruses to successfully replicate.

7 ACKNOWLEDGEMENTS

The work presented in this thesis was performed at laboratories at Department of Infectious Diseases – Virology at Heidelberg University and at Institute for Medical Virology, National Reference Center for Retroviruses, Goethe University, Frankfurt am Main. Thank you for sharing instruments and reagents.

The guidance and support of several individuals has been essential. In particular, I wish to thank:

Hans-Georg Kräusslich, for giving me the opportunity to perform research in his department and for being the first referee of my thesis. Thank you for your supportive advice during and outside my thesis advisory committee meetings.

Oliver Keppler, my supervisor and second referee of the thesis, for inviting me to join his lab. Thank you for the support during the four years, for introducing me to the exciting field of intrinsic immunity, and for sharing your enthusiasm.

Alexander Dalpke, for advice during my thesis advisory committee meetings, and for agreeing to be a referee of my thesis. Thank you also for providing me with my first research experience in Germany.

Britta Brügger, for taking the time to read my thesis and for agreeing to be a referee of it.

Felix Lasitschka, for being a member of my thesis advisory committee and a key collaborator in several projects. Thank you for your very helpful advice when it comes to tissue staining and antibodies.

During my PhD I have had the pleasure of meeting people who have contributed to creating a very nice working atmosphere. I would therefore like to thank the following people:

All past and present members of the Keppler and Schaller lab during my time in the group; in particular Nikolas, Sebe and Torsten for proof reading my thesis and for being great colleagues and friends.

All collaborators and co-authors on the papers in this thesis; without your work this would not have been possible!

Jutta Scheuerer for useful technical support at the Dept. of Pathology, Heidelberg University.

Staff at the animal facility at the Goethe University, Frankfurt am Main; especially Silvia Hettler and Marco Leitenberger for being the responsible caretakers for the Siglec-1 KO mice.

Lab-friends in Heidelberg, Boston and Stockholm: Åsa, Lucho, Alexander and Spiros. Peter and Marie.

Finally, I would like to thank my family for their constant support and my parents for letting me make my own choices (and for making me feel good about them). Thank you for providing such a relaxed view on things.

8 REFERENCES

1. **Ahn, J., C. Hao, J. Yan, M. DeLucia, J. Mehrens, C. Wang, A. M. Gronenborn, and J. Skowronski.** 2012. HIV/simian immunodeficiency virus (SIV) accessory virulence factor Vpx loads the host cell restriction factor SAMHD1 onto the E3 ubiquitin ligase complex CRL4DCAF1. The Journal of biological chemistry **287:**12550-12558.
2. **Allred, D. C., G. M. Clark, R. Elledge, S. A. Fuqua, R. W. Brown, G. C. Chamness, C. K. Osborne, and W. L. McGuire.** 1993. Association of p53 protein expression with tumor cell proliferation rate and clinical outcome in node-negative breast cancer. Journal of the National Cancer Institute **85:**200-206.
3. **Aravind, L., and E. V. Koonin.** 1998. The HD domain defines a new superfamily of metal-dependent phosphohydrolases. Trends in biochemical sciences **23:**469-472.
4. **Arrighi, J. F., M. Pion, E. Garcia, J. M. Escola, Y. van Kooyk, T. B. Geijtenbeek, and V. Piguet.** 2004. DC-SIGN-mediated infectious synapse formation enhances X4 HIV-1 transmission from dendritic cells to T cells. The Journal of experimental medicine **200:**1279-1288.
5. **Banchereau, J., and R. M. Steinman.** 1998. Dendritic cells and the control of immunity. Nature **392:**245-252.
6. **Baribaud, F., S. Pohlmann, G. Leslie, F. Mortari, and R. W. Doms.** 2002. Quantitative expression and virus transmission analysis of DC-SIGN on monocyte-derived dendritic cells. Journal of virology **76:**9135-9142.
7. **Barre-Sinoussi, F., J. C. Chermann, F. Rey, M. T. Nugeyre, S. Chamaret, J. Gruest, C. Dauguet, C. Axler-Blin, F. Vezinet-Brun, C. Rouzioux, W. Rozenbaum, and L. Montagnier.** 1983. Isolation of a T-lymphotropic retrovirus from a patient at risk for acquired immune deficiency syndrome (AIDS). Science **220:**868-871.
8. **Becker, M., A. Sommer, J. R. Kratzschmar, H. Seidel, H. D. Pohlenz, and I. Fichtner.** 2005. Distinct gene expression patterns in a tamoxifen-sensitive human mammary carcinoma xenograft and its tamoxifen-resistant subline MaCa 3366/TAM. Molecular cancer therapeutics **4:**151-168.
9. **Bekeredjian-Ding, I. B., M. Wagner, V. Hornung, T. Giese, M. Schnurr, S. Endres, and G. Hartmann.** 2005. Plasmacytoid dendritic cells control TLR7 sensitivity of naive B cells via type I IFN. Journal of immunology **174:**4043-4050.
10. **Beloglazova, N., R. Flick, A. Tchigvintsev, G. Brown, A. Popovic, B. Nocek, and A. F. Yakunin.** 2013. Nuclease activity of the human SAMHD1 protein implicated in the Aicardi-Goutieres syndrome and HIV-1 restriction. The Journal of biological chemistry **288:**8101-8110.
11. **Bergamaschi, A., D. Ayinde, A. David, E. Le Rouzic, M. Morel, G. Collin, D. Descamps, F. Damond, F. Brun-Vezinet, S. Nisole, F. Margottin-Goguet, G. Pancino, and C. Transy.** 2009. The human immunodeficiency virus type 2 Vpx protein usurps the CUL4A-DDB1 DCAF1 ubiquitin ligase to overcome a postentry block in macrophage infection. Journal of virology **83:**4854-4860.
12. **Berger, A., A. F. Sommer, J. Zwarg, M. Hamdorf, K. Welzel, N. Esly, S. Panitz, A. Reuter, I. Ramos, A. Jatiani, L. C. Mulder, A. Fernandez-Sesma, F. Rutsch, V. Simon, R. Konig, and E. Flory.** 2011. SAMHD1-deficient CD14+ cells from individuals with Aicardi-Goutieres syndrome are highly susceptible to HIV-1 infection. PLoS pathogens **7:**e1002425.
13. **Bhattacharya, A., S. L. Alam, T. Fricke, K. Zadrozny, J. Sedzicki, A. B. Taylor, B. Demeler, O. Pornillos, B. K. Ganser-Pornillos, F. Diaz-Griffero, D. N. Ivanov, and M. Yeager.** 2014. Structural basis of HIV-1 capsid recognition by PF74 and CPSF6. Proceedings of the National Academy of Sciences of the United States of America **111:**18625-18630.
14. **Bieniasz, P. D.** 2004. Intrinsic immunity: a front-line defense against viral attack. Nature immunology **5:**1109-1115.
15. **Bishop, K. N., R. K. Holmes, and M. H. Malim.** 2006. Antiviral potency of APOBEC proteins does not correlate with cytidine deamination. Journal of virology **80:**8450-8458.
16. **Blasius, A. L., E. Giurisato, M. Cella, R. D. Schreiber, A. S. Shaw, and M. Colonna.** 2006. Bone marrow stromal cell antigen 2 is a specific marker of type I IFN-producing cells in

the naive mouse, but a promiscuous cell surface antigen following IFN stimulation. Journal of immunology **177:**3260-3265.

17. **Brandariz-Nunez, A., J. C. Valle-Casuso, T. E. White, N. Laguette, M. Benkirane, J. Brojatsch, and F. Diaz-Griffero.** 2012. Role of SAMHD1 nuclear localization in restriction of HIV-1 and SIVmac. Retrovirology **9:**49.
18. **Brinkman-Van der Linden, E. C., E. R. Sjoberg, L. R. Juneja, P. R. Crocker, N. Varki, and A. Varki.** 2000. Loss of N-glycolylneuraminic acid in human evolution. Implications for sialic acid recognition by siglecs. The Journal of biological chemistry **275:**8633-8640.
19. **Brugger, B., B. Glass, P. Haberkant, I. Leibrecht, F. T. Wieland, and H. G. Krausslich.** 2006. The HIV lipidome: a raft with an unusual composition. Proceedings of the National Academy of Sciences of the United States of America **103:**2641-2646.
20. **Bukrinsky, M.** 2004. A hard way to the nucleus. Molecular medicine **10:**1-5.
21. **Burleigh, L., P. Y. Lozach, C. Schiffer, I. Staropoli, V. Pezo, F. Porrot, B. Canque, J. L. Virelizier, F. Arenzana-Seisdedos, and A. Amara.** 2006. Infection of dendritic cells (DCs), not DC-SIGN-mediated internalization of human immunodeficiency virus, is required for long-term transfer of virus to T cells. Journal of virology **80:**2949-2957.
22. **Cai, D., J. Cao, Z. Li, X. Zheng, Y. Yao, W. Li, and Z. Yuan.** 2009. Up-regulation of bone marrow stromal protein 2 (BST2) in breast cancer with bone metastasis. BMC cancer **9:**102.
23. **Cameron, P. U., P. S. Freudenthal, J. M. Barker, S. Gezelter, K. Inaba, and R. M. Steinman.** 1992. Dendritic cells exposed to human immunodeficiency virus type-1 transmit a vigorous cytopathic infection to CD4+ T cells. Science **257:**383-387.
24. **Cantrell, D. A., and K. A. Smith.** 1984. The interleukin-2 T-cell system: a new cell growth model. Science **224:**1312-1316.
25. **Cao, W., L. Bover, M. Cho, X. Wen, S. Hanabuchi, M. Bao, D. B. Rosen, Y. H. Wang, J. L. Shaw, Q. Du, C. Li, N. Arai, Z. Yao, L. L. Lanier, and Y. J. Liu.** 2009. Regulation of TLR7/9 responses in plasmacytoid dendritic cells by BST2 and ILT7 receptor interaction. The Journal of experimental medicine **206:**1603-1614.
26. **Cavrois, M., J. Neidleman, J. F. Kreisberg, and W. C. Greene.** 2007. In vitro derived dendritic cells trans-infect CD4 T cells primarily with surface-bound HIV-1 virions. PLoS pathogens **3:**e4.
27. **Chan, R., P. D. Uchil, J. Jin, G. Shui, D. E. Ott, W. Mothes, and M. R. Wenk.** 2008. Retroviruses human immunodeficiency virus and murine leukemia virus are enriched in phosphoinositides. Journal of virology **82:**11228-11238.
28. **Chiriva-Internati, M., Y. Liu, J. A. Weidanz, F. Grizzi, H. You, W. Zhou, K. Bumm, B. Barlogie, J. L. Mehta, and P. L. Hermonat.** 2003. Testing recombinant adeno-associated virus-gene loading of dendritic cells for generating potent cytotoxic T lymphocytes against a prototype self-antigen, multiple myeloma HM1.24. Blood **102:**3100-3107.
29. **Chow, A., M. Huggins, J. Ahmed, D. Hashimoto, D. Lucas, Y. Kunisaki, S. Pinho, M. Leboeuf, C. Noizat, N. van Rooijen, M. Tanaka, Z. J. Zhao, A. Bergman, M. Merad, and P. S. Frenette.** 2013. CD169(+) macrophages provide a niche promoting erythropoiesis under homeostasis and stress. Nature medicine **19:**429-436.
30. **Chow, A., D. Lucas, A. Hidalgo, S. Mendez-Ferrer, D. Hashimoto, C. Scheiermann, M. Battista, M. Leboeuf, C. Prophete, N. van Rooijen, M. Tanaka, M. Merad, and P. S. Frenette.** 2011. Bone marrow CD169+ macrophages promote the retention of hematopoietic stem and progenitor cells in the mesenchymal stem cell niche. The Journal of experimental medicine **208:**261-271.
31. **Coleman, C. M., and L. Wu.** 2009. HIV interactions with monocytes and dendritic cells: viral latency and reservoirs. Retrovirology **6:**51.
32. **Coutinho, A., and G. Moller.** 1973. B cell mitogenic properties of thymus-independent antigens. Nature: New biology **245:**12-14.
33. **Crabtree, G. R.** 1989. Contingent genetic regulatory events in T lymphocyte activation. Science **243:**355-361.
34. **Cribier, A., B. Descours, A. L. Valadao, N. Laguette, and M. Benkirane.** 2013. Phosphorylation of SAMHD1 by cyclin A2/CDK1 regulates its restriction activity toward HIV-1. Cell reports **3:**1036-1043.

35. **Crocker, P. R., and T. Feizi.** 1996. Carbohydrate recognition systems: functional triads in cell-cell interactions. Current opinion in structural biology **6:**679-691.
36. **Crocker, P. R., and S. Gordon.** 1985. Isolation and Characterization of Resident Stromal Macrophages and Hematopoietic-Cell Clusters from Mouse Bone-Marrow. Journal of Experimental Medicine **162:**993-1014.
37. **Crocker, P. R., S. Kelm, C. Dubois, B. Martin, A. S. McWilliam, D. M. Shotton, J. C. Paulson, and S. Gordon.** 1991. Purification and properties of sialoadhesin, a sialic acid-binding receptor of murine tissue macrophages. The EMBO journal **10:**1661-1669.
38. **Crocker, P. R., J. C. Paulson, and A. Varki.** 2007. Siglecs and their roles in the immune system. Nature reviews. Immunology **7:**255-266.
39. **Crocker, P. R., M. Vinson, S. Kelm, and K. Drickamer.** 1999. Molecular analysis of sialoside binding to sialoadhesin by NMR and site-directed mutagenesis. The Biochemical journal **341 (Pt 2):**355-361.
40. **Crocker, P. R., Z. Werb, S. Gordon, and D. F. Bainton.** 1990. Ultrastructural localization of a macrophage-restricted sialic acid binding hemagglutinin, SER, in macrophage-hematopoietic cell clusters. Blood **76:**1131-1138.
41. **Curtis, B. M., S. Scharnowske, and A. J. Watson.** 1992. Sequence and expression of a membrane-associated C-type lectin that exhibits CD4-independent binding of human immunodeficiency virus envelope glycoprotein gp120. Proceedings of the National Academy of Sciences of the United States of America **89:**8356-8360.
42. **Daniel, M. D., N. L. Letvin, N. W. King, M. Kannagi, P. K. Sehgal, R. D. Hunt, P. J. Kanki, M. Essex, and R. C. Desrosiers.** 1985. Isolation of T-cell tropic HTLV-III-like retrovirus from macaques. Science **228:**1201-1204.
43. **de Witte, L., M. Bobardt, U. Chatterji, G. Degeest, G. David, T. B. Geijtenbeek, and P. Gallay.** 2007. Syndecan-3 is a dendritic cell-specific attachment receptor for HIV-1. Proceedings of the National Academy of Sciences of the United States of America **104:**19464-19469.
44. **Doitsh, G., M. Cavrois, K. G. Lassen, O. Zepeda, Z. Yang, M. L. Santiago, A. M. Hebbeler, and W. C. Greene.** 2010. Abortive HIV infection mediates CD4 T cell depletion and inflammation in human lymphoid tissue. Cell **143:**789-801.
45. **Doitsh, G., N. L. Galloway, X. Geng, Z. Yang, K. M. Monroe, O. Zepeda, P. W. Hunt, H. Hatano, S. Sowinski, I. Munoz-Arias, and W. C. Greene.** 2014. Cell death by pyroptosis drives CD4 T-cell depletion in HIV-1 infection. Nature **505:**509-514.
46. **Dorfman, T., and H. G. Gottlinger.** 1996. The human immunodeficiency virus type 1 capsid p2 domain confers sensitivity to the cyclophilin-binding drug SDZ NIM 811. Journal of virology **70:**5751-5757.
47. **Dwyer, J. M., and C. Johnson.** 1981. The use of concanavalin A to study the immunoregulation of human T cells. Clinical and experimental immunology **46:**237-249.
48. **Evans, D. T., R. Serra-Moreno, R. K. Singh, and J. C. Guatelli.** 2010. BST-2/tetherin: a new component of the innate immune response to enveloped viruses. Trends in microbiology **18:**388-396.
49. **Fackler, O. T., and O. T. Keppler.** 2013. MxB/Mx2: the latest piece in HIV's interferon puzzle. EMBO reports **14:**1028-1029.
50. **Faria, N. R., A. Rambaut, M. A. Suchard, G. Baele, T. Bedford, M. J. Ward, A. J. Tatem, J. D. Sousa, N. Arinaminpathy, J. Pepin, D. Posada, M. Peeters, O. G. Pybus, and P. Lemey.** 2014. HIV epidemiology. The early spread and epidemic ignition of HIV-1 in human populations. Science **346:**56-61.
51. **Fassati, A., and S. P. Goff.** 2001. Characterization of intracellular reverse transcription complexes of human immunodeficiency virus type 1. Journal of virology **75:**3626-3635.
52. **Figdor, C. G., Y. van Kooyk, and G. J. Adema.** 2002. C-type lectin receptors on dendritic cells and Langerhans cells. Nature reviews. Immunology **2:**77-84.
53. **Finkel, T. H., and N. K. Banda.** 1994. Indirect mechanisms of HIV pathogenesis: how does HIV kill T cells? Current opinion in immunology **6:**605-615.
54. **Fletcher, T. M., 3rd, B. Brichacek, N. Sharova, M. A. Newman, G. Stivahtis, P. M. Sharp, M. Emerman, B. H. Hahn, and M. Stevenson.** 1996. Nuclear import and cell cycle

arrest functions of the HIV-1 Vpr protein are encoded by two separate genes in HIV-2/SIV(SM). The EMBO journal **15:**6155-6165.

55. **Flint, S. J., Enquist, L. W., Racaniello V. R., Skalka, A. M.** 2009. Principles of Virology, 3rd Edition, Volume II: Pathogenesis and Control. ASM Press.
56. **Fornerod, M., M. Ohno, M. Yoshida, and I. W. Mattaj.** 1997. CRM1 is an export receptor for leucine-rich nuclear export signals. Cell **90:**1051-1060.
57. **Fossum, S.** 1980. The architecture of rat lymph nodes. IV. Distribution of ferritin and colloidal carbon in the draining lymph nodes after foot-pad injection. Scandinavian journal of immunology **12:**433-441.
58. **Fujita, M., M. Otsuka, M. Nomaguchi, and A. Adachi.** 2008. Functional region mapping of HIV-2 Vpx protein. Microbes and infection / Institut Pasteur **10:**1387-1392.
59. **Galao, R. P., A. Le Tortorec, S. Pickering, T. Kueck, and S. J. Neil.** 2012. Innate sensing of HIV-1 assembly by Tetherin induces NFkappaB-dependent proinflammatory responses. Cell host & microbe **12:**633-644.
60. **Ganesh, L., E. Burstein, A. Guha-Niyogi, M. K. Louder, J. R. Mascola, L. W. Klomp, C. Wijmenga, C. S. Duckett, and G. J. Nabel.** 2003. The gene product Murr1 restricts HIV-1 replication in resting CD4+ lymphocytes. Nature **426:**853-857.
61. **Gao, D., J. Wu, Y. T. Wu, F. Du, C. Aroh, N. Yan, L. Sun, and Z. J. Chen.** 2013. Cyclic GMP-AMP synthase is an innate immune sensor of HIV and other retroviruses. Science **341:**903-906.
62. **Gao, F., E. Bailes, D. L. Robertson, Y. Chen, C. M. Rodenburg, S. F. Michael, L. B. Cummins, L. O. Arthur, M. Peeters, G. M. Shaw, P. M. Sharp, and B. H. Hahn.** 1999. Origin of HIV-1 in the chimpanzee Pan troglodytes troglodytes. Nature **397:**436-441.
63. **Garcia, E., M. Pion, A. Pelchen-Matthews, L. Collinson, J. F. Arrighi, G. Blot, F. Leuba, J. M. Escola, N. Demaurex, M. Marsh, and V. Piguet.** 2005. HIV-1 trafficking to the dendritic cell-T-cell infectious synapse uses a pathway of tetraspanin sorting to the immunological synapse. Traffic **6:**488-501.
64. **Geijtenbeek, T. B., D. S. Kwon, R. Torensma, S. J. van Vliet, G. C. van Duijnhoven, J. Middel, I. L. Cornelissen, H. S. Nottet, V. N. KewalRamani, D. R. Littman, C. G. Figdor, and Y. van Kooyk.** 2000. DC-SIGN, a dendritic cell-specific HIV-1-binding protein that enhances trans-infection of T cells. Cell **100:**587-597.
65. **Geijtenbeek, T. B., R. Torensma, S. J. van Vliet, G. C. van Duijnhoven, G. J. Adema, Y. van Kooyk, and C. G. Figdor.** 2000. Identification of DC-SIGN, a novel dendritic cell-specific ICAM-3 receptor that supports primary immune responses. Cell **100:**575-585.
66. **Gibbert, K., J. F. Schlaak, D. Yang, and U. Dittmer.** 2013. IFN-alpha subtypes: distinct biological activities in anti-viral therapy. British journal of pharmacology **168:**1048-1058.
67. **Goffinet, C., I. Allespach, S. Homann, H. M. Tervo, A. Habermann, D. Rupp, L. Oberbremer, C. Kern, N. Tibroni, S. Welsch, J. Krijnse-Locker, G. Banting, H. G. Krausslich, O. T. Fackler, and O. T. Keppler.** 2009. HIV-1 antagonism of CD317 is species specific and involves Vpu-mediated proteasomal degradation of the restriction factor. Cell host & microbe **5:**285-297.
68. **Goffinet, C., N. Michel, I. Allespach, H. M. Tervo, V. Hermann, H. G. Krausslich, W. C. Greene, and O. T. Keppler.** 2007. Primary T-cells from human CD4/CCR5-transgenic rats support all early steps of HIV-1 replication including integration, but display impaired viral gene expression. Retrovirology **4:**53.
69. **Goila-Gaur, R., and K. Strebel.** 2008. HIV-1 Vif, APOBEC, and intrinsic immunity. Retrovirology **5:**51.
70. **Goldstone, D. C., V. Ennis-Adeniran, J. J. Hedden, H. C. Groom, G. I. Rice, E. Christodoulou, P. A. Walker, G. Kelly, L. F. Haire, M. W. Yap, L. P. de Carvalho, J. P. Stoye, Y. J. Crow, I. A. Taylor, and M. Webb.** 2011. HIV-1 restriction factor SAMHD1 is a deoxynucleoside triphosphate triphosphohydrolase. Nature **480:**379-382.
71. **Goto, T., S. J. Kennel, M. Abe, M. Takishita, M. Kosaka, A. Solomon, and S. Saito.** 1994. A novel membrane antigen selectively expressed on terminally differentiated human B cells. Blood **84:**1922-1930.
72. **Gottlieb, G. S., P. S. Sow, S. E. Hawes, I. Ndoye, M. Redman, A. M. Coll-Seck, M. A. Faye-Niang, A. Diop, J. M. Kuypers, C. W. Critchlow, R. Respess, J. I. Mullins, and N.**

B. Kiviat. 2002. Equal plasma viral loads predict a similar rate of CD4+ T cell decline in human immunodeficiency virus (HIV) type 1- and HIV-2-infected individuals from Senegal, West Africa. The Journal of infectious diseases **185:**905-914.

73. **Goujon, C., L. Jarrosson-Wuilleme, J. Bernaud, D. Rigal, J. L. Darlix, and A. Cimarelli.** 2006. With a little help from a friend: increasing HIV transduction of monocyte-derived dendritic cells with virion-like particles of SIV(MAC). Gene therapy **13:**991-994.
74. **Goujon, C., O. Moncorge, H. Bauby, T. Doyle, C. C. Ward, T. Schaller, S. Hue, W. S. Barclay, R. Schulz, and M. H. Malim.** 2013. Human MX2 is an interferon-induced post-entry inhibitor of HIV-1 infection. Nature **502:**559-562.
75. **Goujon, C., L. Riviere, L. Jarrosson-Wuilleme, J. Bernaud, D. Rigal, J. L. Darlix, and A. Cimarelli.** 2007. SIVSM/HIV-2 Vpx proteins promote retroviral escape from a proteasome-dependent restriction pathway present in human dendritic cells. Retrovirology **4:**2.
76. **Granelli-Piperno, A., V. Finkel, E. Delgado, and R. M. Steinman.** 1999. Virus replication begins in dendritic cells during the transmission of HIV-1 from mature dendritic cells to T cells. Current biology : CB **9:**21-29.
77. **Gray, E. E., and J. G. Cyster.** 2012. Lymph node macrophages. Journal of innate immunity **4:**424-436.
78. **Greenwell-Wild, T., N. Vazquez, W. Jin, Z. Rangel, P. J. Munson, and S. M. Wahl.** 2009. Interleukin-27 inhibition of HIV-1 involves an intermediate induction of type I interferon. Blood **114:**1864-1874.
79. **Guarner, J., and R. Falcon-Escobedo.** 2009. Comparison of the pathology caused by H1N1, H5N1, and H3N2 influenza viruses. Archives of medical research **40:**655-661.
80. **Gummuluru, S., M. Rogel, L. Stamatatos, and M. Emerman.** 2003. Binding of human immunodeficiency virus type 1 to immature dendritic cells can occur independently of DC-SIGN and mannose binding C-type lectin receptors via a cholesterol-dependent pathway. Journal of virology **77:**12865-12874.
81. **Guo, Y., C. Korteweg, M. A. McNutt, and J. Gu.** 2008. Pathogenetic mechanisms of severe acute respiratory syndrome. Virus research **133:**4-12.
82. **Gurney, K. B., J. Elliott, H. Nassanian, C. Song, E. Soilleux, I. McGowan, P. A. Anton, and B. Lee.** 2005. Binding and transfer of human immunodeficiency virus by DC-SIGN+ cells in human rectal mucosa. Journal of virology **79:**5762-5773.
83. **Habermann, A., J. Krijnse-Locker, H. Oberwinkler, M. Eckhardt, S. Homann, A. Andrew, K. Strebel, and H. G. Krausslich.** 2010. CD317/tetherin is enriched in the HIV-1 envelope and downregulated from the plasma membrane upon virus infection. Journal of virology **84:**4646-4658.
84. **Haller, O., G. Kochs, and F. Weber.** 2006. The interferon response circuit: induction and suppression by pathogenic viruses. Virology **344:**119-130.
85. **Haller, O., P. Staeheli, and G. Kochs.** 2007. Interferon-induced Mx proteins in antiviral host defense. Biochimie **89:**812-818.
86. **Hartnell, A.** 2001. Characterization of human sialoadhesin, a sialic acid binding receptor expressed by resident and inflammatory macrophage populations. Blood **97:**288-296.
87. **Hickman, H. D., K. Takeda, C. N. Skon, F. R. Murray, S. E. Hensley, J. Loomis, G. N. Barber, J. R. Bennink, and J. W. Yewdell.** 2008. Direct priming of antiviral CD8+ T cells in the peripheral interfollicular region of lymph nodes. Nature immunology **9:**155-165.
88. **Hollingsworth, T. D., R. M. Anderson, and C. Fraser.** 2008. HIV-1 transmission, by stage of infection. The Journal of infectious diseases **198:**687-693.
89. **Honda, K., H. Yanai, T. Mizutani, H. Negishi, N. Shimada, N. Suzuki, Y. Ohba, A. Takaoka, W. C. Yeh, and T. Taniguchi.** 2004. Role of a transductional-transcriptional processor complex involving MyD88 and IRF-7 in Toll-like receptor signaling. Proceedings of the National Academy of Sciences of the United States of America **101:**15416-15421.
90. **Honke, K., and N. Kotani.** 2012. Identification of cell-surface molecular interactions under living conditions by using the enzyme-mediated activation of radical sources (EMARS) method. Sensors **12:**16037-16045.
91. **Hornung, V., S. Rothenfusser, S. Britsch, A. Krug, B. Jahrsdorfer, T. Giese, S. Endres, and G. Hartmann.** 2002. Quantitative expression of toll-like receptor 1-10 mRNA in cellular

subsets of human peripheral blood mononuclear cells and sensitivity to CpG oligodeoxynucleotides. Journal of immunology **168:**4531-4537.

92. **Hrecka, K., C. Hao, M. Gierszewska, S. K. Swanson, M. Kesik-Brodacka, S. Srivastava, L. Florens, M. P. Washburn, and J. Skowronski.** 2011. Vpx relieves inhibition of HIV-1 infection of macrophages mediated by the SAMHD1 protein. Nature **474:**658-661.
93. **Iannacone, M., E. A. Moseman, E. Tonti, L. Bosurgi, T. Junt, S. E. Henrickson, S. P. Whelan, L. G. Guidotti, and U. H. von Andrian.** 2010. Subcapsular sinus macrophages prevent CNS invasion on peripheral infection with a neurotropic virus. Nature **465:**1079-1083.
94. **Ishii, K. J., T. Kawagoe, S. Koyama, K. Matsui, H. Kumar, T. Kawai, S. Uematsu, O. Takeuchi, F. Takeshita, C. Coban, and S. Akira.** 2008. TANK-binding kinase-1 delineates innate and adaptive immune responses to DNA vaccines. Nature **451:**725-729.
95. **Ishikawa, H., and G. N. Barber.** 2008. STING is an endoplasmic reticulum adaptor that facilitates innate immune signalling. Nature **455:**674-678.
96. **Ishikawa, J., T. Kaisho, H. Tomizawa, B. O. Lee, Y. Kobune, J. Inazawa, K. Oritani, M. Itoh, T. Ochi, K. Ishihara, and et al.** 1995. Molecular cloning and chromosomal mapping of a bone marrow stromal cell surface gene, BST2, that may be involved in pre-B-cell growth. Genomics **26:**527-534.
97. **Izquierdo-Useros, N., O. Esteban, M. T. Rodriguez-Plata, I. Erkizia, J. G. Prado, J. Blanco, M. F. Garcia-Parajo, and J. Martinez-Picado.** 2011. Dynamic imaging of cell-free and cell-associated viral capture in mature dendritic cells. Traffic **12:**1702-1713.
98. **Izquierdo-Useros, N., M. Lorizate, F. X. Contreras, M. T. Rodriguez-Plata, B. Glass, I. Erkizia, J. G. Prado, J. Casas, G. Fabrias, H. G. Krausslich, and J. Martinez-Picado.** 2012. Sialyllactose in viral membrane gangliosides is a novel molecular recognition pattern for mature dendritic cell capture of HIV-1. PLoS biology **10:**e1001315.
99. **Izquierdo-Useros, N., M. Lorizate, P. J. McLaren, A. Telenti, H. G. Krausslich, and J. Martinez-Picado.** 2014. HIV-1 capture and transmission by dendritic cells: the role of viral glycolipids and the cellular receptor Siglec-1. PLoS pathogens **10:**e1004146.
100. **Izquierdo-Useros, N., M. Lorizate, M. C. Puertas, M. T. Rodriguez-Plata, N. Zangger, E. Erikson, M. Pino, I. Erkizia, B. Glass, B. Clotet, O. T. Keppler, A. Telenti, H. G. Krausslich, and J. Martinez-Picado.** 2012. Siglec-1 is a novel dendritic cell receptor that mediates HIV-1 trans-infection through recognition of viral membrane gangliosides. PLoS biology **10:**e1001448.
101. **Jacquelin, B., V. Mayau, B. Targat, A. S. Liovat, D. Kunkel, G. Petitjean, M. A. Dillies, P. Roques, C. Butor, G. Silvestri, L. D. Giavedoni, P. Lebon, F. Barre-Sinoussi, A. Benecke, and M. C. Muller-Trutwin.** 2009. Nonpathogenic SIV infection of African green monkeys induces a strong but rapidly controlled type I IFN response. The Journal of clinical investigation **119:**3544-3555.
102. **Jakobsen, M. R., R. O. Bak, A. Andersen, R. K. Berg, S. B. Jensen, J. Tengchuan, A. Laustsen, K. Hansen, L. Ostergaard, K. A. Fitzgerald, T. S. Xiao, J. G. Mikkelsen, T. H. Mogensen, and S. R. Paludan.** 2013. IFI16 senses DNA forms of the lentiviral replication cycle and controls HIV-1 replication. Proceedings of the National Academy of Sciences of the United States of America **110:**E4571-4580.
103. **Jalili, A., S. Ozaki, T. Hara, H. Shibata, T. Hashimoto, M. Abe, Y. Nishioka, and T. Matsumoto.** 2005. Induction of HM1.24 peptide-specific cytotoxic T lymphocytes by using peripheral-blood stem-cell harvests in patients with multiple myeloma. Blood **106:**3538-3545.
104. **Jekle, A., O. T. Keppler, E. De Clercq, D. Schols, M. Weinstein, and M. A. Goldsmith.** 2003. In vivo evolution of human immunodeficiency virus type 1 toward increased pathogenicity through CXCR4-mediated killing of uninfected CD4 T cells. Journal of virology **77:**5846-5854.
105. **Jeon, Y. J., H. M. Yoo, and C. H. Chung.** 2010. ISG15 and immune diseases. Biochimica et biophysica acta **1802:**485-496.
106. **Jin, T., A. Perry, J. Jiang, P. Smith, J. A. Curry, L. Unterholzner, Z. Jiang, G. Horvath, V. A. Rathinam, R. W. Johnstone, V. Hornung, E. Latz, A. G. Bowie, K. A. Fitzgerald, and T. S. Xiao.** 2012. Structures of the HIN domain:DNA complexes reveal ligand binding and activation mechanisms of the AIM2 inflammasome and IFI16 receptor. Immunity **36:**561-571.

107. **Johnson, J. E., R. A. Gonzales, S. J. Olson, P. F. Wright, and B. S. Graham.** 2007. The histopathology of fatal untreated human respiratory syncytial virus infection. Modern pathology : an official journal of the United States and Canadian Academy of Pathology, Inc **20:**108-119.
108. **Junt, T., E. A. Moseman, M. Iannacone, S. Massberg, P. A. Lang, M. Boes, K. Fink, S. E. Henrickson, D. M. Shayakhmetov, N. C. Di Paolo, N. van Rooijen, T. R. Mempel, S. P. Whelan, and U. H. von Andrian.** 2007. Subcapsular sinus macrophages in lymph nodes clear lymph-borne viruses and present them to antiviral B cells. Nature **450:**110-114.
109. **Kaletsky, R. L., J. R. Francica, C. Agrawal-Gamse, and P. Bates.** 2009. Tetherin-mediated restriction of filovirus budding is antagonized by the Ebola glycoprotein. Proceedings of the National Academy of Sciences of the United States of America **106:**2886-2891.
110. **Kalvodova, L., J. L. Sampaio, S. Cordo, C. S. Ejsing, A. Shevchenko, and K. Simons.** 2009. The lipidomes of vesicular stomatitis virus, semliki forest virus, and the host plasma membrane analyzed by quantitative shotgun mass spectrometry. Journal of virology **83:**7996-8003.
111. **Kane, M., S. S. Yadav, J. Bitzegeio, S. B. Kutluay, T. Zang, S. J. Wilson, J. W. Schoggins, C. M. Rice, M. Yamashita, T. Hatziioannou, and P. D. Bieniasz.** 2013. MX2 is an interferon-induced inhibitor of HIV-1 infection. Nature **502:**563-566.
112. **Karpova, A. Y., M. Trost, J. M. Murray, L. C. Cantley, and P. M. Howley.** 2002. Interferon regulatory factor-3 is an in vivo target of DNA-PK. Proceedings of the National Academy of Sciences of the United States of America **99:**2818-2823.
113. **Kawai, S., Y. Azuma, E. Fujii, K. Furugaki, S. Ozaki, T. Matsumoto, M. Kosaka, and H. Yamada-Okabe.** 2008. Interferon-alpha enhances CD317 expression and the antitumor activity of anti-CD317 monoclonal antibody in renal cell carcinoma xenograft models. Cancer science **99:**2461-2466.
114. **Kawai, S., Y. Koishihara, S. Iida, S. Ozaki, T. Matsumoto, M. Kosaka, and H. Yamada-Okabe.** 2006. Construction of a conventional non-radioisotope method to quantify HM1.24 antigens: correlation of HM1.24 levels and ADCC activity of the humanized antibody against HM1.24. Leukemia research **30:**949-956.
115. **Kelm, S., R. Brossmer, R. Isecke, H. J. Gross, K. Strenge, and R. Schauer.** 1998. Functional groups of sialic acids involved in binding to siglecs (sialoadhesins) deduced from interactions with synthetic analogues. European journal of biochemistry / FEBS **255:**663-672.
116. **Kelm, S., R. Schauer, J. C. Manuguerra, H. J. Gross, and P. R. Crocker.** 1994. Modifications of cell surface sialic acids modulate cell adhesion mediated by sialoadhesin and CD22. Glycoconjugate journal **11:**576-585.
117. **Keppler, O. T., R. Horstkorte, M. Pawlita, C. Schmidt, and W. Reutter.** 2001. Biochemical engineering of the N-acyl side chain of sialic acid: biological implications. Glycobiology **11:**11R-18R.
118. **Kim, T., T. Y. Kim, Y. H. Song, I. M. Min, J. Yim, and T. K. Kim.** 1999. Activation of interferon regulatory factor 3 in response to DNA-damaging agents. The Journal of biological chemistry **274:**30686-30689.
119. **Kirchberger, S., O. Majdic, P. Steinberger, S. Bluml, K. Pfistershammer, G. Zlabinger, L. Deszcz, E. Kuechler, W. Knapp, and J. Stockl.** 2005. Human rhinoviruses inhibit the accessory function of dendritic cells by inducing sialoadhesin and B7-H1 expression. Journal of immunology **175:**1145-1152.
120. **Kirchhoff, F.** 2010. Immune evasion and counteraction of restriction factors by HIV-1 and other primate lentiviruses. Cell host & microbe **8:**55-67.
121. **Kirchhoff, F.** 2009. Is the high virulence of HIV-1 an unfortunate coincidence of primate lentiviral evolution? Nature reviews. Microbiology **7:**467-476.
122. **Klaas, M., and P. R. Crocker.** 2012. Sialoadhesin in recognition of self and non-self. Seminars in immunopathology **34:**353-364.
123. **Klein, F., H. Mouquet, P. Dosenovic, J. F. Scheid, L. Scharf, and M. C. Nussenzweig.** 2013. Antibodies in HIV-1 vaccine development and therapy. Science **341:**1199-1204.
124. **Kluge, S. F., K. Mack, S. S. Iyer, F. M. Pujol, A. Heigele, G. H. Learn, S. M. Usmani, D. Sauter, S. Joas, D. Hotter, F. Bibollet-Ruche, L. J. Plenderleith, M. Peeters, M. Geyer, P.**

M. Sharp, O. T. Fackler, B. H. Hahn, and F. Kirchhoff. 2014. Nef Proteins of Epidemic HIV-1 Group O Strains Antagonize Human Tetherin. Cell host & microbe **16:**639-650.

125. **Kondo, T., J. Kobayashi, T. Saitoh, K. Maruyama, K. J. Ishii, G. N. Barber, K. Komatsu, S. Akira, and T. Kawai.** 2013. DNA damage sensor MRE11 recognizes cytosolic double-stranded DNA and induces type I interferon by regulating STING trafficking. Proceedings of the National Academy of Sciences of the United States of America **110:**2969-2974.
126. **Krutzik, P. O., and G. P. Nolan.** 2003. Intracellular phospho-protein staining techniques for flow cytometry: monitoring single cell signaling events. Cytometry. Part A : the journal of the International Society for Analytical Cytology **55:**61-70.
127. **Kuka, M., and M. Iannacone.** 2014. The role of lymph node sinus macrophages in host defense. Annals of the New York Academy of Sciences **1319:**38-46.
128. **Kupzig, S., V. Korolchuk, R. Rollason, A. Sugden, A. Wilde, and G. Banting.** 2003. Bst-2/HM1.24 is a raft-associated apical membrane protein with an unusual topology. Traffic **4:**694-709.
129. **Kutluay, S. B., T. Zang, D. Blanco-Melo, C. Powell, D. Jannain, M. Errando, and P. D. Bieniasz.** 2014. Global changes in the RNA binding specificity of HIV-1 gag regulate virion genesis. Cell **159:**1096-1109.
130. **Kwon, D. S., G. Gregorio, N. Bitton, W. A. Hendrickson, and D. R. Littman.** 2002. DC-SIGN-mediated internalization of HIV is required for trans-enhancement of T cell infection. Immunity **16:**135-144.
131. **Laguette, N., B. Sobhian, N. Casartelli, M. Ringeard, C. Chable-Bessia, E. Segeral, A. Yatim, S. Emiliani, O. Schwartz, and M. Benkirane.** 2011. SAMHD1 is the dendritic- and myeloid-cell-specific HIV-1 restriction factor counteracted by Vpx. Nature **474:**654-657.
132. **Lahouassa, H., W. Daddacha, H. Hofmann, D. Ayinde, E. C. Logue, L. Dragin, N. Bloch, C. Maudet, M. Bertrand, T. Gramberg, G. Pancino, S. Priet, B. Canard, N. Laguette, M. Benkirane, C. Transy, N. R. Landau, B. Kim, and F. Margottin-Goguet.** 2012. SAMHD1 restricts the replication of human immunodeficiency virus type 1 by depleting the intracellular pool of deoxynucleoside triphosphates. Nature immunology **13:**223-228.
133. **Le Tortorec, A., and S. J. Neil.** 2009. Antagonism to and intracellular sequestration of human tetherin by the human immunodeficiency virus type 2 envelope glycoprotein. Journal of virology **83:**11966-11978.
134. **Lederman, M. M., R. E. Offord, and O. Hartley.** 2006. Microbicides and other topical strategies to prevent vaginal transmission of HIV. Nature reviews. Immunology **6:**371-382.
135. **Lewis, P. F., and M. Emerman.** 1994. Passage through mitosis is required for oncoretroviruses but not for the human immunodeficiency virus. Journal of virology **68:**510-516.
136. **Lippmann, J., S. Rothenburg, N. Deigendesch, J. Eitel, K. Meixenberger, V. van Laak, H. Slevogt, D. N'Guessan P, S. Hippenstiel, T. Chakraborty, A. Flieger, N. Suttorp, and B. Opitz.** 2008. IFNbeta responses induced by intracellular bacteria or cytosolic DNA in different human cells do not require ZBP1 (DLM-1/DAI). Cellular microbiology **10:**2579-2588.
137. **Liu, Z., Q. Pan, S. Ding, J. Qian, F. Xu, J. Zhou, S. Cen, F. Guo, and C. Liang.** 2013. The interferon-inducible MxB protein inhibits HIV-1 infection. Cell host & microbe **14:**398-410.
138. **Luchansky, S. J., and C. R. Bertozzi.** 2004. Azido sialic acids can modulate cell-surface interactions. Chembiochem : a European journal of chemical biology **5:**1706-1709.
139. **Magerus-Chatinet, A., H. Yu, S. Garcia, E. Ducloux, B. Terris, and M. Bomsel.** 2007. Galactosyl ceramide expressed on dendritic cells can mediate HIV-1 transfer from monocyte derived dendritic cells to autologous T cells. Virology **362:**67-74.
140. **Malim, M. H., and P. D. Bieniasz.** 2012. HIV Restriction Factors and Mechanisms of Evasion. Cold Spring Harbor perspectives in medicine **2:**a006940.
141. **Mangeat, B., P. Turelli, G. Caron, M. Friedli, L. Perrin, and D. Trono.** 2003. Broad antiretroviral defence by human APOBEC3G through lethal editing of nascent reverse transcripts. Nature **424:**99-103.
142. **Mansouri, M., K. Viswanathan, J. L. Douglas, J. Hines, J. Gustin, A. V. Moses, and K. Fruh.** 2009. Molecular mechanism of BST2/tetherin downregulation by K5/MIR2 of Kaposi's sarcoma-associated herpesvirus. Journal of virology **83:**9672-9681.

143. **May, A. P., R. C. Robinson, M. Vinson, P. R. Crocker, and E. Y. Jones.** 1998. Crystal structure of the N-terminal domain of sialoadhesin in complex with 3' sialyllactose at 1.85 A resolution. Molecular cell **1:**719-728.
144. **May, M. T., M. Gompels, V. Delpech, K. Porter, C. Orkin, S. Kegg, P. Hay, M. Johnson, A. Palfreeman, R. Gilson, D. Chadwick, F. Martin, T. Hill, J. Walsh, F. Post, M. Fisher, J. Ainsworth, S. Jose, C. Leen, M. Nelson, J. Anderson, C. Sabin, and U. K. C. H. C. Study.** 2014. Impact on life expectancy of HIV-1 positive individuals of CD4+ cell count and viral load response to antiretroviral therapy. Aids **28:**1193-1202.
145. **Miyagi, E., A. J. Andrew, S. Kao, and K. Strebel.** 2009. Vpu enhances HIV-1 virus release in the absence of Bst-2 cell surface down-modulation and intracellular depletion. Proceedings of the National Academy of Sciences of the United States of America **106:**2868-2873.
146. **Monroe, K. M., Z. Yang, J. R. Johnson, X. Geng, G. Doitsh, N. J. Krogan, and W. C. Greene.** 2014. IFI16 DNA sensor is required for death of lymphoid CD4 T cells abortively infected with HIV. Science **343:**428-432.
147. **Moore, R. C., I. Y. Lee, G. L. Silverman, P. M. Harrison, R. Strome, C. Heinrich, A. Karunaratne, S. H. Pasternak, M. A. Chishti, Y. Liang, P. Mastrangelo, K. Wang, A. F. Smit, S. Katamine, G. A. Carlson, F. E. Cohen, S. B. Prusiner, D. W. Melton, P. Tremblay, L. E. Hood, and D. Westaway.** 1999. Ataxia in prion protein (PrP)-deficient mice is associated with upregulation of the novel PrP-like protein doppel. Journal of molecular biology **292:**797-817.
148. **Moseman, E. A., M. Iannacone, L. Bosurgi, E. Tonti, N. Chevrier, A. Tumanov, Y. X. Fu, N. Hacohen, and U. H. von Andrian.** 2012. B cell maintenance of subcapsular sinus macrophages protects against a fatal viral infection independent of adaptive immunity. Immunity **36:**415-426.
149. **Munch, J., L. Standker, W. G. Forssmann, and F. Kirchhoff.** 2014. Discovery of modulators of HIV-1 infection from the human peptidome. Nature reviews. Microbiology **12:**715-722.
150. **Naito-Matsui, Y., S. Takada, Y. Kano, T. Iyoda, M. Sugai, A. Shimizu, K. Inaba, L. Nitschke, T. Tsubata, S. Oka, Y. Kozutsumi, and H. Takematsu.** 2014. Functional evaluation of activation-dependent alterations in the sialoglycan composition of T cells. The Journal of biological chemistry **289:**1564-1579.
151. **Naito, Y., H. Takematsu, S. Koyama, S. Miyake, H. Yamamoto, R. Fujinawa, M. Sugai, Y. Okuno, G. Tsujimoto, T. Yamaji, Y. Hashimoto, S. Itohara, T. Kawasaki, A. Suzuki, and Y. Kozutsumi.** 2007. Germinal center marker GL7 probes activation-dependent repression of N-glycolylneuraminic acid, a sialic acid species involved in the negative modulation of B-cell activation. Molecular and cellular biology **27:**3008-3022.
152. **Nath, D., P. A. van der Merwe, S. Kelm, P. Bradfield, and P. R. Crocker.** 1995. The amino-terminal immunoglobulin-like domain of sialoadhesin contains the sialic acid binding site. Comparison with CD22. The Journal of biological chemistry **270:**26184-26191.
153. **Neil, S. J., T. Zang, and P. D. Bieniasz.** 2008. Tetherin inhibits retrovirus release and is antagonized by HIV-1 Vpu. Nature **451:**425-430.
154. **Nguyen, D. G., and J. E. Hildreth.** 2003. Involvement of macrophage mannose receptor in the binding and transmission of HIV by macrophages. European journal of immunology **33:**483-493.
155. **Oetke, C., M. C. Vinson, C. Jones, and P. R. Crocker.** 2006. Sialoadhesin-deficient mice exhibit subtle changes in B- and T-cell populations and reduced immunoglobulin M levels. Molecular and cellular biology **26:**1549-1557.
156. **Ohtomo, T., Y. Sugamata, Y. Ozaki, K. Ono, Y. Yoshimura, S. Kawai, Y. Koishihara, S. Ozaki, M. Kosaka, T. Hirano, and M. Tsuchiya.** 1999. Molecular cloning and characterization of a surface antigen preferentially overexpressed on multiple myeloma cells. Biochemical and biophysical research communications **258:**583-591.
157. **Oldham-Ott, C. K., and J. Gilloteaux.** 1997. Comparative morphology of the gallbladder and biliary tract in vertebrates: variation in structure, homology in function and gallstones. Microscopy research and technique **38:**571-597.

158. **Ozaki, S., M. Kosaka, Y. Wakahara, Y. Ozaki, M. Tsuchiya, Y. Koishihara, T. Goto, and T. Matsumoto.** 1999. Humanized anti-HM1.24 antibody mediates myeloma cell cytotoxicity that is enhanced by cytokine stimulation of effector cells. Blood **93:**3922-3930.
159. **Pedersen, N. C., E. W. Ho, M. L. Brown, and J. K. Yamamoto.** 1987. Isolation of a T-lymphotropic virus from domestic cats with an immunodeficiency-like syndrome. Science **235:**790-793.
160. **Perez-Caballero, D., T. Zang, A. Ebrahimi, M. W. McNatt, D. A. Gregory, M. C. Johnson, and P. D. Bieniasz.** 2009. Tetherin inhibits HIV-1 release by directly tethering virions to cells. Cell **139:**499-511.
161. **Phan, T. G., J. A. Green, E. E. Gray, Y. Xu, and J. G. Cyster.** 2009. Immune complex relay by subcapsular sinus macrophages and noncognate B cells drives antibody affinity maturation. Nature immunology **10:**786-793.
162. **Pizzato, M., O. Erlwein, D. Bonsall, S. Kaye, D. Muir, and M. O. McClure.** 2009. A one-step SYBR Green I-based product-enhanced reverse transcriptase assay for the quantitation of retroviruses in cell culture supernatants. Journal of virological methods **156:**1-7.
163. **Plesa, G., J. Dai, C. Baytop, J. L. Riley, C. H. June, and U. O'Doherty.** 2007. Addition of deoxynucleosides enhances human immunodeficiency virus type 1 integration and 2LTR formation in resting CD4+ T cells. Journal of virology **81:**13938-13942.
164. **Pollard, V. W., and M. H. Malim.** 1998. The HIV-1 Rev protein. Annual review of microbiology **52:**491-532.
165. **Pope, M., S. Gezelter, N. Gallo, L. Hoffman, and R. M. Steinman.** 1995. Low levels of HIV-1 infection in cutaneous dendritic cells promote extensive viral replication upon binding to memory CD4+ T cells. The Journal of experimental medicine **182:**2045-2056.
166. **Powell, R. D., P. J. Holland, T. Hollis, and F. W. Perrino.** 2011. Aicardi-Goutieres syndrome gene and HIV-1 restriction factor SAMHD1 is a dGTP-regulated deoxynucleotide triphosphohydrolase. The Journal of biological chemistry **286:**43596-43600.
167. **Pulliam, L., B. Sun, and H. Rempel.** 2004. Invasive chronic inflammatory monocyte phenotype in subjects with high HIV-1 viral load. Journal of neuroimmunology **157:**93-98.
168. **Puryear, W. B., H. Akiyama, S. D. Geer, N. P. Ramirez, X. Yu, B. M. Reinhard, and S. Gummuluru.** 2013. Interferon-inducible mechanism of dendritic cell-mediated HIV-1 dissemination is dependent on Siglec-1/CD169. PLoS pathogens **9:**e1003291.
169. **Puryear, W. B., X. Yu, N. P. Ramirez, B. M. Reinhard, and S. Gummuluru.** 2012. HIV-1 incorporation of host-cell-derived glycosphingolipid GM3 allows for capture by mature dendritic cells. Proceedings of the National Academy of Sciences of the United States of America **109:**7475-7480.
170. **Rempel, H., C. Calosing, B. Sun, and L. Pulliam.** 2008. Sialoadhesin expressed on IFN-induced monocytes binds HIV-1 and enhances infectivity. PloS one **3:**e1967.
171. **Rennert, P. D., J. L. Browning, R. Mebius, F. Mackay, and P. S. Hochman.** 1996. Surface lymphotoxin alpha/beta complex is required for the development of peripheral lymphoid organs. The Journal of experimental medicine **184:**1999-2006.
172. **Roe, T., T. C. Reynolds, G. Yu, and P. O. Brown.** 1993. Integration of murine leukemia virus DNA depends on mitosis. The EMBO journal **12:**2099-2108.
173. **Rollason, R., V. Korolchuk, C. Hamilton, M. Jepson, and G. Banting.** 2009. A CD317/tetherin-RICH2 complex plays a critical role in the organization of the subapical actin cytoskeleton in polarized epithelial cells. The Journal of cell biology **184:**721-736.
174. **Rosenberg, N., and P. Jolicoeur.** 1997. Retroviral Pathogenesis. *In* J. M. Coffin, S. H. Hughes, and H. E. Varmus (ed.), Retroviruses, Cold Spring Harbor (NY).
175. **Ryoo, J., J. Choi, C. Oh, S. Kim, M. Seo, S. Y. Kim, D. Seo, J. Kim, T. E. White, A. Brandariz-Nunez, F. Diaz-Griffero, C. H. Yun, J. A. Hollenbaugh, B. Kim, D. Baek, and K. Ahn.** 2014. The ribonuclease activity of SAMHD1 is required for HIV-1 restriction. Nature medicine **20:**936-941.
176. **Sauter, D., M. Schindler, A. Specht, W. N. Landford, J. Munch, K. A. Kim, J. Votteler, U. Schubert, F. Bibollet-Ruche, B. F. Keele, J. Takehisa, Y. Ogando, C. Ochsenbauer, J. C. Kappes, A. Ayouba, M. Peeters, G. H. Learn, G. Shaw, P. M. Sharp, P. Bieniasz, B. H. Hahn, T. Hatziioannou, and F. Kirchhoff.** 2009. Tetherin-driven adaptation of Vpu and Nef

function and the evolution of pandemic and nonpandemic HIV-1 strains. Cell host & microbe **6:**409-421.

177. **Schaumann, D. H., J. Tuischer, W. Ebell, R. A. Manz, and R. Lauster.** 2007. VCAM-1-positive stromal cells from human bone marrow producing cytokines for B lineage progenitors and for plasma cells: SDF-1, flt3L, and BAFF. Molecular immunology **44:**1606-1612.
178. **Serra-Moreno, R., B. Jia, M. Breed, X. Alvarez, and D. T. Evans.** 2011. Compensatory changes in the cytoplasmic tail of gp41 confer resistance to tetherin/BST-2 in a pathogenic nef-deleted SIV. Cell host & microbe **9:**46-57.
179. **Sharova, N., Y. Wu, X. Zhu, R. Stranska, R. Kaushik, M. Sharkey, and M. Stevenson.** 2008. Primate lentiviral Vpx commandeers DDB1 to counteract a macrophage restriction. PLoS pathogens **4:**e1000057.
180. **Sharp, P. M., E. Bailes, M. Stevenson, M. Emerman, and B. H. Hahn.** 1996. Gene acquisition in HIV and SIV. Nature **383:**586-587.
181. **Silveira, N. J., L. Varuzza, A. Machado-Lima, M. S. Lauretto, D. G. Pinheiro, R. V. Rodrigues, P. Severino, F. G. Nobrega, Head, G. Neck Genome Project, W. A. Silva, Jr., B. P. C. A. de, and E. H. Tajara.** 2008. Searching for molecular markers in head and neck squamous cell carcinomas (HNSCC) by statistical and bioinformatic analysis of larynx-derived SAGE libraries. BMC medical genomics **1:**56.
182. **Smith, K. A.** 1988. Interleukin-2: inception, impact, and implications. Science **240:**1169-1176.
183. **Sonnenburg, J. L., T. K. Altheide, and A. Varki.** 2004. A uniquely human consequence of domain-specific functional adaptation in a sialic acid-binding receptor. Glycobiology **14:**339-346.
184. **Srivastava, S., S. K. Swanson, N. Manel, L. Florens, M. P. Washburn, and J. Skowronski.** 2008. Lentiviral Vpx accessory factor targets VprBP/DCAF1 substrate adaptor for cullin 4 E3 ubiquitin ligase to enable macrophage infection. PLoS pathogens **4:**e1000059.
185. **Stevenson, M., T. L. Stanwick, M. P. Dempsey, and C. A. Lamonica.** 1990. HIV-1 replication is controlled at the level of T cell activation and proviral integration. The EMBO journal **9:**1551-1560.
186. **Sun, L., J. Wu, F. Du, X. Chen, and Z. J. Chen.** 2013. Cyclic GMP-AMP synthase is a cytosolic DNA sensor that activates the type I interferon pathway. Science **339:**786-791.
187. **Sundquist, W. I., and H. G. Krausslich.** 2012. HIV-1 assembly, budding, and maturation. Cold Spring Harbor perspectives in medicine **2:**a006924.
188. **Swiecki, M., and M. Colonna.** 2010. Unraveling the functions of plasmacytoid dendritic cells during viral infections, autoimmunity, and tolerance. Immunological reviews **234:**142-162.
189. **Tebas, P., D. Stein, W. W. Tang, I. Frank, S. Q. Wang, G. Lee, S. K. Spratt, R. T. Surosky, M. A. Giedlin, G. Nichol, M. C. Holmes, P. D. Gregory, D. G. Ando, M. Kalos, R. G. Collman, G. Binder-Scholl, G. Plesa, W. T. Hwang, B. L. Levine, and C. H. June.** 2014. Gene editing of CCR5 in autologous CD4 T cells of persons infected with HIV. The New England journal of medicine **370:**901-910.
190. **Tokarev, A., M. Suarez, W. Kwan, K. Fitzpatrick, R. Singh, and J. Guatelli.** 2013. Stimulation of NF-kappaB activity by the HIV restriction factor BST2. Journal of virology **87:**2046-2057.
191. **Towers, G. J.** 2007. The control of viral infection by tripartite motif proteins and cyclophilin A. Retrovirology **4:**40.
192. **Tumanov, A. V., S. I. Grivennikov, A. N. Shakhov, S. A. Rybtsov, E. P. Koroleva, J. Takeda, S. A. Nedospasov, and D. V. Kuprash.** 2003. Dissecting the role of lymphotoxin in lymphoid organs by conditional targeting. Immunological reviews **195:**106-116.
193. **Turville, S. G., P. U. Cameron, A. Handley, G. Lin, S. Pohlmann, R. W. Doms, and A. L. Cunningham.** 2002. Diversity of receptors binding HIV on dendritic cell subsets. Nature immunology **3:**975-983.
194. **Turville, S. G., J. J. Santos, I. Frank, P. U. Cameron, J. Wilkinson, M. Miranda-Saksena, J. Dable, H. Stossel, N. Romani, M. Piatak, Jr., J. D. Lifson, M. Pope, and A. L. Cunningham.** 2004. Immunodeficiency virus uptake, turnover, and 2-phase transfer in human dendritic cells. Blood **103:**2170-2179.

195. **Unterholzner, L.** 2013. The interferon response to intracellular DNA: why so many receptors? Immunobiology **218:**1312-1321.
196. **Unterholzner, L., S. E. Keating, M. Baran, K. A. Horan, S. B. Jensen, S. Sharma, C. M. Sirois, T. Jin, E. Latz, T. S. Xiao, K. A. Fitzgerald, S. R. Paludan, and A. G. Bowie.** 2010. IFI16 is an innate immune sensor for intracellular DNA. Nature immunology **11:**997-1004.
197. **Valbuena, G., and D. H. Walker.** 2006. The endothelium as a target for infections. Annual review of pathology **1:**171-198.
198. **Van Damme, N., D. Goff, C. Katsura, R. L. Jorgenson, R. Mitchell, M. C. Johnson, E. B. Stephens, and J. Guatelli.** 2008. The interferon-induced protein BST-2 restricts HIV-1 release and is downregulated from the cell surface by the viral Vpu protein. Cell host & microbe **3:**245-252.
199. **van der Kuyl, A. C., R. van den Burg, F. Zorgdrager, F. Groot, B. Berkhout, and M. Cornelissen.** 2007. Sialoadhesin (CD169) expression in CD14+ cells is upregulated early after HIV-1 infection and increases during disease progression. PloS one **2:**e257.
200. **Vinson, M., P. A. van der Merwe, S. Kelm, A. May, E. Y. Jones, and P. R. Crocker.** 1996. Characterization of the sialic acid-binding site in sialoadhesin by site-directed mutagenesis. The Journal of biological chemistry **271:**9267-9272.
201. **Wang, W., Y. Nishioka, S. Ozaki, A. Jalili, S. Abe, S. Kakiuchi, M. Kishuku, K. Minakuchi, T. Matsumoto, and S. Sone.** 2009. HM1.24 (CD317) is a novel target against lung cancer for immunotherapy using anti-HM1.24 antibody. Cancer immunology, immunotherapy : CII **58:**967-976.
202. **Wenzel, J., B. Bekisch, M. Uerlich, O. Haller, T. Bieber, and T. Tuting.** 2005. Type I interferon-associated recruitment of cytotoxic lymphocytes: a common mechanism in regressive melanocytic lesions. American journal of clinical pathology **124:**37-48.
203. **West, A. P., Jr., L. Scharf, J. F. Scheid, F. Klein, P. J. Bjorkman, and M. C. Nussenzweig.** 2014. Structural insights on the role of antibodies in HIV-1 vaccine and therapy. Cell **156:**633-648.
204. **White, T. E., A. Brandariz-Nunez, J. C. Valle-Casuso, S. Amie, L. A. Nguyen, B. Kim, M. Tuzova, and F. Diaz-Griffero.** 2013. The retroviral restriction ability of SAMHD1, but not its deoxynucleotide triphosphohydrolase activity, is regulated by phosphorylation. Cell host & microbe **13:**441-451.
205. **Worobey, M., M. Gemmel, D. E. Teuwen, T. Haselkorn, K. Kunstman, M. Bunce, J. J. Muyembe, J. M. Kabongo, R. M. Kalengayi, E. Van Marck, M. T. Gilbert, and S. M. Wolinsky.** 2008. Direct evidence of extensive diversity of HIV-1 in Kinshasa by 1960. Nature **455:**661-664.
206. **Wu, J., L. Sun, X. Chen, F. Du, H. Shi, C. Chen, and Z. J. Chen.** 2013. Cyclic GMP-AMP is an endogenous second messenger in innate immune signaling by cytosolic DNA. Science **339:**826-830.
207. **Wu, L., T. D. Martin, R. Vazeux, D. Unutmaz, and V. N. KewalRamani.** 2002. Functional evaluation of DC-SIGN monoclonal antibodies reveals DC-SIGN interactions with ICAM-3 do not promote human immunodeficiency virus type 1 transmission. Journal of virology **76:**5905-5914.
208. **Yang, Y., J. Luban, and F. Diaz-Griffero.** 2014. The fate of HIV-1 capsid: a biochemical assay for HIV-1 uncoating. Methods in molecular biology **1087:**29-36.
209. **Yoder, A., D. Yu, L. Dong, S. R. Iyer, X. Xu, J. Kelly, J. Liu, W. Wang, P. J. Vorster, L. Agulto, D. A. Stephany, J. N. Cooper, J. W. Marsh, and Y. Wu.** 2008. HIV envelope-CXCR4 signaling activates cofilin to overcome cortical actin restriction in resting CD4 T cells. Cell **134:**782-792.
210. **Yondola, M. A., F. Fernandes, A. Belicha-Villanueva, M. Uccelini, Q. Gao, C. Carter, and P. Palese.** 2011. Budding capability of the influenza virus neuraminidase can be modulated by tetherin. Journal of virology **85:**2480-2491.
211. **Yoneyama, M., W. Suhara, and T. Fujita.** 2002. Control of IRF-3 activation by phosphorylation. Journal of interferon & cytokine research : the official journal of the International Society for Interferon and Cytokine Research **22:**73-76.
212. **York, M. R., T. Nagai, A. J. Mangini, R. Lemaire, J. M. van Seventer, and R. Lafyatis.** 2007. A macrophage marker, Siglec-1, is increased on circulating monocytes in patients with

systemic sclerosis and induced by type I interferons and toll-like receptor agonists. Arthritis and rheumatism **56:**1010-1020.

213. **Yu, X., Y. Yu, B. Liu, K. Luo, W. Kong, P. Mao, and X. F. Yu.** 2003. Induction of APOBEC3G ubiquitination and degradation by an HIV-1 Vif-Cul5-SCF complex. Science **302:**1056-1060.
214. **Zack, J. A., S. J. Arrigo, S. R. Weitsman, A. S. Go, A. Haislip, and I. S. Chen.** 1990. HIV-1 entry into quiescent primary lymphocytes: molecular analysis reveals a labile, latent viral structure. Cell **61:**213-222.
215. **Zhang, F., S. J. Wilson, W. C. Landford, B. Virgen, D. Gregory, M. C. Johnson, J. Munch, F. Kirchhoff, P. D. Bieniasz, and T. Hatziioannou.** 2009. Nef proteins from simian immunodeficiency viruses are tetherin antagonists. Cell host & microbe **6:**54-67.
216. **Zhang, Z., B. Yuan, M. Bao, N. Lu, T. Kim, and Y. J. Liu.** 2011. The helicase DDX41 senses intracellular DNA mediated by the adaptor STING in dendritic cells. Nature immunology **12:**959-965.
217. **Zhong, B., Y. Yang, S. Li, Y. Y. Wang, Y. Li, F. Diao, C. Lei, X. He, L. Zhang, P. Tien, and H. B. Shu.** 2008. The adaptor protein MITA links virus-sensing receptors to IRF3 transcription factor activation. Immunity **29:**538-550.
218. **Zou, Z., A. Chastain, S. Moir, J. Ford, K. Trandem, E. Martinelli, C. Cicala, P. Crocker, J. Arthos, and P. D. Sun.** 2011. Siglecs facilitate HIV-1 infection of macrophages through adhesion with viral sialic acids. PloS one **6:**e24559.